

# POLITECNICO DI TORINO

Corso di Laurea Magistrale in  
Automotive Engineering (Ingegneria dell'autoveicolo)

Tesi di Laurea Magistrale

**SCR modelling for road transport applications: realization,  
validation and implementation on light-duty vehicle**



**Politecnico  
di Torino**

Relatori:

Dr. Ezio Spessa

Dr. Roberto Finesso

Candidato:

Francesco Esposito

Anno Accademico 2020/2021



## ABSTRACT

Vehicle modelling is a standard procedure employed today by all the major OEMs in order to comply with the market requirements as well as with the several industrial norms, aiming at reducing the number of modifications during the design phase. For these reasons, its implementation on tools such as Simulink® is of fundamental relevance and constitutes the so-called virtual prototyping process.

The aim of this thesis is to examine the longitudinal behaviour and optimize the emissions treatment of a vehicle already present on the market, a 2014 remarkable van. In particular, the attention was shifted on the NOx emissions, being the most relevant emission, together with the particulate matter, in Diesel engines such as the one employed on this van.

The whole vehicle layout was implemented on a specific Simulink® tool, commercially known as Simscape™ and able to create an apparatus based on physical relationships, where each single block performs the functions of a specific element of the real van.

Particular attention was put on the engine mock-up, realised through the GT-Power® software and governed by a BMEP-target principle, according to the required engine speed and accelerator pedal position. Successively, the engine interface was coupled to the Simulink net through a dedicated interface, ensuring the management of the entire system directly on Simulink®. After the selection of a Selective Catalyst Reduction (SCR) suitable to the engine characteristics, the trivial chance to customize a component ex novo was exploited. This constitutes a new methodology practicable through a thorough understanding of the source codes and of the mathematical principles governing the components. Finally, a validation procedure was conducted on the SCR thermal evolution according to the experimental data provided.

The complete simulation, performed on the current standard homologation cycle, the Worldwide harmonized Light-duty vehicles Test Cycle (WLTC), has demonstrated the ability of the model to correctly replicate the vehicle dynamics. This was achieved according to a continuous reference and model speed matching principle that brought the margin of error below 1 km/h for more than 80% of the time. Moreover, the BMEP target-based approach was tested on a 0-100 km/h launch, where the computed time error, related to the empirical data, was found to be less than 2%. In addition, the investigation has revealed that the conversion efficiency of the selected 12 litres catalyst achieves values higher than 90% in general, when the residence time and SCR Temperature are high enough.

These results confirms the pivotality of the adoption of the methodology to reasonably simulate the vehicle behaviour in advance. Consequently, the best possible NOx emission level can be reached, according to the current State of Art.

Overall, the procedure leads to a higher level of detail while still maintaining the design costs low. In this analysis, the focus was limited to the mechanical and thermal behaviour of the main elements of a van. Nevertheless, this approach can be extended to characterize all the properties of any device installed onboard, opening infinite scenarios in the future vehicle modelling.



# INDEX

LIST OF FIGURES.....	pag.7
LIST OF TABLES.....	pag.10
1. INTRODUCTION .....	pag.12
1.1 Objective.....	pag.12
1.2 Motivation.....	pag.12
2. THE VEHICLE.....	pag.13
3. THE VIRTUAL PROTOTYPING.....	pag.15
3.1 Longitudinal Driver.....	pag.17
3.1.1 <i>Drive cycle</i> .....	pag.18
3.2 Engine.....	pag.19
3.3 Transmission.....	pag.21
3.4 Final Drive.....	pag.23
3.5 Wheels.....	pag.24
3.6 Vehicle Body.....	pag.24
3.7 SCR.....	pag.25
3.7.1 Thermal Model.....	pag.26
3.7.2 Chemical Model.....	pag.28
4. ENGINE MOCK-UP.....	pag.29
5. SIMSCAPE LANGUAGE.....	pag.31
6. THERMAL MODEL DEVELOPMENT.....	pag.32
7. SCR MODEL IMPLEMENTATION IN SIMSCAPE.....	pag.35
8. MODEL VALIDATION.....	pag.40
8.1 Powertrain.....	pag.40
8.2 Selective Catalyst Reduction.....	pag.41
9. RESULTS .....	pag.44
9.1 Speed.....	pag.44
9.2 Acceleration.....	pag.46
9.3 Torque.....	pag.48

9.4 Gears.....	pag.51
9.5 Final Drive.....	pag.55
9.6 Braking.....	pag.57
9.7 Wheels.....	pag.60
9.8 Engine-out.....	pag.64
9.9 SCR.....	pag.70
9.9.1 Thermal model.....	pag.70
9.9.2 Chemical model.....	pag.80
10. MODEL LIMITATIONS.....	pag.82
11. CONCLUSIONS.....	pag.84
REFERENCES.....	pag.85

# LIST OF FIGURES

Figure 1. IVECO DAILY 50C15 MY 2014.....	pag.13
Figure 2. Vehicle model.....	pag.16
Figure 3. Longitudinal Driver Controller block.....	pag.17
Figure 4. Worldwide harmonized Light-duty vehicles Test Cycle – Class 3b.....	pag.18
Figure 5. Engine sub-group Simscape model.....	pag.20
Figure 6. StateFlow Gearshift logic chart.....	pag.21
Figure 7. Transmission sub-group Simscape model.....	pag.22
Figure 8. Final Drive sub-group Simscape model.....	pag.23
Figure 9. Brakes sub-group Simscape model.....	pag.23
Figure 10. Wheels sub-group Simscape model.....	pag.24
Figure 11. Vehicle Body block.....	pag.25
Figure 12. SCR overall model.....	pag.26
Figure 13. SCR Simscape thermal model.....	pag.27
Figure 14. GT-Power Engine scheme.....	pag.30
Figure 15. SCR discretization by 0D model.....	pag.32
Figure 16. SCR elementary block.....	pag.35
Figure 17. SCR parameters.....	pag.36
Figure 18. Signs convention.....	pag.39
Figure 19. 0-100 km/h acceleration.....	pag.40
Figure 20. SCR validation model.....	pag.42
Figure 21. Model Thermal trend – Comparison with experimental data.....	pag.43
Figure 22. Speed comparison between WLTP and model output.....	pag.45
Figure 23. Accelerator vs Decelerator Command during WLTC.....	pag.46
Figure 24. Imposition of Acceleration cut-off during gear shifting.....	pag.47
Figure 25. Accelerator vs Decelerator Command during WLTC – zoom in first 200 seconds.....	pag.48
Figure 26. Engine Torque trend during the WLTC.....	pag.49
Figure 27. Engine map.....	pag.49
Figure 28. Fuel consumption and BSFC maps.....	pag.50

Figure 29. Gear selection and related engine rpm.....	pag.51
Figure 30. Gear selection detailed charts.....	pag.52
Figure 31. Clutch Pressure application for gear shifting.....	pag.52
Figure 32. Gearbox principle – Speed conversion.....	pag.53
Figure 33. Gearbox principle – Detailed view of first 200 seconds.....	pag.54
Figure 34. Differential characteristic diagram.....	pag.55
Figure 35. Differential principle – Speed conversion.....	pag.56
Figure 36. Brakes Actuation – From Deceleration Command to Braking Torque.....	pag.57
Figure 37. Brakes Actuation – Deceleration Command imposition on the Speed Profiles.....	pag.58
Figure 38. Brakes Actuation – First 200 seconds zoom in.....	pag.58
Figure 39. Brakes Actuation – Deceleration Command computation.....	pag.59
Figure 40. Left vs Right tyre rotational speed.....	pag.60
Figure 41. Wheel Normal Load trend.....	pag.60
Figure 42. Wheel Normal Load trend – Filtered Signal.....	pag.61
Figure 43. Wheel Normal Load trend vs Speed.....	pag.61
Figure 44. Wheel Rolling Resistance and Normal Load relationship.....	pag.62
Figure 45. Wheel Normal Load vs Longitudinal Load trend.....	pag.63
Figure 46. Engine-out Temperature.....	pag.64
Figure 47. Engine-out Temperature vs Acceleration Command.....	pag.65
Figure 48. Engine-out Mass Flow Rate.....	pag.66
Figure 49. Engine-out Mass Flow Rate vs Engine Speed.....	pag.66
Figure 50. Engine-out Volumetric Flow Rate.....	pag.67
Figure 51. Engine-out Flows.....	pag.67
Figure 52. Engine-out NOx emission.....	pag.68
Figure 53. Engine-out NOx emission vs exhaust gas Temperature.....	pag.69
Figure 54. Inlet fluid Temperature vs Wall Temperature, first block – detailed .....	pag.71
Figure 55. Inlet fluid Temperature vs Wall Temperature, first block.....	pag.72
Figure 56. Outlet fluid Temperature vs Wall Temperature, first block.....	pag.72
Figure 57. Outlet fluid Temperature vs Wall Temperature, first block – Detailed.....	pag.73
Figure 58. Complete thermal evolution, first block.....	pag.74
Figure 59. Heat Flow Rate, first block.....	pag.75

Figure 60. First block and Second block interaction.....	pag.76
Figure 61. First block and Second block interaction with walls.....	pag.77
Figure 62. Fluid Thermal evolution across the catalyst.....	pag.78
Figure 63. SCR Thermal evolution.....	pag.79
Figure 64. NOx conversion efficiency.....	pag.80
Figure 65. NOx conversion efficiency and emissions.....	pag.81

**LIST OF TABLES**

Table 1. Main Engine Data.....pag.14  
Table 2. Selected SCR catalyst – Main data.....pag.38



# 1. INTRODUCTION

## 1.1 Objective

The goal of the entire project is the modelling of an iconic van of the IVECO brand, the Daily Diesel 50C15H V MY 2014, equipped with a 3.0L Diesel F1CFL411E engine able to develop a maximum power of 107 kW. More in deep, the focus is on the powertrain of the vehicle and on the emission reduction, starting from the engine data evolution. Therefore, the van behaviour is tested in a virtual environment according to the Worldwide Harmonized Light Vehicles Test Procedure (WLTP), class 3.

The engine is coupled to a 12 litres catalyst to reduce its NO<sub>x</sub> emissions: the Selective Catalytic Reduction (SCR). Here, the NO<sub>x</sub> molecules present in the exhaust gases are chemically reacting with the active sites of the catalyst, to remove their oxygen content (reduction reaction). This step effectiveness (i.e., the NO<sub>x</sub> conversion efficiency) is directly related to the Temperature level and flow rate amount. The modelling, simulation and analysis of this device, and in particular of its thermal behaviour, is consequently of fundamental importance and requires particular attention as standing alone component.

## 1.2 Motivation

The simulation of the behaviour of a generic vehicle is nowadays a must-do step along the design phase. This allows to estimate in advance significant quantities which are linked to the design of other components and thus avoids a trial-and-error procedure in which the cost of the changes in the plan are high and increasing as the time goes by. Moreover, it is possible to forecast the product behaviour before the physical vehicle is actually available.

In this area, one of the most relevant topic today is the emissions control, especially in Diesel engines. This is due to the strong correlation between this type of engine and its emissions, considered very dangerous.

In the particular case of NO<sub>x</sub> production, it is characteristic of the Diesel engine, and it is of high relevance since almost 50% of the global NO<sub>x</sub> emission can be related to the vehicles' activity, according to recent studies. Moreover, the NO<sub>x</sub> emissions contribute to the formation of the so called "photochemical smog", a mix of many dangerous substances, such as the Ozone, that constitute a localized danger for the human health. For these reasons, it is necessary to make a big effort in the treatment of the Diesel emissions and big steps can still be done in this direction.

## 2. THE VEHICLE

The object of the analysis is the IVECO DAILY 50C15H V MY 2014. The daily family is an iconic model of the IVECO original equipment manufacturer (OEM) and it is commonly available in different versions: van, semi-windowed van, minibus, chassis cab, crew cab,... For the purpose, the van version was selected for its fame and data accessibility.

Through the several improvements employed during its design across the years, this version has reached an incredible goal in terms of aerodynamic performance. Consequently, the final drag coefficient ( $C_x$ ) is set to 0.316, extremely close to the optimum results achievable with a passenger car.

Moreover, the new van architecture led to an increase in the load volume ( $19.6\text{m}^3$ ) and an easier accessibility to the load compartment. This, combined with an enhanced versatility, made this van very popular and enjoyed by the typical customer. The success was confirmed by the conferment of the van of the year 2015 award.



Figure 1. IVECO DAILY 50C15 MY 2014

The van is equipped with a Diesel engine known as F1CFL411E or simply F1C. This engine is characterized by a total displacement of 3 Litres approximately and a maximum power of 107 kW, ensuring a top class performance thanks to the adoption of the rear drive too. This improves the traction and the pick-up at the start, optimizing the van behaviour in the traffic.

A 6-gears transmission is designed to reach the best performance-fuel consumption trade-off and to reach high speeds too, allowing the achievement of the top capability on highway as well.

The main engine data are reported in table 1:

<b>F1C DATA</b>	
<b>Total displacement</b>	2998 cm <sup>3</sup>
<b>Max power</b>	146 hp/107 kW at 3000-3500 rpm
<b>Max torque</b>	350 Nm at 1400-2600 rpm
<b>N° cylinders</b>	4 vertical cylinders in line
<b>N° valves</b>	16 valves/4 per cylinder
<b>Timing system</b>	Double Overhead Camshaft (DOHC)
<b>Engine type</b>	Turbocharged

Table 1. Main engine data

### 3. THE VIRTUAL PROTOTYPING

The whole powertrain of the IVECO DAILY is implemented on Simulink®, exploiting the specific Simscape™ tool. This facility allows the creation of models of physical systems inside the environment, based on physical relationships that directly combine with the components integrated into the diagrams. This type of tool exploits bidirectional physical signals transmitted along the entire net. Unlike the classic Simulink® approach, this logic allows to handle different types of signals (or variables) on the same line of the net. The entire model is shown in figure 2.

When the blocks are connected together, the resulting diagram is corresponding to the mathematical representation of the system under design, based on the Physical Network approach. In the end, several functional elements will cooperate with each other by swapping energy through their nondirectional ports, as they mimic physical connections between elements. Associating Simscape blocks becomes like connecting real modules, such as pumps, valves, pipes... The Physical Network methodology autonomously figures out all the usual matters with variables, directionality, and so on, as in real world. The sum of linking ports for each component is defined according to the number of energy flows exchanged with other elements in the scheme.

The energy flows are linked to two variable types, one Through and one Across. Their product is the energy flow in watts. These are the so-called basic (or conjugate) variables. For example, the basic variables for a mechanical translational system are force and velocity, for a mechanical rotational system they are torque and angular velocity, for a hydraulic system the two are flow rate and pressure whereas for an electrical system, current and voltage.

Therefore, Simscape allows to apply this method in a wide variety of fields, included in its Physical Foundation Domains (Electric, Gas, Thermal, Mechanical, Hydraulic...). For instance, in the general Iveco Daily powertrain structure, the links are of mechanical type, meaning that each line can be assumed as a mechanical shaft or linkage system. On the other hand, the SCR thermal model is connected by gas links, that can be imagined as straight pipes in which the exhaust gases are continuously flowing. Here, the thermodynamic properties rule.

Going more in deep in the model analysis, each main sub-group is represented with a dedicated mask:

- the longitudinal driver controller
- the engine
- the transmission
- the final drive
- the wheels
- the vehicle body
- the SCR

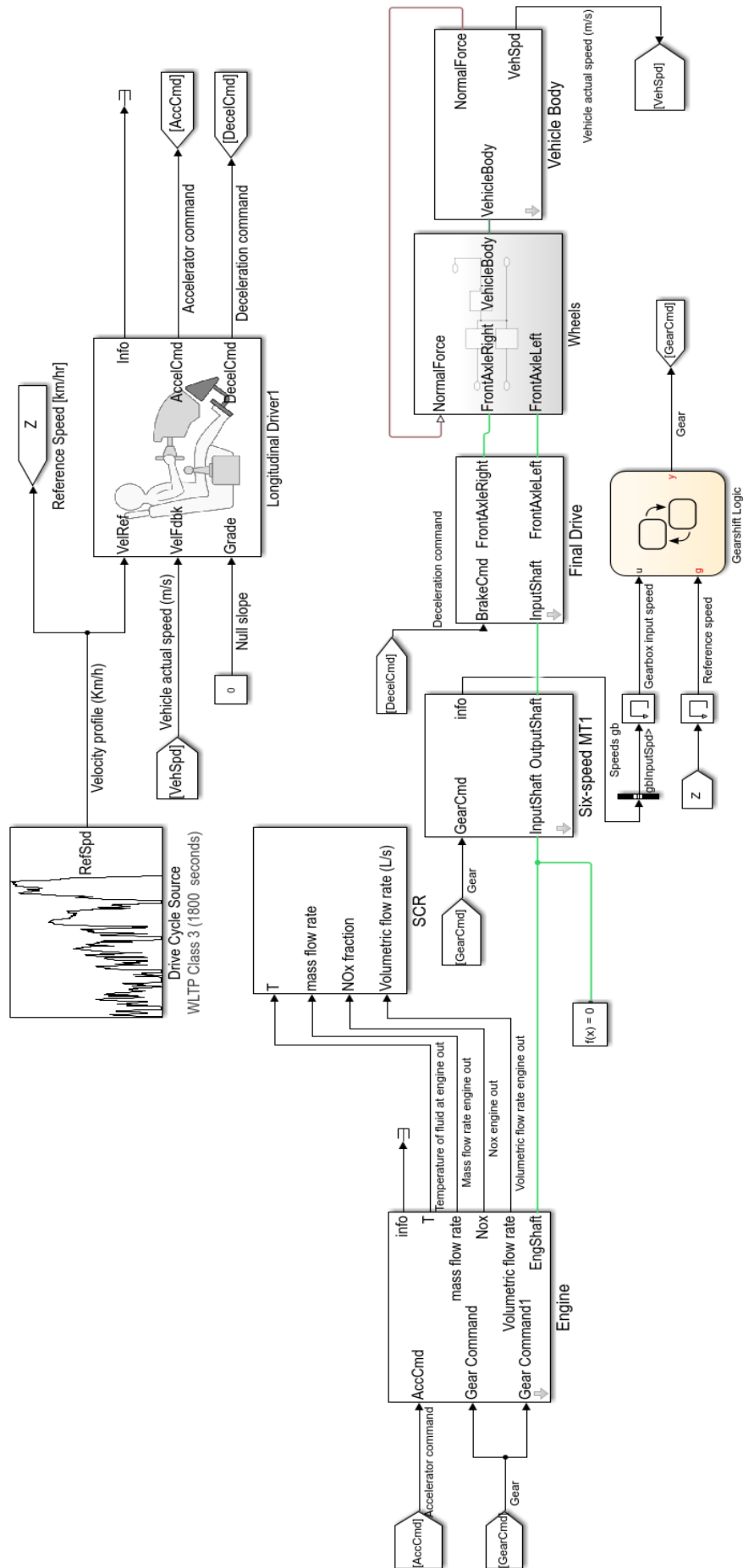


Figure 2. Vehicle model

Besides the masks, many other elements can be noticed in the complex diagram.

The trapezoidal-shape components are a sort of connecting portals. These are of two types, From and Goto ports, and they allow to link a variable, specified within the block shape, between two elements without the need of a connecting line, to avoid a too much complex wiring system.

When a block output is not relevant for the analysis, a Terminator sequence can be linked to the related port. Its symbol is:  $\equiv$

Moreover, a strange block with the wording  $f(x)=0$  can be pointed out. This represents the so-called Solver Configuration, necessary to define the mathematical settings for the model simulation. This block can be placed anywhere as long as it is connected to each Simscape chart.

In conclusion, a memory block  is located prior to the Gearshift Logic section, for both Reference Speed and Gearbox input Speed. This component is able to apply a one integration step delay during the computation. This step is necessary since the model is characterized by Algebraic loops; thus, it is necessary to provide a previous condition in order to make the mathematical resolution possible. Therefore, the output of this component is the preceding input value.

### 3.1 Longitudinal Driver

This particular block examines the reference speed (VelRef in next picture) coming from the drive cycle profile at each instant of time and compares it with the feedback velocity, the actual velocity of the vehicle computed by the model (VelFdbk). According to the difference between the two, it determines the relative acceleration (AccelCmd) or deceleration command (DecelCmd) to apply on the engine to follow continuously the drive cycle evolution. The road grade (Grade) is null, as required by the drive cycle itself, whereas the Info port is negligible for the intended purpose.

In this specific case, the controller is of proportional- integral type (PI controller). The two gains are calibrated in order to find the proper compromise between the speed matching capability (i.e., minimizing the velocity error) and the flexibility in the computation of the model. The unit of the two speeds to compare is the [m/s].

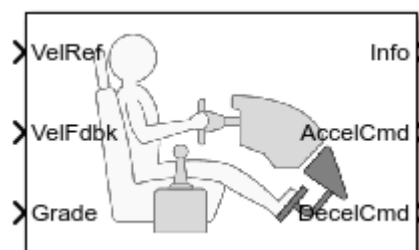


Figure 3. Longitudinal Driver Controller block

### 3.1.1 Drive cycle

The considered drive cycle is the current standard in Europe, the so-called WLTP. Introduced on 1<sup>st</sup> September 2017, it is now the reference cycle for the emission collection procedure. It has replaced the older NEDC, considered highly unrealistic and far from the actual driving as the maximum acceleration during the transient parts reaches approximately 1 m/s<sup>2</sup> and the average speed is low, especially in the urban part. The new cycle is still not that representative of real driving and big efforts are required in the future to cover the gap. On this direction, Real Driving Emission (RDE) tests have been introduced with the EURO 6 regulation, boosted by the DieselGate scandal.

The WLTP is characterized by different cycles (WLTC) according to the class of the vehicle. In particular, three classes have been introduced, according to the reference parameter used, the Power-to-Weight ratio (PWR), expressed in [W/kg]:

- Class 1, low power and/or big vehicles with  $PWR \leq 22$
- Class 2, vehicles with  $22 < PWR \leq 34$ ;
- Class 3, high power and/or small vehicles with  $PWR > 34$ .

The Iveco Daily under analysis belongs to the last category, as its PWR is roughly 42. This category is the most common as the vast majority of the standard passenger vehicles fall in this range. The duration of each of the four parts of the WLTC (Low, Medium, High and Extra-High speed) is constant between classes, whereas the acceleration and speed profiles are dissimilar. For the class 3 these are:

- Low, with a top speed of 56.5 km/h
- Medium, with a top speed of 76.6 km/h
- High, with a top speed of 97.4 km/h
- Extra-high, with a top speed of 131.3 km/h.

These driving segments simulate urban, suburban, rural and highway conditions respectively.

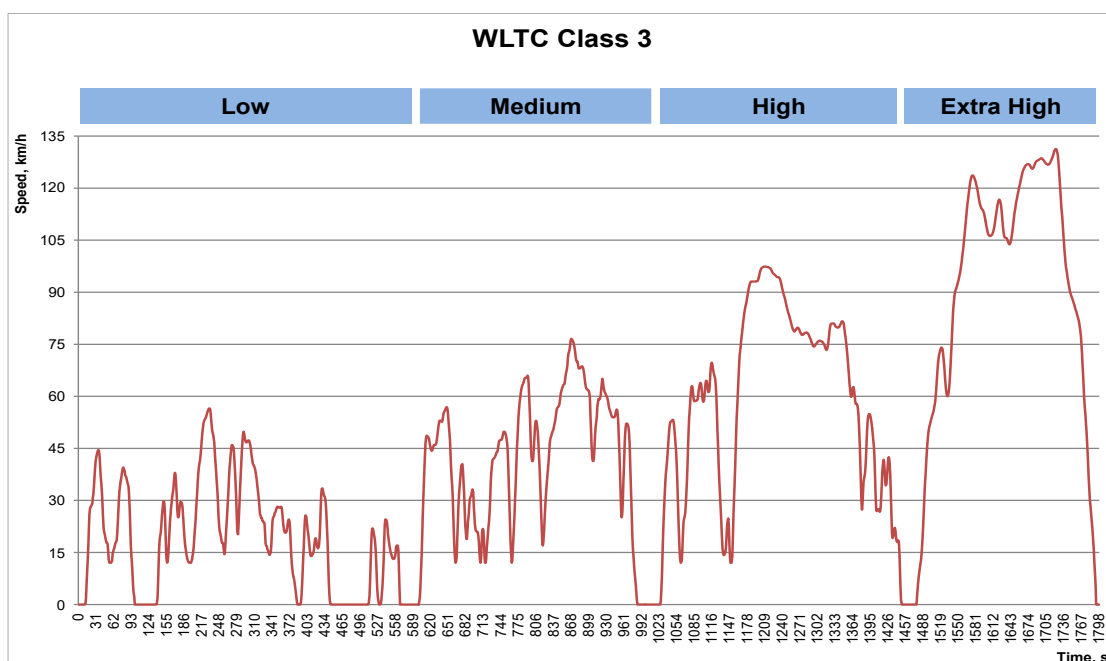


Figure 4. Worldwide harmonized Light-duty vehicles Test Cycle – Class 3b

## 3.2 Engine

This is the core of the project and first real macro-block involved in the Simscape model. Here, the acceleration command derived from the driver controller is the starting point. This signal ranges between 0 (no throttle) and 1 (full throttle) and it is considered in combination with the engine speed to compute the engine working point. In particular, a BMEP target is computed according to a 2-D look up table, function of pedal position and engine rpm.

At this point, the behaviour of the 3.0L is simulated thanks to the GT-Power coupling: for each time step, the previous data are sent in the dedicated software, where the engine functioning is replicated by all the components (from the cylinders up to the turbine). This software is able to determine all the main quantities in each component, simultaneously to the Simulink model, considering the engine inertia. The most indicative ones, according to the user choice, are passed again to Simulink, thanks to the coupling interface.

In this circumstance, these are:

- BMEP Target, linked to the acceleration required to match the reference speed
- Engine Torque, the actual torque including the negative friction contribution. This is the only parameter actually useful at the mechanical level: this raw value is passed to an ideal Torque source where a torque, proportional to the input physical signal, is generated at its terminals. The source is ideal since it is supposed to be capable of maintaining the specified torque regardless of the angular velocity.
- Exhaust Gas Temperature, the Temperature (in [K]) of the gas discharged by the engine (engine-out)
- Mass flow rate at engine-out, related again to the exhaust gases and expressed in [kg/s]
- Volumetric flow rate at engine-out, expressed in [L/s] and then converted in [m<sup>3</sup>/h]
- NO<sub>x</sub> fraction at engine-out, mass fraction of the total exhaust flow

The actual chart is slightly more complex due to the necessity of some additional controller, for a realistic governing of the engine, and some extra Simscape component, in order to consistently implement the physical quantities computed by GT software into the model.

Figure 5 is showing the general principle:

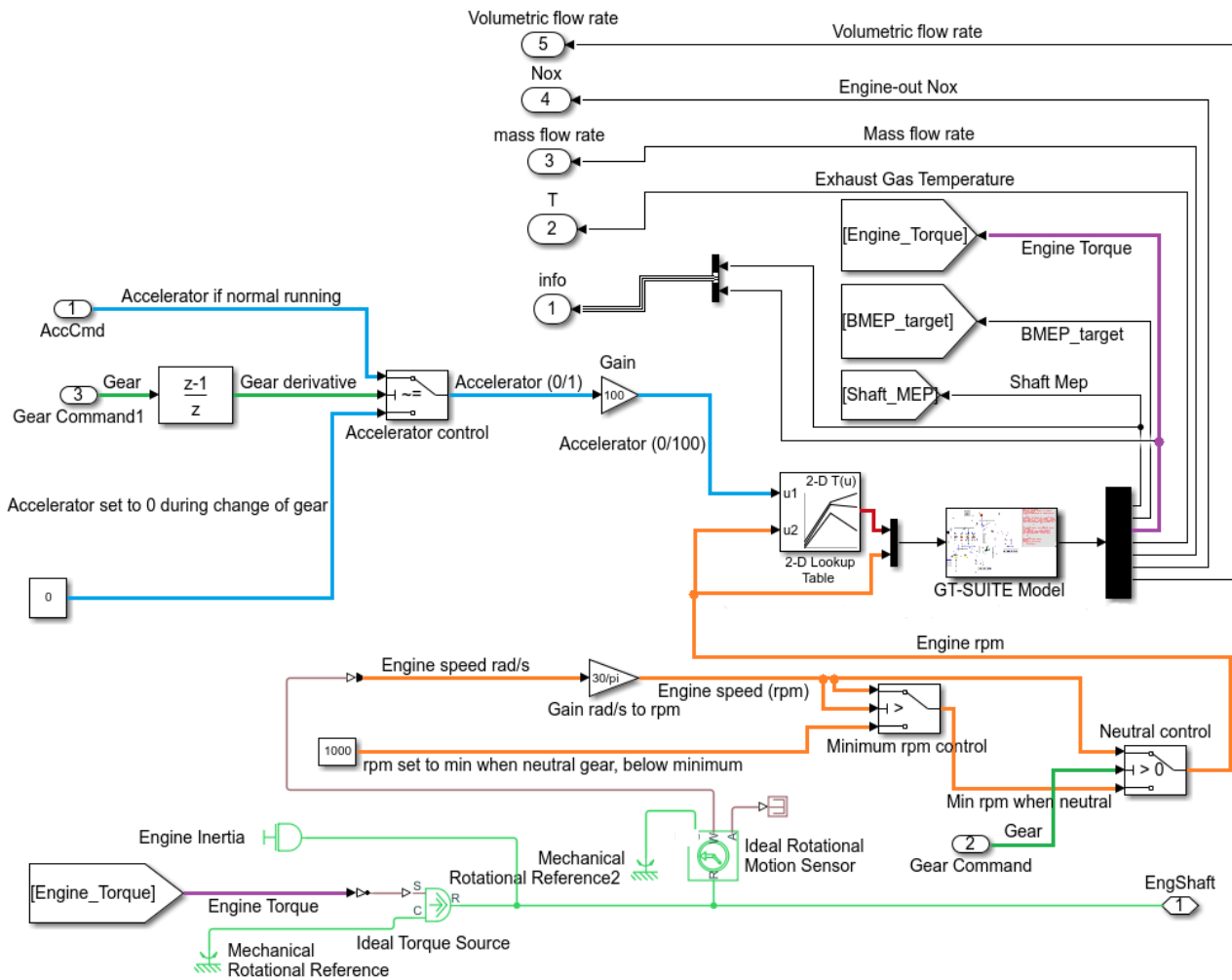


Figure 5. Engine sub-group Simscape model

The scheme is developing from left to right. The starting point is represented by the Gear and Accelerator Command signals introduction, respectively in cyan and dark green . The Gear Signal is derived by a proper block and passed to a switch that acts as a controller: if the gear derivative is not 0, meaning that a gear shifting is in progress, the accelerator is imposed to 0 to avoid a peak in the Torque transferred to the clutch, otherwise the original Accelerator Command is considered.

As a consequence, the Accelerator value is always ranging between 0 and 1. Then, it is converted in % by the “Gain” element and combined with the engine rpm (in orange) to calculate the working point in the 2-D look up table. The outcome is the BMEP target (in red), passed into the GT-Power coupling together with the instantaneous engine rotational speed, later described.

Among all the quantities previously described, the Average Engine Torque (in violet) is the parameter used to trigger the Simscape model. This value is transformed into a variable thanks to the Simulink to PS (Physical Signal) converter block (double arrow sign, in black and white). The Torque Variable is then controlling an Ideal Torque Source, able to generate torque at its terminals proportional to the input physical signal, simulating the engine functioning. As the engine is connected to the frame, this component must be linked to a Mechanical Rotational Reference in one of its ports. The engine inertia is also considered by a dedicated element.

Now, the engine rotational speed must be sensed and considered for the look-up table previously mentioned. For this reason, an Ideal Rotational Motion Sensor is connected in parallel to the mechanical circuit (in light green), measuring the speed difference at its terminals, A and B, without the application of inertia, friction, delay or energy consumption of any kind.

This block senses the angular speed (in orange) in [rad/s] and it requires a further Mechanical Rotational Reference. This value is then converted in rpm and examined by a couple of other switches. The first one is essential to set the minimum rotational limit. The second one is required to ensure this limit is applied only when the engine is in idle condition, that is in neutral condition (when the Gear signal is at 0). In the opposite case, the original rpm is directly transferred to the look-up table. At this point, the engine schematic loop is completed.

### 3.3 Transmission

The engine is successively connected mechanically to a 6-speeds transmission. The engine shaft rpm is sensed by a dedicated two terminals sensor (in [rad/S]). The sensor is again ideal since it does not account for inertia, friction, delays, energy consumption, and so on. This velocity coincides with the gearbox speed at the input shaft, employed as evaluating parameter in the gear selection after the conversion in round per minute (rpm).

The gearshift logic is implemented in a simple StateFlow block, visible in figure 6. StateFlow is a particular Simulink control logic tool constituted by state machines and flow charts, able to establish hierarchies, parallelisms and histories of the instructions located in the State charts. Moreover, it allows to implement truth tables and state transition tables, according to a Boolean logic.

Starting from a neutral condition, when the engine rpm is above the minimum (around 850 rpm) and the reference speed is positive, the first gear is engaged. The successive gear ratios are involved when the engine speed is higher than 2000 rpm for a fraction of second at least, to avoid a change of gear in case of sudden but temporary oscillations of speed. Concerning the downshifts, they are performed when a rotational speed below 1000 rpm is kept for at least 2 seconds, when the engine working point is going towards low efficiency areas for too long. In this direction, the proper gear is continuously selected.

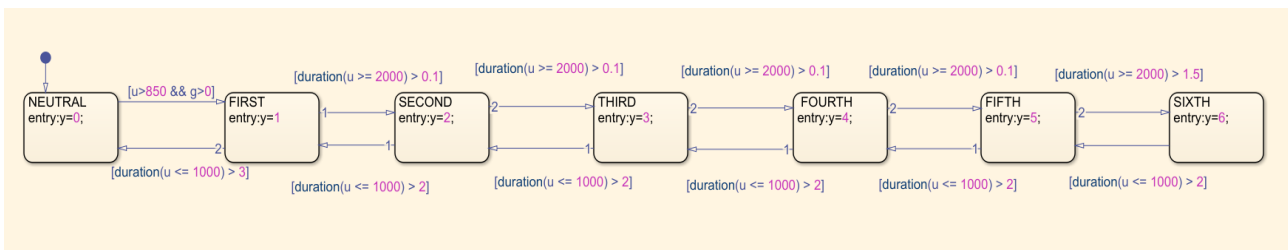


Figure 6. StateFlow Gearshift logic chart

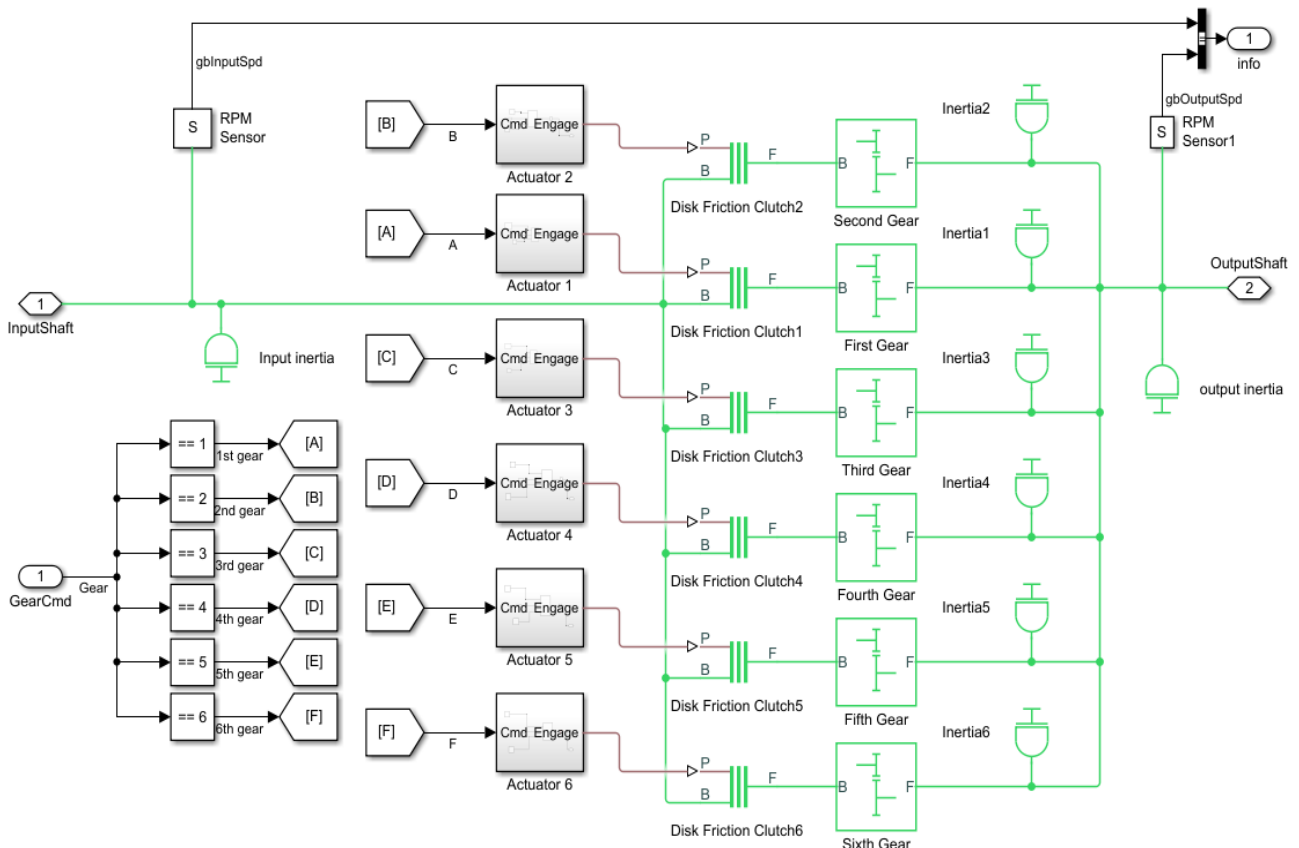


Figure 7. Transmission sub-group Simscape model

Once the proper gear is selected, this signal is sent to the Transmission circuit, noticeable in figure 7.

For the continuity of the circuit, a different path must be fitted for each gear ratio; therefore, one clutch for each line should be employed. Consequently, the proper clutch is controlled by the gear command: when the n-th gear must be engaged, only the n-th path is triggered by imposing a strong enough pressure on the relative disk clutch.

Differently, a null pressure is exerted on the not actuated clutches. Specifically, the clutches are friction-controlled disks that allows or denies transmission of torque between the driving and driven shafts. Each clutch is described by a bidirectional functioning, with four active surfaces and 130 mm effective torque radius.

The gears are simple gear-pinion meshing with fixed gear ratios. The meshing losses are included too, according to specific efficiencies. In the end, all the gears are characterized by a specific inertia, considered again by the proper blocks.

### 3.4 Final Drive

Going on along the Simscape circuit, the final drive is the following stage. This can be easily implemented thanks to a Differential block, with the specific carrier to driveshaft teeth ratio. This is organized as a planetary bevel gear train supplied with an additional bevel gear transmission between driveshaft and carrier. The pinion gear is connected to the driveshaft while the large bevel crown gear is attached to the carrier. Again, the meshing losses are included thanks to the sun-sun and carrier-driveshaft ordinary efficiencies. The differential element is splitting the torque between left and right wheel of the same axle, the front one.

In the same mask, also the brakes circuit is incorporated: the brake command derived from the longitudinal driver controller is converted into a brake torque thanks to an Ideal Torque Source, controlled directly by the raw value. This block is of the same type of the torque actuator used for the engine, except for the opposite sign torque. Again, a Mechanical Rotational Reference is mandatory to simulate the system frame.

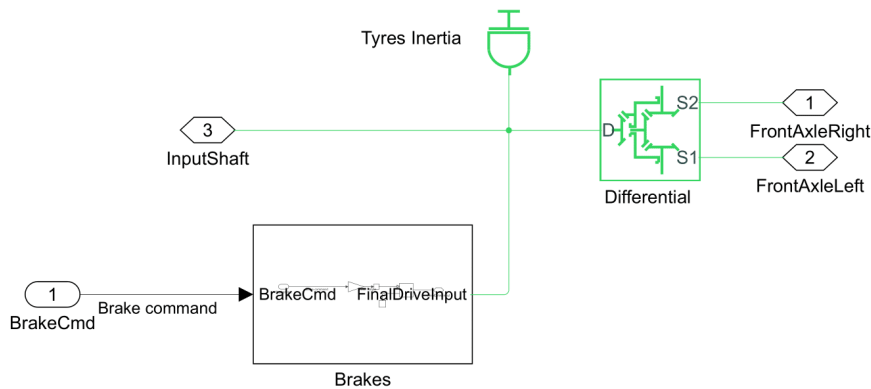


Figure 8. Final Drive sub-group Simscape model

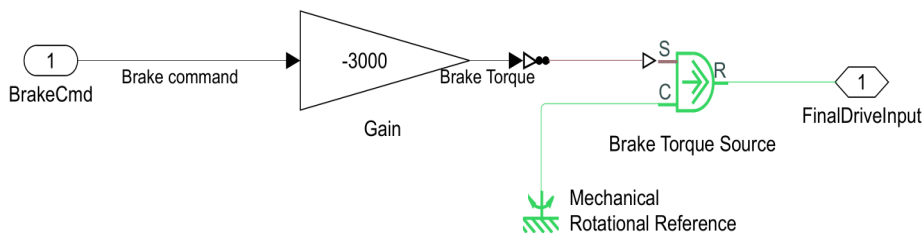


Figure 9. Brakes sub-group Simscape model

### 3.5 Wheels

The next step is the simulation of the wheels: here, the rolling radius and the tyres inertia are evaluated, considering that the van is equipped with 195/75 R16 tyres. This is physically implemented by the Tire block.

A rolling resistance model is also included. For this purpose, a constant coefficient model is employed. The resistance to the tire rolling is calculated starting from the normal force, or vertical weight force, applied at each wheel and computed in the next block.

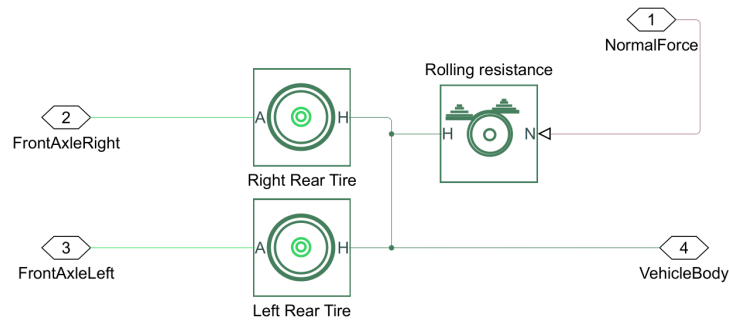


Figure 10. Wheels sub-group Simscape model

### 3.6 Vehicle Body

The last step of the mechanical circuit is the vehicle body evaluation. A dedicated block, shown in figure 11, is employed to compute the aerodynamic drag of the van, considering:

- Curb Mass, equal to 2577 kg
- Road inclination beta, null slope for the WLTP
- Wind speed W, null again
- Centre of Gravity position, relatively to axles and ground level
- Air density, assumed equal to  $1.18 \text{ kg/m}^3 @ 25 \text{ }^\circ\text{C}$
- Drag coefficient, equal to 0.316, an excellent result achieved thanks to the continuous improvement of the van design
- Frontal area, computed starting from the knowledge of the coast-down test coefficients (F0,F1,F2), considering the aerodynamic force and the rolling resistance. The only unknown is thus the area, equal to  $4.4 \text{ m}^2$

Combining everything, the vehicle speed is processed for each instant of simulation. This is the actual speed of the van that is then related to the reference speed in the controller block. The last computation is the normal force NF/NR (along the vertical axis) previously mentioned.

This is the last component of the Simscape mechanical circuit in a visual order, thanks to the H port connection. Actually, the circuit can be thought as a loop in which each quantity is circulating back and forth, thanks to the bidirectionality of the Simscape logic.

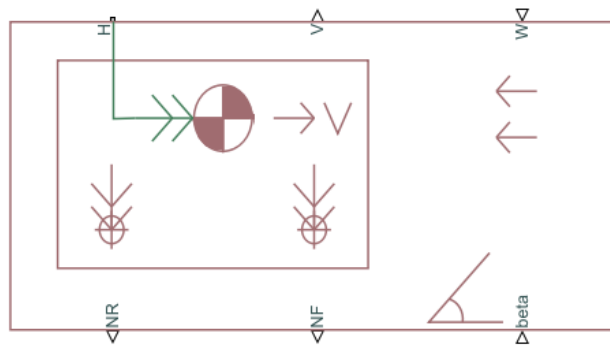


Figure 11. Vehicle Body block

### 3.7 SCR

In this prototype, the engine outlet is assumed to be coupled directly to a classic Selective Catalyst Reduction, acting as a simplified after-treatment system and able to treat the NO<sub>x</sub> emission at the engine-out. More in detail, the exhaust gases rich of NO<sub>x</sub> (due to the lean operation, typical of Diesel engines) enters into a big monolith, full of active sites.

This component has a huge volume, normally four times the engine displacement, and therefore a large area is available for the chemical reaction of the NO<sub>x</sub> with the ammonia, produced starting from the urea in water solution commercially called AdBlue®. Thanks to this passage, the NO<sub>x</sub> can be reduced with a very high efficiency, especially in case of long residence time in the monolith and high wall Temperatures.

The device can be generally decomposed in two successive areas, for the model purpose:

- A thermal model, to evaluate the evolution of fluid and catalyst (or wall) Temperature
- A chemical model, to compute the NO<sub>x</sub> conversion efficiency in function of the computed Temperature and flow rate

The overall organization is represented in figure 12:

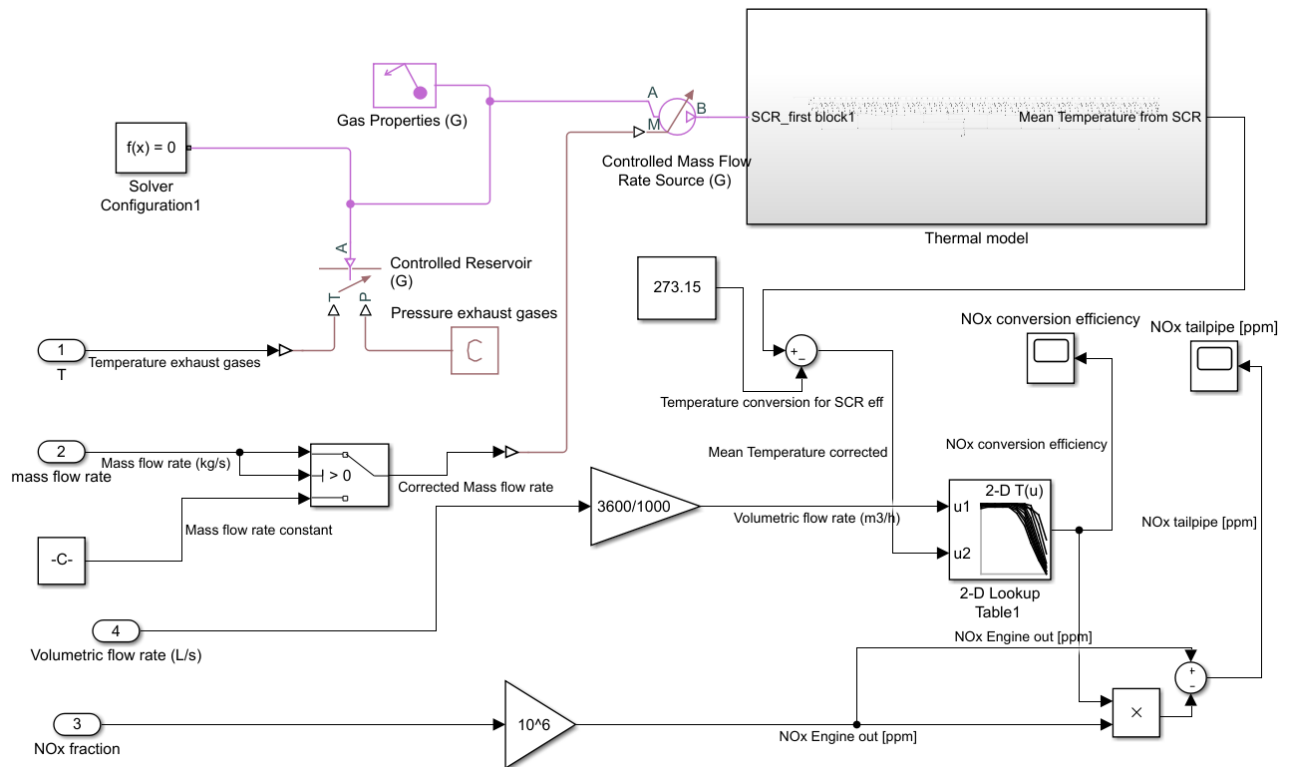


Figure 12. SCR overall model

### 3.7.1 Thermal Model

The preliminary requirement of the thermal model is the knowing of Temperature of exhaust gases (in [K]) and their mass flow rate (in [kg/s]) at the engine-out. In fact, the Simscape gas model needs a reservoir as starting block, controlled by the Temperature of the gas. This component represents a boundary condition at infinite capacity volume, able to maintain constant the properties for each instant of time. Thus, the flow is considered quasi-steady and the gas is characterized by the same pressure and temperature of the reservoir itself, at its outlet, without any interference.

The following stage is the imposition of the mass flow rate value, according to the quantity computed by GT-Power. This is done thanks to a dedicated gas library component, a Mass Flow rate Source controlled indirectly by the raw value, thanks to a physical port. The indirectivity is due to a switch controller that adds an infinitesimal small amount of mass flow rate, relevant only in the first transition seconds, to avoid a zero amount of mass flow rate that would case the simulation to collapse due to mathematical inconsistency. This block maintains a mass flow rate regardless of the pressure differential. In this case, no delta Pressure is imposed at the circuit terminals as simplifying hypothesis (some hundreds of millibar during normal operation, quite negligible). The flow resistance and the heat exchange with the environment are neglected. As done for the mechanical Simscape circuit, a Solver Configuration block is necessary to set the resolution properties of the model.

At this point, the true SCR can be implemented in a block set, to better represent the thermal behaviour, as it will be discussed in chapter 7:

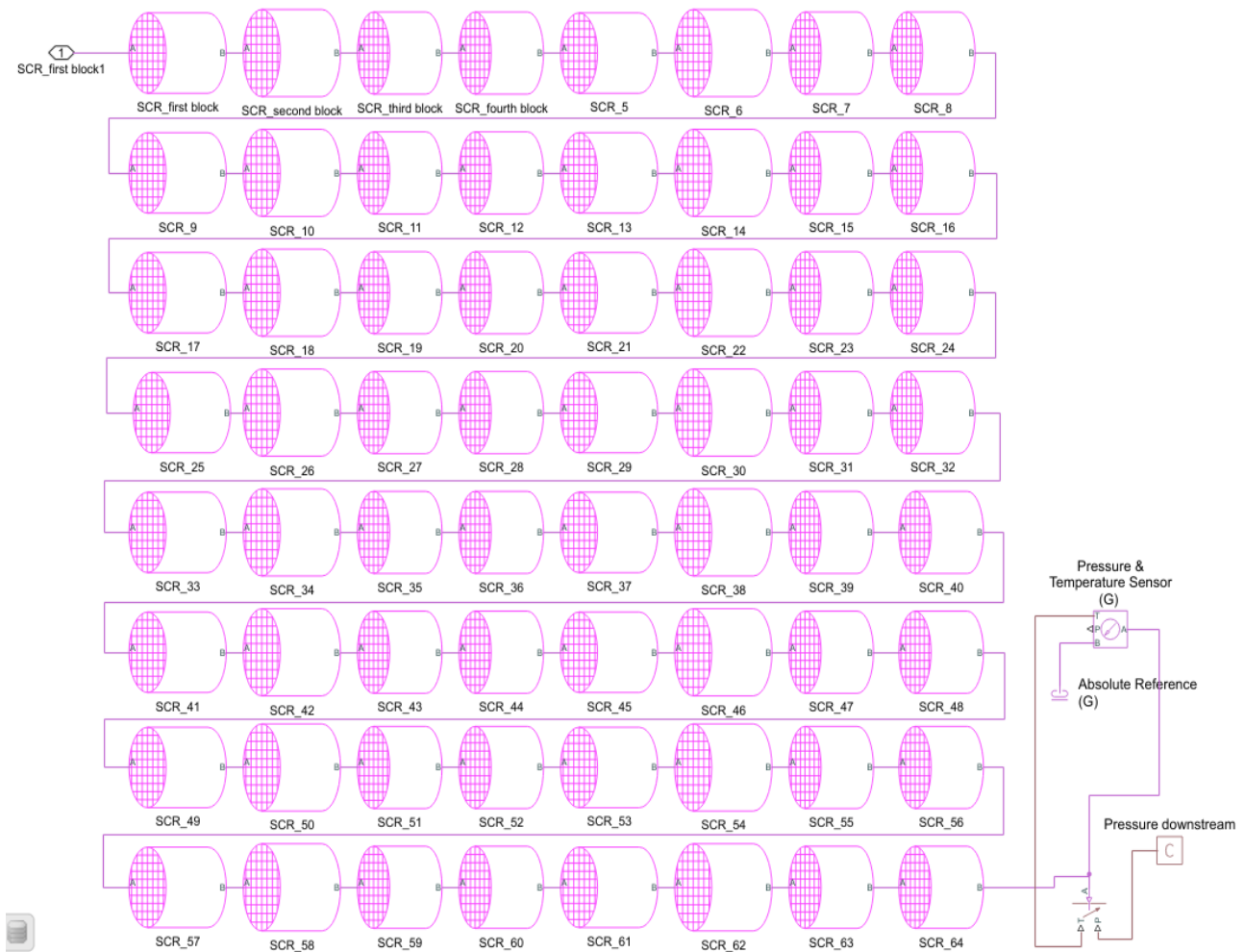


Figure 13. SCR Simscape thermal model

For the circuit continuity, the temperature of the fluid at the outlet of each block matches the inlet fluid temperature of the next one. Simultaneously, the catalyst temperature is obtained for each block and instant of time.

The last stage of this circuit is a further controller reservoir, governed by the specified Pressure downstream of the catalyst and by the fluid Temperature at the SCR outlet, to avoid any interference in the last blocks. An interesting deepening could be the supplementary examination about the heat exchange between SCR and environment, especially at its output terminal.

At the end, the mean temperature of the SCR wall can be extracted, for each time instant, ready to be used in the last step, the chemical model.

### 3.7.2 Chemical Model

Once the mean SCR Temperature is known and converted in Celsius degrees, it must be combined with the volumetric flow rate (expressed in [m<sup>3</sup>/h]) in order to obtain the conversion efficiency by linear interpolation of a 2-D look up table. Here, the higher is the Temperature, the better is the abatement of the NOx emitted by the engine.

This is true up to a certain Temperature threshold, approximately 500 °C, when the oxidation reactions of the urea, in contact with the lean gases, are favoured, causing the conversion efficiency to drop. On the other hand, a higher volumetric flow rate ensures shorter residence time of the NOx-active sites contact. Consequently, the flow rate amount is decreasing with the NOx conversion efficiency.

In general, the NOx conversion efficiency is calculated as:

$$\frac{\dot{m}_{NOx, in} - \dot{m}_{NOx, out}}{\dot{m}_{NOx, in}} \quad (1)$$

where in=engine and out=tailpipe

The same law can be applied with the volumetric version (assuming the density variation null) or even with the integral quantities (mass or volume).

Since the NOx engine out-is known and transferred by GT-Power to the model (in mass fraction terms of the total exhaust stream), the tailpipe NOx can be computed by inverting the formula. This is physically implemented by a series of Simulink elements acting as sum and multiplier, in the overall SCR model picture (figure 12).

## 4. ENGINE MOCK-UP

GT-POWER is the industry standard to simulate the engine performance in a virtual environment, discretizing the engine in each functional sub-element. This software is used by all major engine manufacturers and vehicle OEMs as it is able to calculate engine performance quantities such as power, torque, airflow, volumetric efficiency, fuel consumption, turbocharger performance...

GT-POWER engine mock-ups are straightforwardly converted into real-time models (also identified as Fast Running Models – FRMs) for Software-in-the-loop (SiL) or Hardware-in-the-loop (HiL) simulations. This program belongs to the GT-Suite software family specifically programmed for the vehicle simulation, starting from the chassis up to the entire automobile body.

In the proposed case, the FPT F1C turbocharged engine has been replicated in all the facets, from the compressor, going towards the cylinders, in yellow in the next figure, up to the turbine and EGR valve. Charge Air Cooler (CAC), EGR-cooler and intercooler can be appreciated along the boundaries of the circuit. The whole model starts from the BMEP generator, chosen according to the target transferred by the Simulink coupling. This interface is represented by the so-called Simulink Harness. Here, the inputs (from GT to Simulink), outputs (from Simulink to GT) and same simulation pace with Simulink are specified.

The outputs are the BMEP target and the engine rpm, according to which the engine functioning is governed. Once all the components of the scheme are simulated, the inputs are available too. Each component is characterized by its own quantities and many of them can be found in several blocks (for example the flow rate), therefore the proper choice of the inputs is relative to a specific component too. The selected ones are Shaft MEP, BMEP target, Average brake Torque, Exhaust gas Temperature, Mass flow rate, NOx Mass Fraction and Volumetric flow rate. These quantities have been already discussed and will be re-utilized at Simulink/Simscape level for each time step.

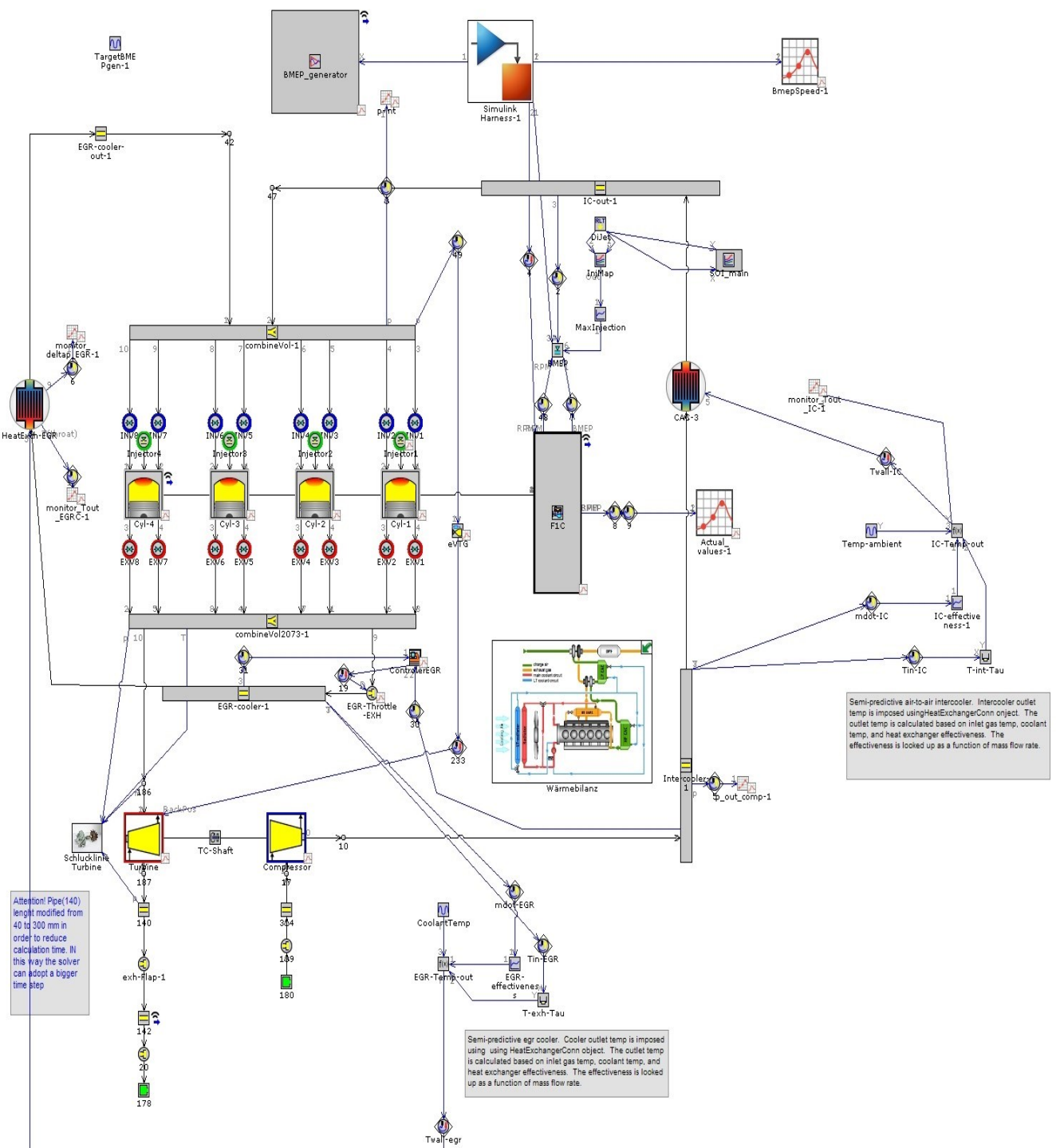


Figure 14. GT-Power Engine scheme

## 5. SIMSCAPE LANGUAGE

Simscape™ enables a quick design of physical models within the Simulink® environment. With Simscape it is possible to build physical component models based on physical connections that directly integrate with block diagrams and other modelling paradigms. These systems can be electric motors, bridge rectifiers, hydraulic actuators, refrigeration systems...

The customization of the Simscape physical components requires a thorough understanding of the Simscape language. This is a specific textual language for modelling physical systems, based on the MATLAB® programming language and contains additional constructs specific to physical modelling.

The basic component customization usually needs a couple of nodes, conserving ports of the block.

These nodes correspond to inlet and outlet points of each component and they must be assigned to an existing domain, implemented in the MATLAB® library. Some common domains are the Electrical, Mechanical, Gas,...

Through the ports, it is possible to link each component to the rest of the circuit.

A further step is the definition of all the variables associated with the current component. Simscape distinguishes between two types of variables:

- Across variables, they are defined as differential entities “across” the inlet and outlet port. Therefore, they are measured with a gauge connected in parallel to the element. In the classic example of a Ohmic Resistor component, the Across variable is the voltage difference at its terminals.
- Through variables, they are defined as flowing entities “through” the ports. Therefore, they are measured with a gauge connected in series to the element. In each branch point, the sum of all the values of a through variable entering equals the sum of all its values leaving. Referring again to the Ohmic Resistor case, the Through variable is the current.

Independently on the type, each variable is defined as “value with unit”, where value is the initial value imposed and unit is the unit of measure. Simscape allows also to impose a kind of priority to the variables’ initial values, according to the different levels under the priority field: high, low or none.

Once all the variables are defined, it is fundamental to link the Through variables to the nodes. To establish this relationship, Branches must be defined. Specifically, branches define the starting and arriving nodes of the Through variables.

Here, it is also required to link the component Through variables to the variables defined in the library domain, also called Domain Through variables. This step ensures the continuity of the circuit.

Moreover, parameters and intermediates are defined to support the equations. The parameters are fixed values and can be adjusted in the block dialog box too, when building the model. The parameters, like the variables, are defined as “value with unit” and will appear in the equations. On the other hand, the intermediates are terms that will be used in the equations but not necessarily fixed values.

## 6. THERMAL MODEL DEVELOPMENT

The SCR is a device able to treat the NO<sub>x</sub> gaseous mixture emitted by the engine, thanks to its several active sites disposed onto the monolith walls. This apparatus is characterized by a fluctuating temperature, according to the engine working conditions. For this reason, a thermal model is indispensable to evaluate its behaviour.

For the purpose, a 0D model was selected with the aim of predicting the monolith temperature (i.e., the wall temperature  $T_w$ ), given the inlet fluid temperature  $T_f^{in}$  and the mass flow rate  $\dot{m}_f$ .

To derive the thermal model of the catalyst, a simple pipe with uniform wall temperature  $T_w$  was considered, assuming that the heat conduction inside the wall is sufficient to match its temperature.

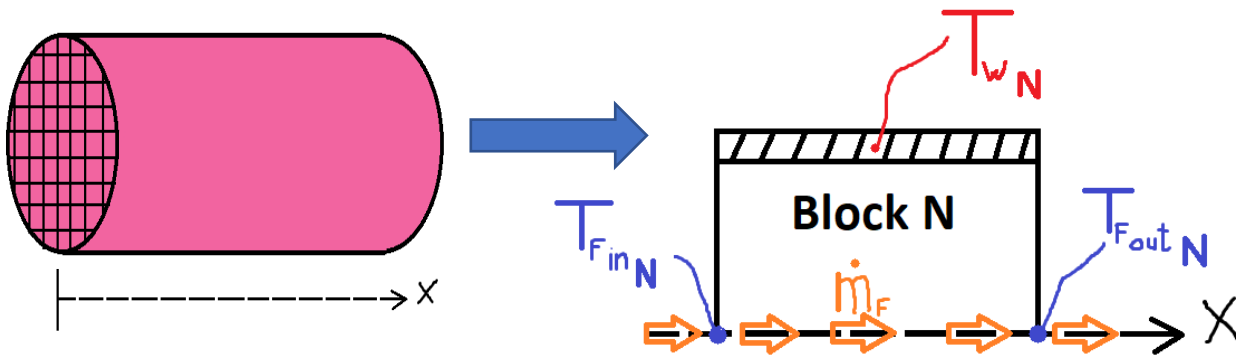


Figure 15. SCR discretization by 0D model

The starting point of the modelling of the thermal analysis is a fluid energy balance. Under the hypothesis that the catalyst wall Temperature is uniform, the convective heat exchange between fluid and walls is:

$$q_{conv}(x) = h(T_f(x) - T_w) \quad (2)$$

where  $x$  is the generic section,  $h$  the convective heat transfer coefficient [W/(m<sup>2</sup>\*K)] and  $q_{conv}$  the specific convective heat [J/kg].

At this point, the fluid energy balance is easily computed in the passages (3), (4) and (5):

$$\dot{Q}(x) = \Delta A_h q_{conv}(x) = \dot{m}_f c_{p,f} (T_f(x) - T_f(x + \Delta x)) \quad (3)$$

$$P_h \Delta x h (T_f(x) - T_w) = \dot{m}_f c_{p,f} (T_f(x) - T_f(x + \Delta x)) \quad (4)$$

$$P_h h (T_f(x) - T_w) = \dot{m}_f c_{p,f} \frac{T_f(x) - T_f(x + \Delta x)}{\Delta x} \quad (5)$$

Where  $c_{p,f}$  is the fluid heat capacity [J/(kg\*K)],  $A_h$  is the heat exchange Area [m<sup>2</sup>] and  $P_h$  is the heat exchange Perimeter [m]

Considering the limit for  $\Delta x \rightarrow 0$ :

$$P_h h(T_f(x) - T_w) = \dot{m}_f c_{p,f} \frac{dT_f}{dx} \quad (6)$$

Therefore, the derivative of the fluid temperature in the axial direction can be isolated:

$$\frac{dT_f}{dx} = \frac{hP_h}{\dot{m}_f c_{p,f}} (T_w - T_f) \quad (7)$$

To solve the first order differential equation, it is necessary to consider the exponential exact solution:

$$T_f(x) = T_w + (T_f^{in} - T_w) e^{\frac{hP_h}{\dot{m}_f c_{p,f}} x} \quad (8)$$

In the end, it is possible to assume a linearized simplified profile:

$$T_f(x) = \frac{T_f^{in} + T_w \frac{hP_h}{\dot{m}_f c_{p,f}} x}{1 + \frac{hP_h}{\dot{m}_f c_{p,f}} x} = \frac{T_f^{in} + T_w \frac{hA_h}{\dot{m}_f c_{p,f}}}{1 + \frac{hA_h}{\dot{m}_f c_{p,f}}} = T_f^{out} \quad (9)$$

On the other hand, the energy balance can also be applied on the monolith (solid phase) to compute the trend of the wall Temperature:

$$m_w c_{p,w} \frac{dT_w}{dt} = hA_h (T_f^m - T_w) \quad (10)$$

Where  $T_f^m$  is the average flow temperature [K],  $c_{p,w}$  the wall heat capacity [J/(kg\*K)],  $m_w$  the monolith mass [kg]. For the average flow temperature,  $T_f^{in}$  and  $T_f^{out}$  are considered.

The following assumptions are formulated:

- Uniform wall temperature
- Heat developed during the chemical reactions in the washcoat is negligible
- Heat transfer to the atmosphere is not evaluated

Again, the thermal variation in the axial direction is extracted:

$$\frac{dT_w}{dt} = \frac{hA_h}{m_w c_{p,w}} (T_f^m - T_w) \quad (11)$$

And assuming a linearization of the model:

$$\frac{dT_w}{dt} = \frac{hA_h}{m_w c_{p,w}} \frac{2 + \frac{hA_h}{\dot{m}_f c_{p,f}}}{2 \left(1 + \frac{hA_h}{\dot{m}_f c_{p,f}}\right)} (T_f^{in} - T_w) \quad (12)$$

Overall, the model is constituted by an ordinary differential equation (or state equation, to characterize the catalyst thermal performance) and an algebraic equation (from the linearization of the fluid thermal behaviour).

Therefore, the outcome of the computations is a 2-equations mathematical system:

$$\left\{ \begin{array}{l} \frac{dT_w}{dt} = \frac{hA_h}{m_w c_{p,w}} \frac{2 + \frac{hA_h}{\dot{m}_f c_{p,f}}}{2 \left(1 + \frac{hA_h}{\dot{m}_f c_{p,f}}\right)} (T_f^{in} - T_w) \quad (13) \\ T_f^{out} = \frac{T_f^{in} + T_w \frac{hA_h}{\dot{m}_f c_{p,f}}}{1 + \frac{hA_h}{\dot{m}_f c_{p,f}}} \quad (14) \end{array} \right.$$

Where:

- $T_w$  is the system state
- $T_f^{out}$  is the system output
- $\dot{m}_f$  and  $T_f^{in}$  are the exogenous inputs
- $h$ ,  $A_h$ ,  $c_{p,f}$ ,  $m_w$  and  $c_{p,w}$  are the model's parameters

## 7. SCR MODEL IMPLEMENTATION IN SIMSCAPE

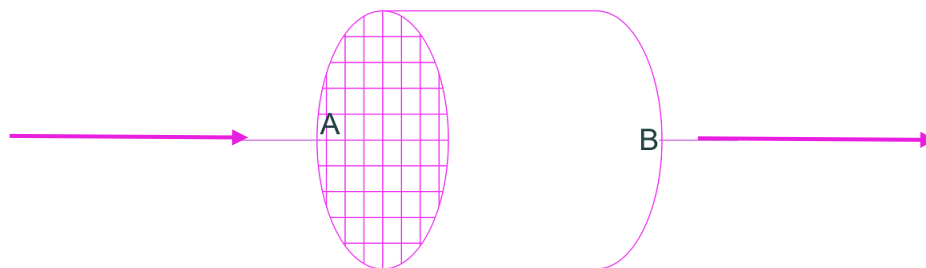
A huge advantage of the Simscape™ environment is the possibility to create own customized components. This is mandatory when the design requirements are not matching with the standard blocks and their libraries. A precondition for this step is the utilization of the appropriate domain for the component's nodes: a Simscape Foundation domain or one created for the purpose. The choice of the domain constitutes also the starting point of the model creation.

In this case, the selected domain is the Gas Domain, already implemented in the standard libraries. Therefore, the nodes A (inlet) and B (outlet) are associated to it by the expression *foundation.gas.gas*. This allows the linking of the physical entities such as Temperature, Pressure, Enthalpy... defined in the Gas library to the inlet and outlet nodes. Thanks to this step, each entity is treated as a unique signal transmitted on the entire circuit (i.e., the same signal is also employed in the standards blocks used, such as sensors and sources).

The functional core of the custom component is the implementation of the previously described 2-equations system. Combining the notions of the last chapters, the classification of the different players involved in the equations is now immediate. The fluid Temperature  $T_f$  is a variable of across type, being measured at the terminals of each block only. Concerning the mass flow rate  $\dot{m}_f$ , it consists of a through variable, being characterized by the conservation equation at each node.

By converse,  $T_w$  represents a state of the system: it expresses the temperature of the monolith at the wall level. for a particular section along the axial length: the catalyst is subdivided in several successive blocks indeed. This Temperature is initialized to the room temperature (e.g., 300K) in case of cold start or to whatever specific Temperature in case of hot running.

All these variables are treated in each elementary block, of the following type:



SCR

Figure 16. SCR elementary block

This is marked by a couple of the already described nodes or ports: A and B. The former constitutes the inlet node whereas the latter describes the outlet node. At these terminals, the equations are solved, while the model is “blind” in the middle points.

This is the reason why, for the achievement of a proper level of accuracy of the results, it is necessary to discretize the monolith in many successive blocks, each of which characterized by its own fluid temperature at inlet and outlet and monolith temperature.

For the continuity of the circuit, for a fixed instant of time, the temperature of the fluid leaving a block is the same of the fluid entering the successive block.

In each block, by knowing mass flow rate and fluid temperature at the inlet port, it is possible to compute the 2-equations model previously described. To fully evaluate the trend of the wall Temperature and of the fluid Temperature at the outlet it is also necessary the estimation of the few parameters left:

- The heat exchange Area  $A_h$  is expressed in  $[m^2]$ . This is computed by:

$$A_h = GSA * L * A_{f,empty} \quad (15)$$

$L$  is the total axial length of the SCR,  $A_{f,empty}$  its frontal cross-sectional area without the solid part of the walls and  $GSA$  is the Geometric Surface Area:

$$GSA = \frac{A_h}{A_{f,empty} * L} = \frac{4(l - t_w)}{l^2} \quad (16)$$

where  $l$  is the side of the single square and  $t_w$  the wall thickness.

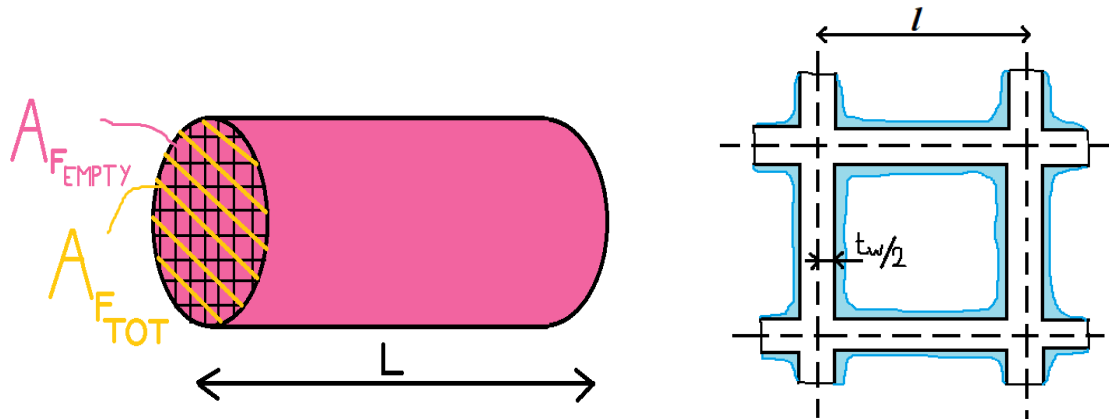


Figure 17. SCR parameters. In left figure, total and empty frontal areas and axial length. On the right, square cell length and wall thickness

For this calculation, it is possible to refer to an already known catalyst, applied to a Euro IV NEF4 118kW Diesel engine. This is characterized by a Cell Density of 400 cpsi (cells per square inch), Volume of 13 l and the axial length equal to 0.1778 m. The total and empty areas are respectively 72928  $mm^2$  and 61697  $mm^2$ , whereas the mass is 6.802 kg.

The only missing data is the GSA, but it can be immediately obtained once  $l$  and  $t_w$  are known: the cell density is also defined as  $n_c = \frac{1}{l^2}$ , consequently,  $l = 1.27 \text{ mm}$ . On the other hand, the wall thickness can be extracted by the Open Frontal Area formula (17):

$$OFA = \frac{A_{f,empty}}{A_{f,tot}} = \frac{(l - t_w)^2}{l^2} = 0.846 \quad (17)$$

Therefore,  $t_w = 0.102 \text{ mm}$ ,  $GSA = 2.897 \frac{mm^2}{mm^3}$  and  $A_h \approx 32 \text{ m}^2$

At this point, it is necessary to scale this value linearly according to the total volume of the actual SCR. In fact, the geometry of the two devices is exactly the same while the mass and volume must be scaled. In the IVECO DAILY MY 2014 case, the SCR volume can be approximated to 12 litres, according to rule of thumb:  $V_{SCR} = 4 * V_{engine}$

In the end,  $A'_h = \frac{12}{13} * A_h \approx 29.5 \text{ m}^2$

- The wall heat capacity  $c_{p,w}$  is 113 J/(mol\*K) @ T=550K, very common working point within the 300-600K range of the gamma-alumina ( $\gamma\text{-Al}_2\text{O}_3$ ) used for the catalyst. Its molar mass is 101.986 g/mol, therefore  $c_{p,w} = 1108 \text{ J}/(\text{kg} * \text{K})$
- The fluid heat capacity  $c_{p,f}$  matches 1040 J/(kg\*K), computed considering the specific heat capacity of the air (negligible difference with the exhaust gases, considering the relatively small fractions of NOX usually present) in the same working Temperature considered for the catalyst, being continuously close to the fluid Temperature.
- The convective heat transfer coefficient is again simplified as a constant value, independently of the Temperature, and equal to 50 W/(m<sup>2</sup>\*K). This is evaluated as:

$$h = Nu \frac{k_f}{R_\Omega}, \text{ where:} \quad (18)$$

- $K_f$  is the thermal conductivity, again it is possible to refer to the air properties and, considering a typical working Temperature of 450K,  $K_f$  can be approximated to 36.8 W/(m\*K)
- $R_\Omega$  is the hydraulic radius, it is computed by:

$$R_\Omega = \frac{OFA}{GSA} = \frac{1}{4} \left( \frac{1}{\sqrt{n_c}} - t_w \right) = 254,6 \mu\text{m} \quad (19)$$

- Nu is the Nusselt number, equal to 3.66 in a duct characterized by forced convection due to laminar internal flow. The laminarity is demonstrated by computing the Reynolds number:

$$\text{Re} = \frac{\rho_f u_f 2R_\Omega}{\mu_f} = \frac{\dot{m}_f}{A_{f,empty}} \frac{2R_\Omega}{\mu_f} \approx 5 \ll 2000 \quad (20)$$

Where 2000 is the approximated turbulence transition threshold in a rectangular pipe

- The monolith mass  $m_w$  is 6.28 kg, scaled linearly on the volume again.

Overall, the main data related to the selected catalyst can be summed up in Table 2:

Selected SCR features	
<b>Volume</b>	12 litres
<b>Cell density</b>	400 cells per square inch (cpsi)
<b>Mass</b>	6.28 kg
<b>Total transversal area (<math>A_{f,tot}</math>)</b>	72928 mm <sup>2</sup>
<b>Open Frontal Area (OFA)</b>	0.846
<b>Geometrical Surface Area (GSA)</b>	2.897 $\frac{mm^2}{mm^3}$
<b>Heat exchange area (<math>A_h</math>)</b>	29.5 m <sup>2</sup>
<b>Wall heat capacity (<math>c_{p,w}</math>)</b>	1108 $\frac{J}{kg \cdot K}$ @ T=550K
<b>Heat transfer coefficient (h)</b>	50 $\frac{W}{m^2 \cdot K}$
<b>Hydraulic radius (<math>R_\Omega</math>)</b>	254,6 $\mu m$

Table 2. Selected SCR catalyst – Main data

The 2-equations model is not enough to fully describe the Gas library related to the blocks. In particular, the Pressure continuity in A and B must be guaranteed through the adoption of a fictitious variable of Pressure type, aligned to the two library Pressures. At the end, this ensures a null drop of pressure across the entire SCR. This is a valid assumption, as the variation of Pressure in an actual case is typically negligible: some hundreds of millibar during normal operation, according to the exhaust gas flow amount. This is not necessary for the Temperatures as they are already included in the core equations of the model, but they must be aligned to the library ones as well.

A further step in the additional characterising equations definition is the energy balance computation across each block, derived from the first principle of thermodynamics. In this circumstance, the mechanical power is null, the exchanged heat is obtained by the convection formulation

$$\dot{Q}_{exch} = \dot{m}_A c_{p,f}(T_B - T_A) \quad (21)$$

and the energy flow rates (or powers) in port A and B are defined as through variables, computed by the model.

To effectively distinguish across and through variables in the model, these latter are associated to the library mass flow rates and powers in the nodes through the branches. Here, the through variables are marked with their initial and final point. It is common to refer to a couple of variables for each type (two mass flow rates and two powers), one associated to node A and the other one to node B.

Therefore, for the continuity equation:

$$\vec{\dot{m}}_A + \vec{\dot{m}}_B = 0 \quad (22)$$

The two are characterised by opposite sign for convention reasons. Once the mass flow direction is fixed, for example from left to right as shown in figure 18, the sign is computed according to the normal to the section surface. At the inlet, the mass flow is concordant to the normal vector  $\vec{i}$  therefore the sign is positive and vice versa at the outlet the sign is negative for the normal vector  $\vec{j}$ .



Figure 18. Signs convention

The conclusive step is the connection of the convection library for the gas to the initial and final node (A and B). In this way, the mass flow rates and thermal powers are obtained directly from the library equations, provided that the enthalpy in A is converted into enthalpy in B plus the heat exchanged along the block.

## 8. MODEL VALIDATION

Like any model worth this name, it is fundamental to undergo a confirming process about the achievement of the intended purpose. This will involve the investigation of the model predictivity by comparing model simulations to independent experimental data. For the purpose, the mechanical and thermal sections will still be separated, referring to different situations.

### 8.1 Powertrain

For the mechanical model, no big load of data are commercially available. For this reason, the proposed validation is bearing on a simplified case study. Specifically, the analysis is supported by the time required during a 0-100 km/h acceleration, in a flat road condition and with no load applied. This information is not explicitly sponsored by the brand but it can be estimated by the examination of some test drives on the YouTube platform. By looking at different video sources, the common factor is a time of about 18 seconds for the 0-100 km/h acceleration.

It is now necessary to evaluate the model computed time, imposing a full throttle condition up to the achievement of a sufficient speed. The outcome can be noticed in figure 19:

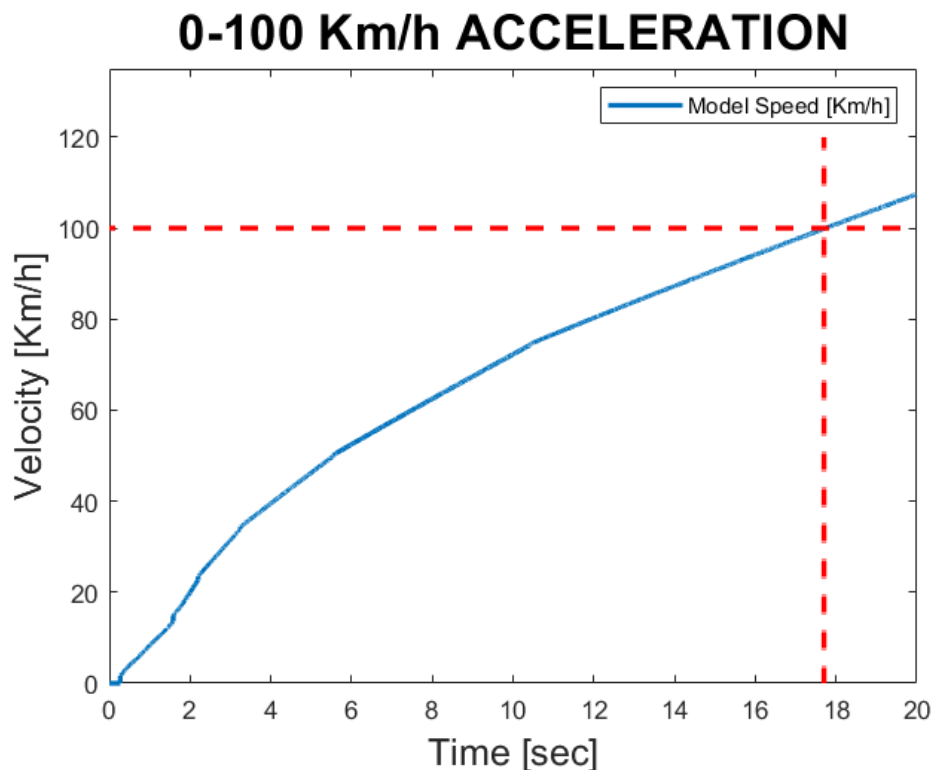


Figure 19. 0-100 km/h acceleration

With no load applied and flat road, the computed time is approximately 17.7 seconds, very well fitting the empirical 18 seconds around.

## 8.2 Selective Catalyst Reduction

Concerning the Selective Catalyst Reduction, the chemical part is a direct consequence of the thermal model. As a result, it is enough to apply the validation process to the thermal part only. For the purpose, a set of experimental data have been provided by the Fiat Powertrain Technologies industry, also known as FPT Industrial.

These data are referred to few validation cycles of the industry domain but available in terms of the needed parameters. In particular, these are the engine-out mass flow rates and the fluid Temperature upstream of the catalyst, for each instant of time. These latter are essentially the only inputs needed by the thermal model itself. Above all, the most interesting dataset is the Temperature at SCR-out.

Moreover, these data are relative to the already mentioned SCR, applied to a Euro IV NEF4 118kW Diesel engine. This catalyst is characterized by a 13litres volume and applied to a different engine to the one under investigation. Therefore, for the validation of the thermal model it is mandatory to implement it in the older configuration, under the same conditions involved for the computation of the experimental data.

Practically, this implies to adapt the total mass and total exchange surface to the 13 l case. In this case, the catalyst mass and total exchange area are known. Being the SCR geometry and material employed identical, all the other parameters can be maintained unvaried. Once the mass flow rates and inlet fluid Temperature used for the experimental campaign are imposed, it is possible to simulate the whole model and extract the computed fluid Temperature downstream of the catalyst. The imposition is feasible thanks to the “from file” command, where the data of “double” type can be directly extracted from an Excel file with two columns: Time of simulation and Data. In the end, the processed fluid Temperature downstream of the catalyst, output of the model, can be compared to the Experimental Temperature dataset, again at the outlet of the SCR.

The missing step is the selection of the number of the blocks in the set. As previously described, the many assumptions of the mathematical formulations behind the model make it necessary to implement  $n$  successive blocks for the best accuracy of the model itself. The proper number “ $n$ ” is determined according to the best trade-off between quality of the results and lightness of the computation: a higher number of sections make the model more precise but also heavier from the computational point of view. The best trade-off for this validation was found in 64 successive elements, characterized by a heat exchange area of  $0.5 \text{ m}^2$  approximately.

The same logic can be applied to the original model, simply scaling the mass and exchange area with respect to the volume of the SCR. Here, the imposition of the mass flow rate and of the engine-out Temperature is directly provided by the GT-Power simulation.

The schematic diagram can be better examined in the next page:

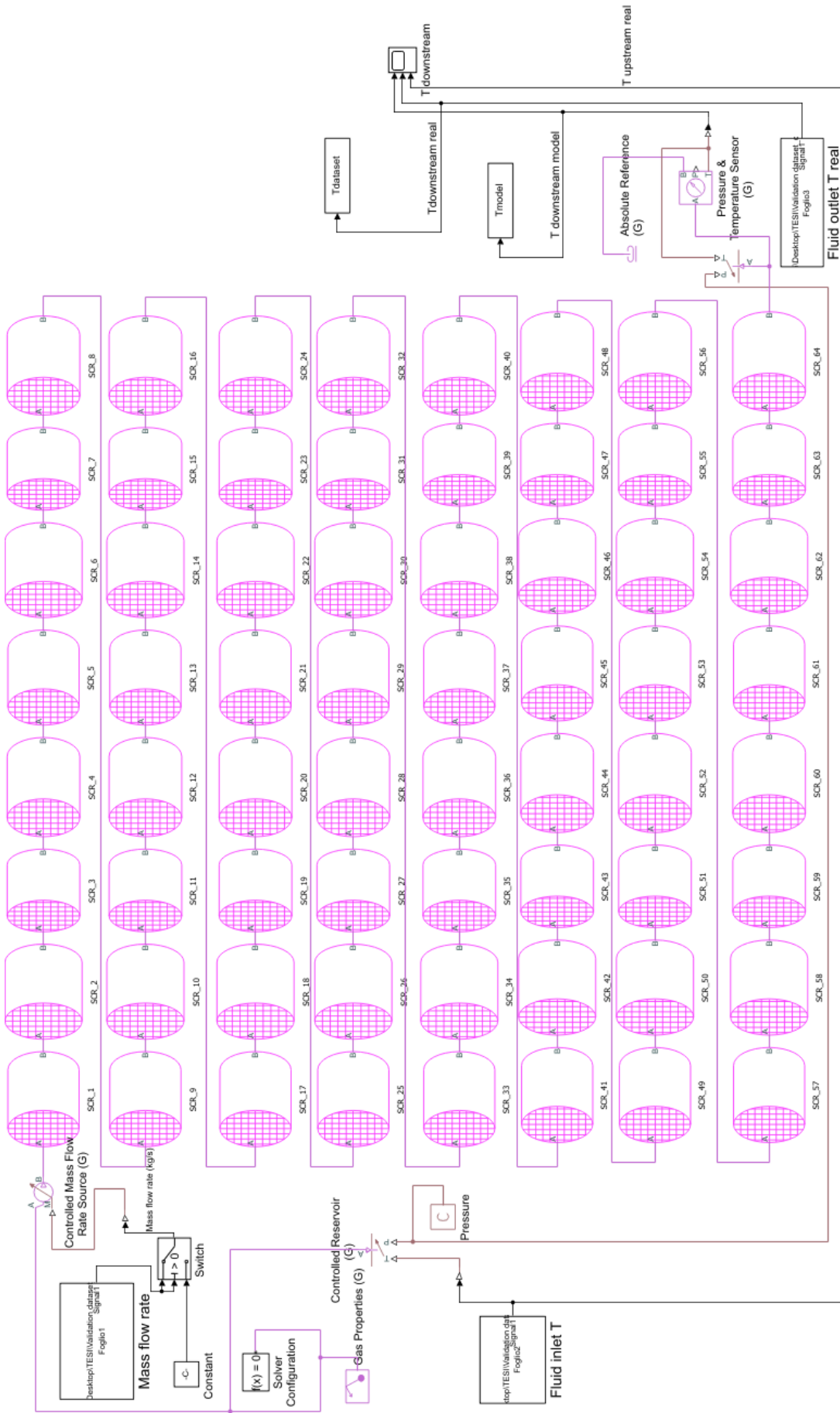


Figure 20. SCR validation model

In the following, the Temperatures evolution can be appreciated:

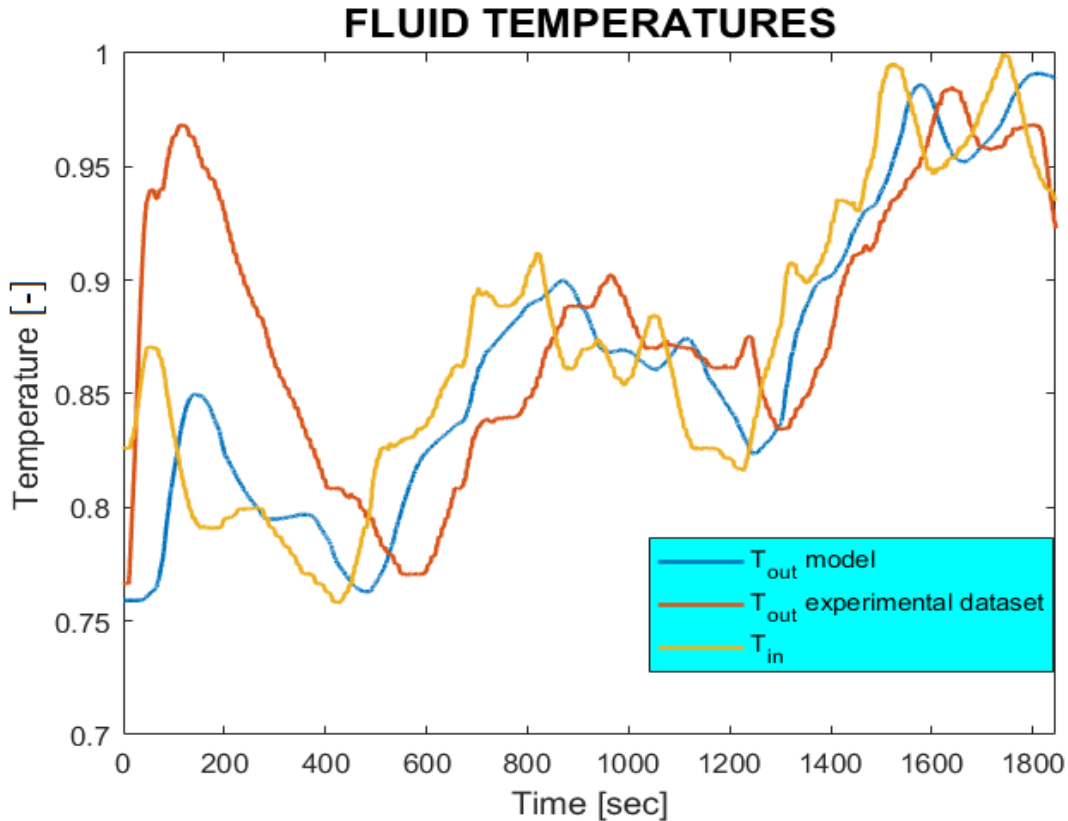


Figure 21. Model Thermal trend – Comparison with experimental data

The reference object for the “in” and “out” reference is the SCR; as a consequence,  $T_{in}$  is the Temperature upstream of the catalyst, imposed according to the experimental values, whereas  $T_{out}$  is the Temperature downstream of it, evaluated with the model calculation and with the experimental actual values. Due to the strong assumptions made, such as the negligence of the heat developed during the chemical reactions and the atmosphere heat exchange, the behaviour at the outlet could seem quite far from the real data, especially in the initial part of the test, up to 400 seconds. The big initial peak experienced at the outlet in the experimental Temperature reaches much higher values than the one of the actual inlet Temperature, suggesting that this trend could be referred to the chemical reactions. As a consequence, the model is correctly reaching Temperatures downstream of the catalyst that are lower of the upstream condition, in the first part.

Besides this initial incongruence, the model seems to be able to fit well the experimental curve, following the trend of the experimental curve in a quite faithful manner in the remaining portion of the computation.

A goodness of the model capability to match the expected results can be estimated by the NRMSE (Normalized root mean square error), in terms of percentage, to obtain a sort of accuracy :

$$\text{Accuracy [\%]} = (1 - \text{NRMSE}) * 100 = \left( 1 - \frac{\|\hat{y} - y\|}{\|\hat{y} - \text{mean}(\hat{y})\|} \right) * 100 \quad (23)$$

Neglecting the first 400 seconds for the explained reasons, the model accuracy reaches 80.3% in the 64 cell blocks case. This validation case study was conducted according to a “hot” cycle, that is a collecting procedure of the data after a specific time dedicated to the engine warm-up . The same can be repeated with a “cold” starting condition, reaching a lower accuracy of approximately 73%.

## 9. RESULTS

### 9.1 Speed

The concept starts from the analysis of the WLTC class 3, reference cycle for the speed profile to follow. The driver controller has the task to provide the proper acceleration/deceleration command to continuously adjust the actual speed, computed by the model, to the reference one. This will be achieved thanks to the engine actuation through GT-Power software and considering all the inertias and the successive mechanical stages throughout the path, up to the wheels.

Nevertheless, it is meaningful to jump directly to the most relevant output of the model, the speeds matching, which can be immediately examined in the following chart:

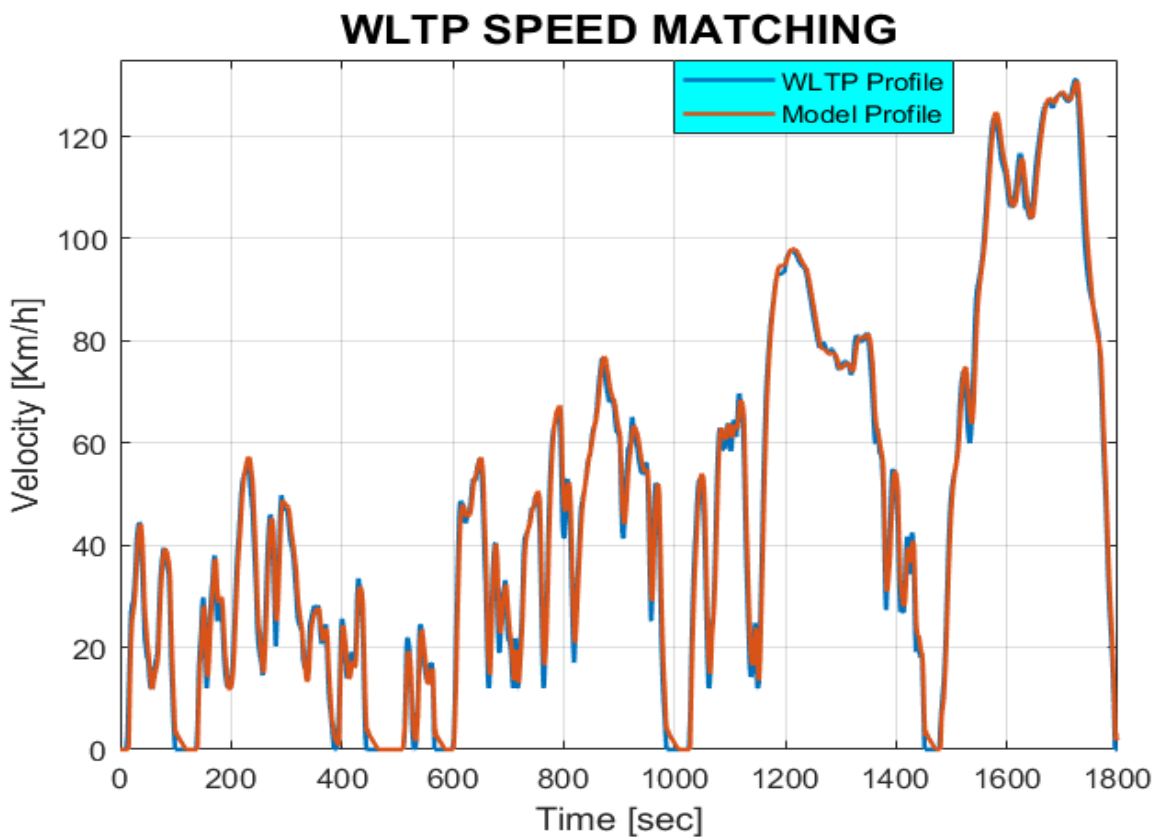


Figure 22. Speed comparison between WLTP and model output

After few seconds of idling prescribed by the cycle, almost 15 seconds, the model is immediately able to follow up the sudden rise of speed. This officially starts the Low-speed phase, ending at second 600 approximately. This section is characterized by continuous acceleration and deceleration between 0 and more than 56 km/h maximum, introducing a highly oscillatory trend. This phase is thus the most demanding for the model, risking of obtaining a not fast enough change of speed. On the contrary, the model is responding very well to this transient, even during the several decelerations.

The only critical point is the achievement of a complete stopping condition. As it can be noticed, this takes more than needed in the very last part of the deceleration, reducing the steepness of the profile.

This is due to the simplified gearshift logic introduced: in order to let the model able to operate in different working conditions and thus increase its flexibility, the neutral gear is employed only when the engine rpm is below a minimum threshold (1000 rpm during first gear) for few seconds, a range of time long enough to avoid an automatic gear disengagement during normal driving at very low speeds.

Even the other gears follow a similar approach, contributing to the stopping delay. This is therefore a limit of the model implementation and not a real criticism.

The next segment is the Middle-speed phase, characterized by a top speed of almost 80 km/h and again very dynamic in terms of accelerations but with less stopping time and as a consequence higher average speed. The same principles in the model functioning are still holding in this session, ending at second 1000 roughly.

The model behaviour is even improving in the last phases, the High and Extra High-speed segments. These latter are characterized by a full speed of almost 100 km/h and more than 130 km/h respectively. On the other hand, their speed profiles are much less oscillating, providing a more favourable situation for the model speed follow-up. Overall, the margin of error is below the 1km/h threshold for most of the time, precisely for more than 80% of the cycle.

## 9.2 Acceleration

To keep the vehicle continuously on the correct speed profile, the proper acceleration or deceleration must be continuously employed, acting on the pedals. As already mentioned, this is replicated by commands imposed by the longitudinal controller on the engine digital twin.

The trend on the whole WLTC may be analysed in figure 23:

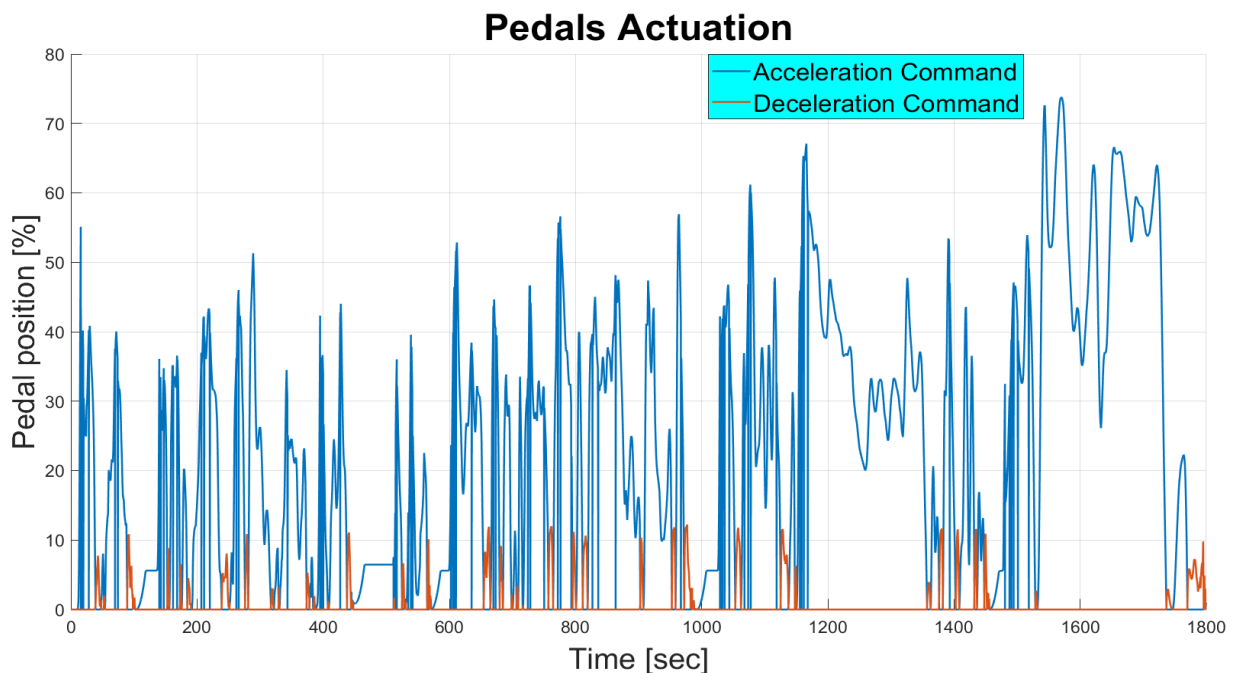


Figure 23. Accelerator vs Decelerator Command during WLTC

Being the cycle quite extended, around 30 minutes, the overall situation is highly chaotic; nevertheless, some features are already well-perceptible and can be highlighted.

First of all, the driving cycle, introduced to replace the old and unrealistic NEDC, is still not extremely demanding, as already mentioned in chapter 3.1.1, since the acceleration capability is never fully exploited. Actually, an accelerator position deeper than 70% is seldomly employed.

Moreover, the dynamicity of the cycle is evident from the endless oscillations recorded at the pedal level. This is also due to acceleration cut-off during the gear shifting, imposed by the specific controller. The correct functioning of this mechanism is evident from figure 24:

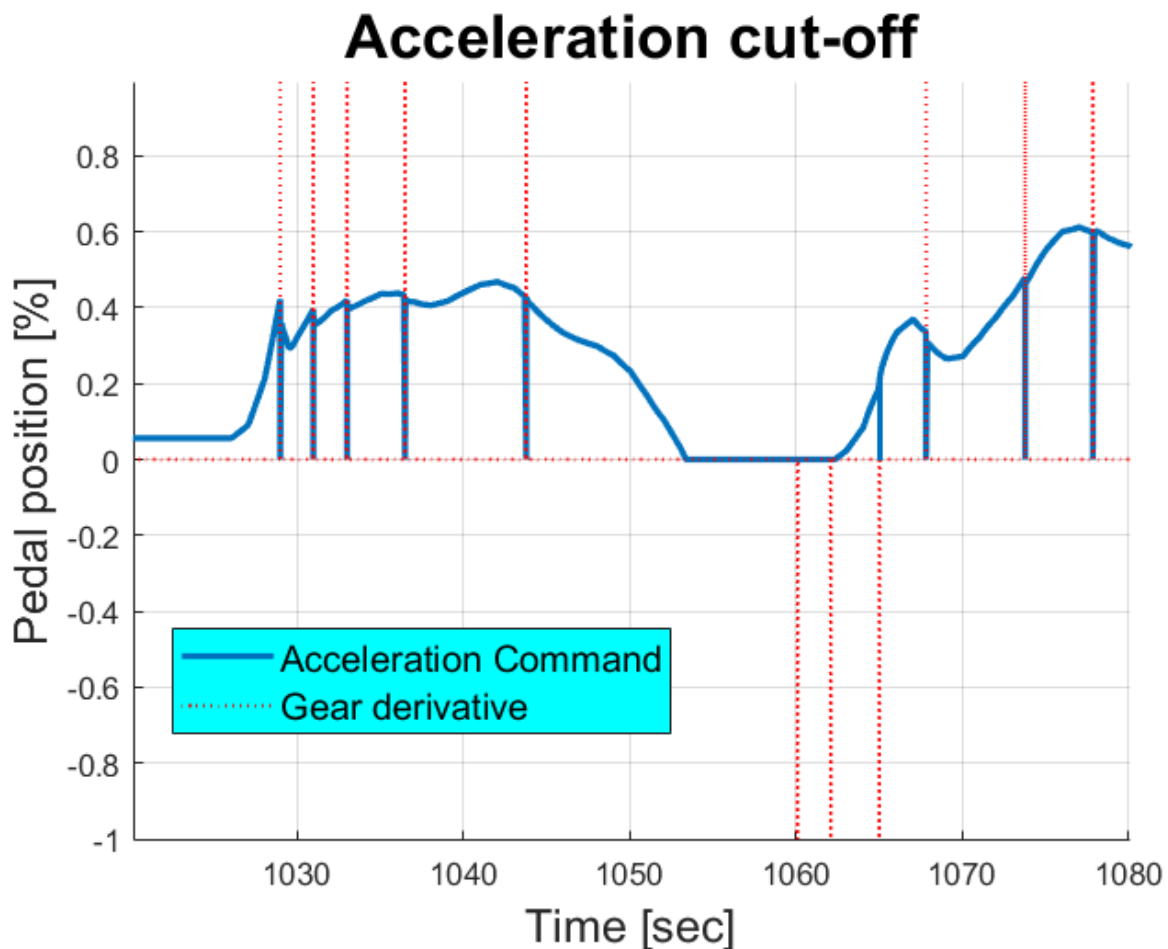


Figure 24. Imposition of Acceleration cut-off during gear shifting

Here, a short timelapse has been considered to better analyse the principle. When the gear derivative is different from zero, a gear shifting is in progress. In particular, when the gear derivative is positive, an upshift is in course and the other way around if it is negative. Being the gear engagement almost immediate, the derivative actual value is tending to infinity but this has been cut in the chart for feasibility reasons. Coming back to the plot, it is worth to notice that in both upshifts and downshifts, the accelerator is correctly forced to reduce to zero during shifts of gear, unless it is already not actuated.

Referring again to the Pedals Actuation plot, another feature which can be observed is the complementarity of the accelerator and decelerator pedal. When the accelerator pedal is pressed, the brake pedal is released and vice versa, as one could expect considering normal driving. The behaviour can be better examined by zooming in:

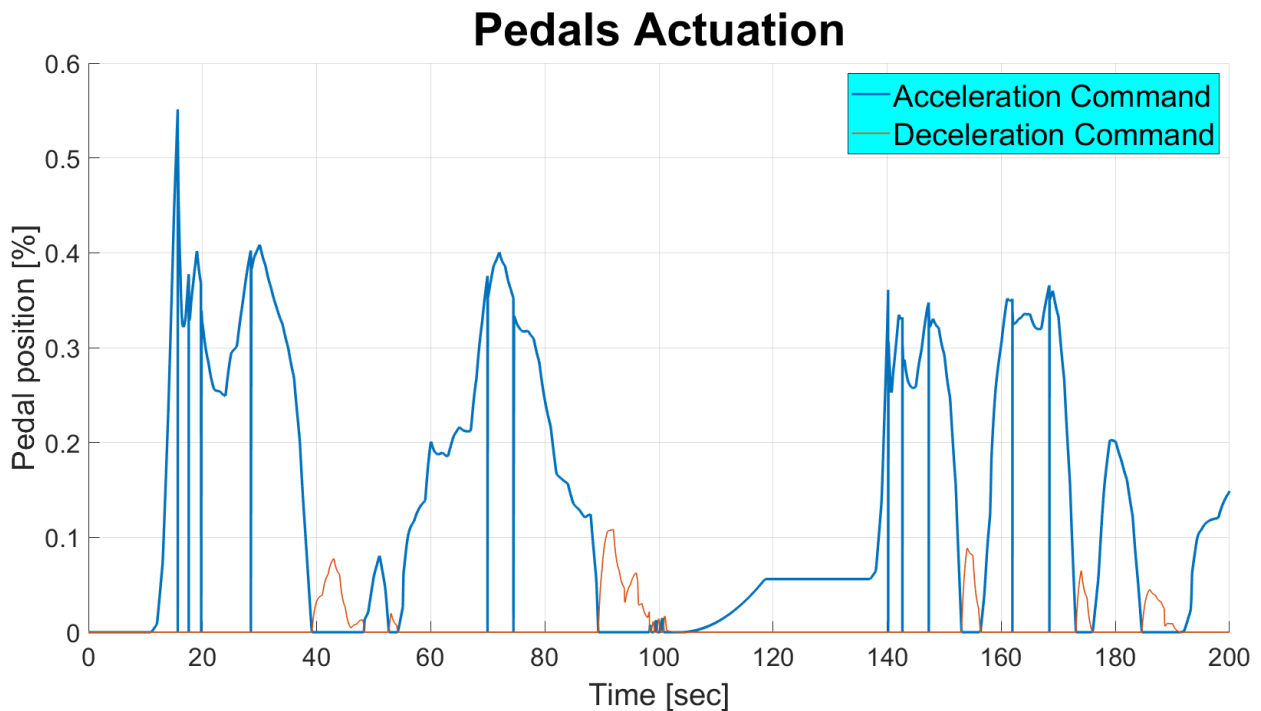


Figure 25. Accelerator vs Decelerator Command during WLTC – zoom in first 200 seconds

In this portion of the lowest speed phase, the maximum accelerator position is slightly above 50% during the first acceleration. By looking at the whole cycle Pedal chart, it is noticeable that the trend is to achieve higher top accelerator positions as the speed of the relative phase is increasing.

### 9.3 Torque

Combining the acceleration command and the instantaneous engine speed, the engine Torque is calculated according to the BMEP target coming from the look-up table representing the engine working map. The instantaneous engine speed is computed in turn according to the torque applied, therefore an initial condition setup for the GT-model is mandatory. These values will be considered for the very first step of the simulation only.

Moreover, the minimum engine rotational speed is imposed by the proper controller, replicating the real limitation, whereas the engine inertia is set by the specific Simscape block.

The Torque trend can be easily computed along the entire cycle:

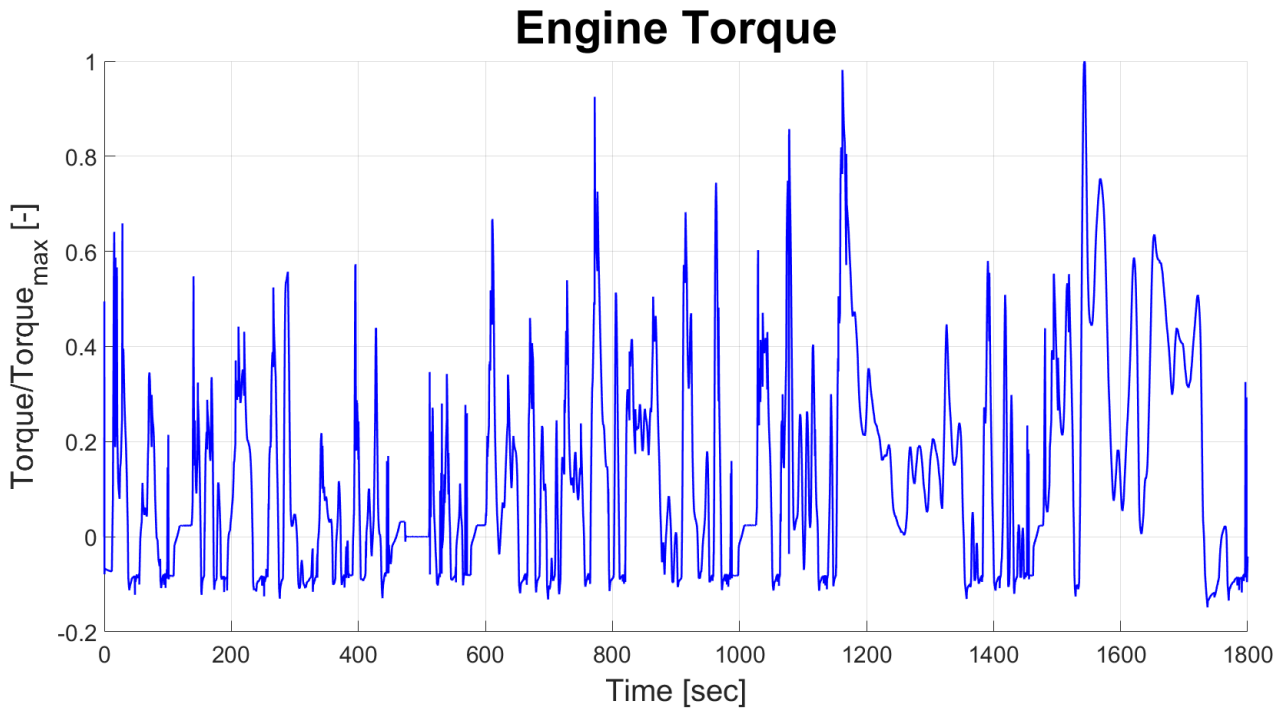


Figure 26. Engine Torque trend during the WLTC

The plot is showing a huge amount of variation of the engine Torque, normalized with respect to the max Torque developable by the engine, due to the dynamicity of the cycle. The achievement of a maximum torque is due to the steep enough acceleration segments, while the negative values are linked to the coasting phases, where the engine is let decelerating spontaneously, acting as a brake for the vehicle motion, or directly during the braking phases, when the deceleration command is triggering the brakes. Nevertheless, the analysis of the plot is limited by the huge disorder in the dynamicity of the Torque variation. Therefore, it is common practise to refer to the classic Engine Map, showing the normalized BMEP working points, function of the engine rotational speed:

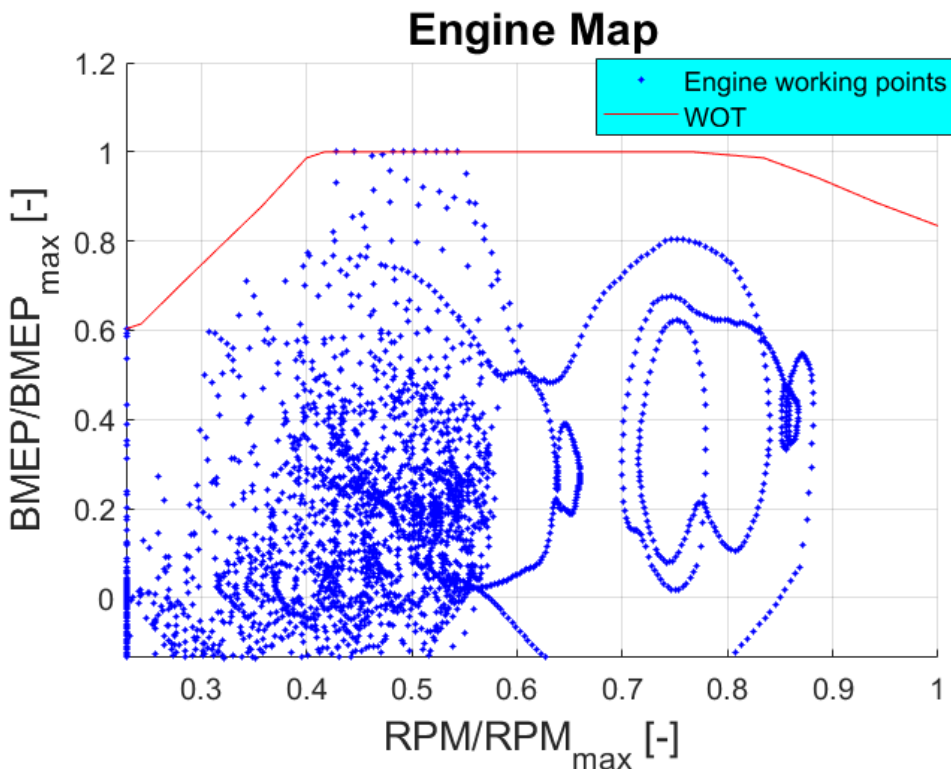


Figure 27. Engine map

In figure 27, the characterization of the working points achieved by the F1C engine is represented. As already mentioned in chapter 3.1.1, the introduction of the WLTP aimed at providing a more realistic picture of the utilisation of an engine during the typical driving. Nevertheless, still big efforts can be done in this direction. This is confirmed by the computation of the F1C working points. The engine rotational speed is typically in the range between 30 and 60 % of the maximum rotational speed, whereas it overcomes the 80% in the wide acceleration segments only.

This is certainly affected by the simplified gearshift logic applied that plans to shift the gears at fixed rpm, in order to reduce the power and time computation, while the WLTC is characterized by a more flexible gear shift scheme.

Concerning the BMEP, the condition is not highly influenced by the previous factors instead. The Wide Open Throttle curve (WOT), representing the maximum BMEP capability of the engine, is reached for very limited portions of the cycle, confirming the limits of this cycle. The most common working condition is constituted by a BMEP below 60% bars indeed. In the end, a classic working point, i.e., the area where the points are more crowded, could be defined by the 30% BMEP x 50% rpm.

Since the fuel consumption breakpoints are known too, the fuel consumption colour map can be obtained. In this plot, the fuel consumption is expressed in [g/s], prior to the normalization. Nevertheless, a high fuel consumption of this type could be even convenient in terms of travelled distance, for example, as at higher rpms the speed increases with the fuel consumption. To better evaluate this topic, it is common to refer to the Brake Specific Fuel Consumption, also known as BSFC, related to a fuel consumption expressed in [g/kWh], computed by normalizing the previous fuel consumption with respect to the power. Thus, a similar map can be drawn:

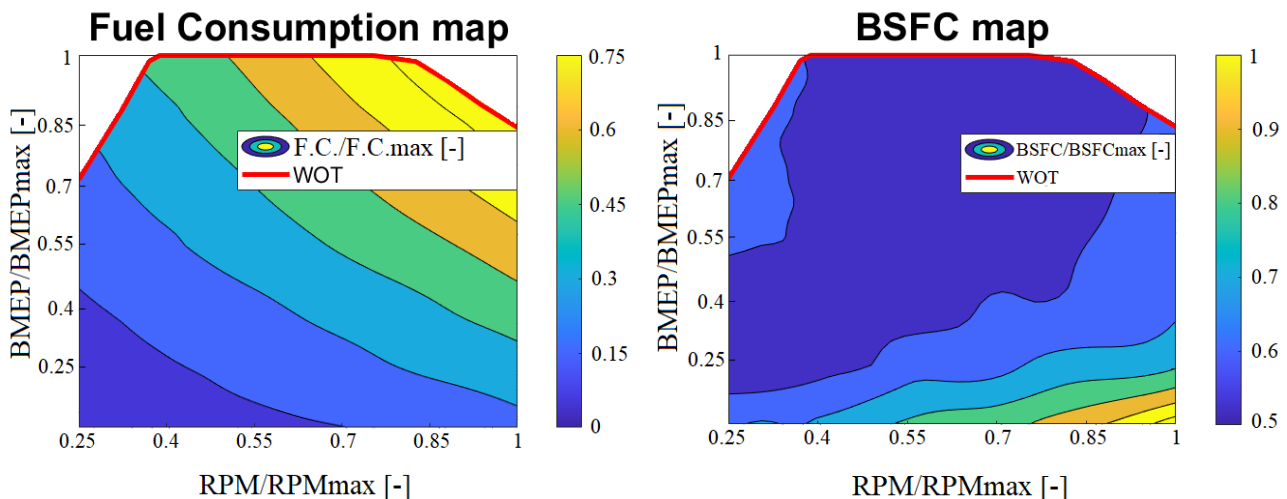


Figure 28. Fuel consumption and BSFC maps

By looking at the fuel consumption map, the fuel consumption is describing the amount of fuel injected in the cylinders in the time, not taking into account of the vehicle condition in any manner. As expected, to achieve higher BMEPs and/or speeds it is required to increase the amount of fuel to burn, in order to obtain a higher chemical power, converted then into mechanical power.

By converse, the BSFC map, more realistic picture, is showing a most efficient area of utilization of the engine (in dark blue), close to the WOT curve and around middle engine speeds. At this point, considering the typical WLTC engine working points previously analysed, it is now evident why the WLTC results are far from the real driving, especially in terms of emissions: during the cycle, the working points typically grasped are close to the best efficiency area, where the minimum BSFC and CO<sub>2</sub> emissions are achieved. This proves that the same principles applicable for the classic passenger vehicles are also valid for the IVECO DAILY van, equipped with the F1C engine.

## 9.4 Gears

After the engine classification, the next mechanical step is the gearbox replication. Here, according to the vehicle speed requirements, the engine rotational velocity is continuously adjusted. The gearbox input shaft is typically directly connected to the engine shaft, thus rotating at the same frequency. As a consequence, it will be common to refer to these two indistinctly.

In particular, the gearshiftings are realised evaluating the gearbox input shaft rotational speed, according to a temporal reference. This reference is represented by a fraction of second for upshifts, when the engine rotational speed is above the already discussed thresholds, whereas it is more significant during downshifts, to avoid unwanted disengagements at low rpms.

According to this principle, the correct gear is continuously selected, according to the vehicle conditions. The overall recording can be pointed out in the next chart:

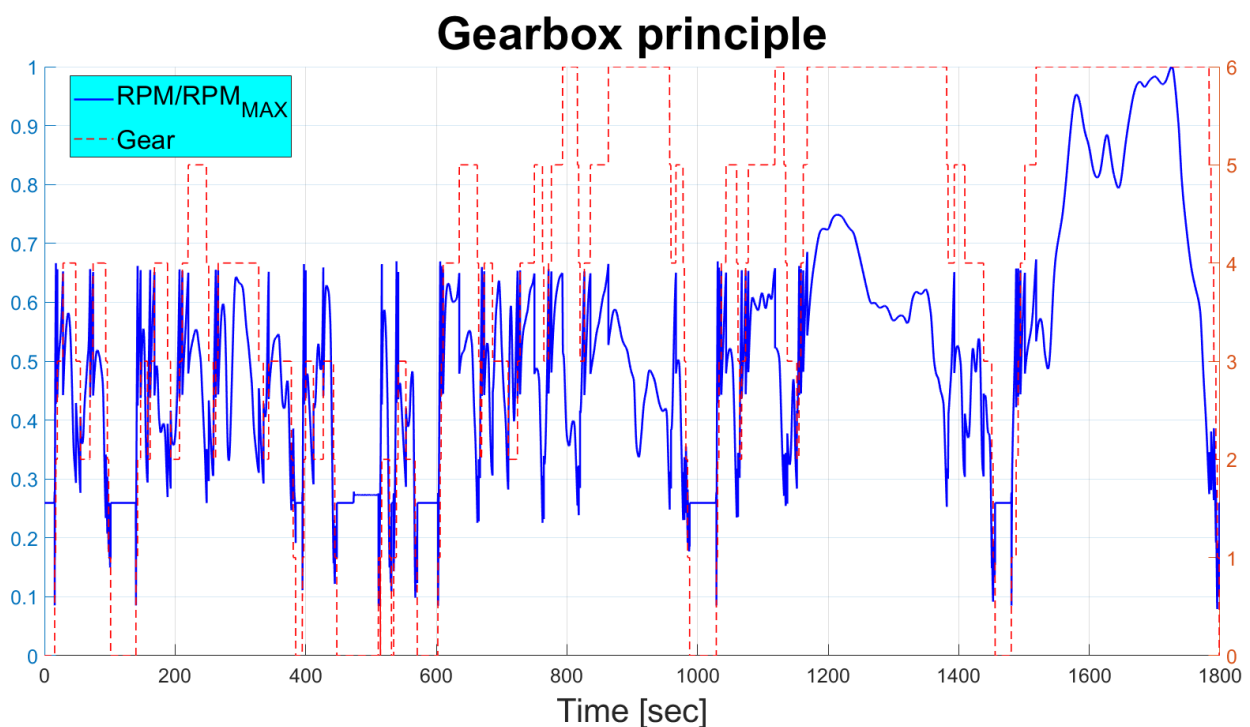


Figure 29. Gear selection and related engine rpm

The dynamicity of the cycle is highlighted once again, in terms of spread and variation of the normalized engine rotational speed. Due to the imposed thresholds for gearshifting, the engine rotational speed can reach the maximum values in the last gear only. This is achieved in the very fast sections, that are the High and Extra-High speed phases. The situation can be better examined by considering a detailed view of the first 100 seconds:

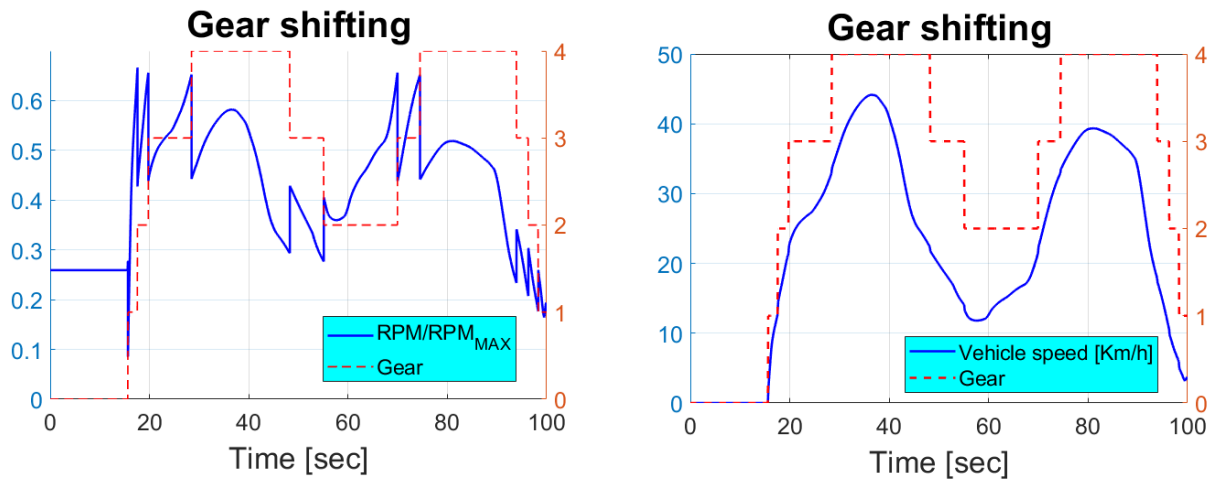


Figure 30. Gear selection detailed charts. On the left chart, selected gear and related engine rpm for first 200 seconds. On the right chart, the vehicle speed, expressed in [km/h] is considered too, for the same timelapse.

The cycle starts from a neutral condition in the first seconds, where no gear is engaged as the vehicle is still. Slightly after 15 seconds from the start of the test, the vehicle starts to move, requiring the engagement of the first gear. This requires the application of a strong enough pressure on the first clutch of the Simscape model, reminding that each gear has a separate path.

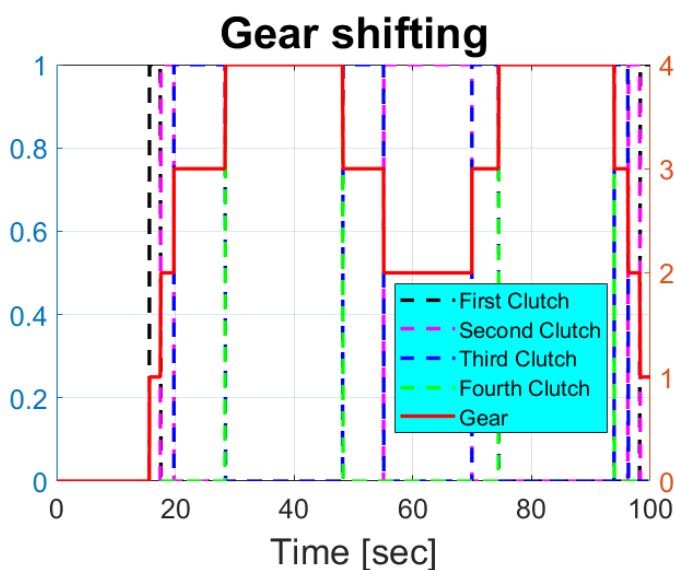


Figure 31. Clutch Pressure application for gear shifting

The behaviour can be highlighted on the left chart. Here, the normalized pressure applied on each clutch is shown on the left y axis, whereas the engaged gear is indicated on the right one. When the first gear must be engaged, the black dotted curve immediately steps up to 1, constituting the maximum pressure applied, limiting the clutch slipping to a short fraction of time. The same applies for the other gears and clutches.

This can also be pointed out in figure 30, where the first gear engagement causes a fast drop in the engine speed below the minimum rotational speed.

This is due to the fast connection of the engine inertia, characterized by the minimum rotational speed, to the still vehicle inertia, much higher. The final synchronization speed, minimum value of the engine rpm drop after the synchronization phase, is closer to 0 rather than the starting neutral condition of the engine, according to the transmission ratio and to the critical synchronization of the inertia of the mechanical chain downstream of the engine .

This phenomenon is managed by acting softly on the clutch pedal in the real world, smoothening the clutch transition. However, the speed drop is almost immediate in the model, confirming the extremely limited clutch slipping. After that, the engine speed rises again, indicating that the clutch has achieved the stick state in a fraction of time, to follow up the reference speed that is not null anymore.

When the engine speed largely overcomes the 60% of the max speed, the upshift into 2<sup>nd</sup> gear is performed. As a consequence, the first clutch is disengaged and the second one is actuated. Here and for the other upshifts, the same principle of the first gear engagement still holds, with the difference that now both vehicle and engine are running, therefore the final synchronization speed is not below the minimum engine regime. As expected, the effect is reversed during downshifts, performed for the first time after 40 seconds due to the first deceleration, since the engine shaft is accelerated by the higher reduction ratios. Successively, in the vehicle speed chart, a similar second sequence is initiated and the whole procedure is repeated. By proceeding in this way, the entire cycle is then computed.

The transmission dedicated mask has the task to duplicate the gearbox functioning, converting the gearbox input rotational speed, or engine rotational speed when the clutch is acting, into gearbox output rotational speed, through a couple of shafts. This represents a simple gear-pinion coupling per each transmission ratio, in order to continuously adjust the engine working conditions to the requirements at the vehicle level. The general principle can be therefore replicated during the entire cycle:

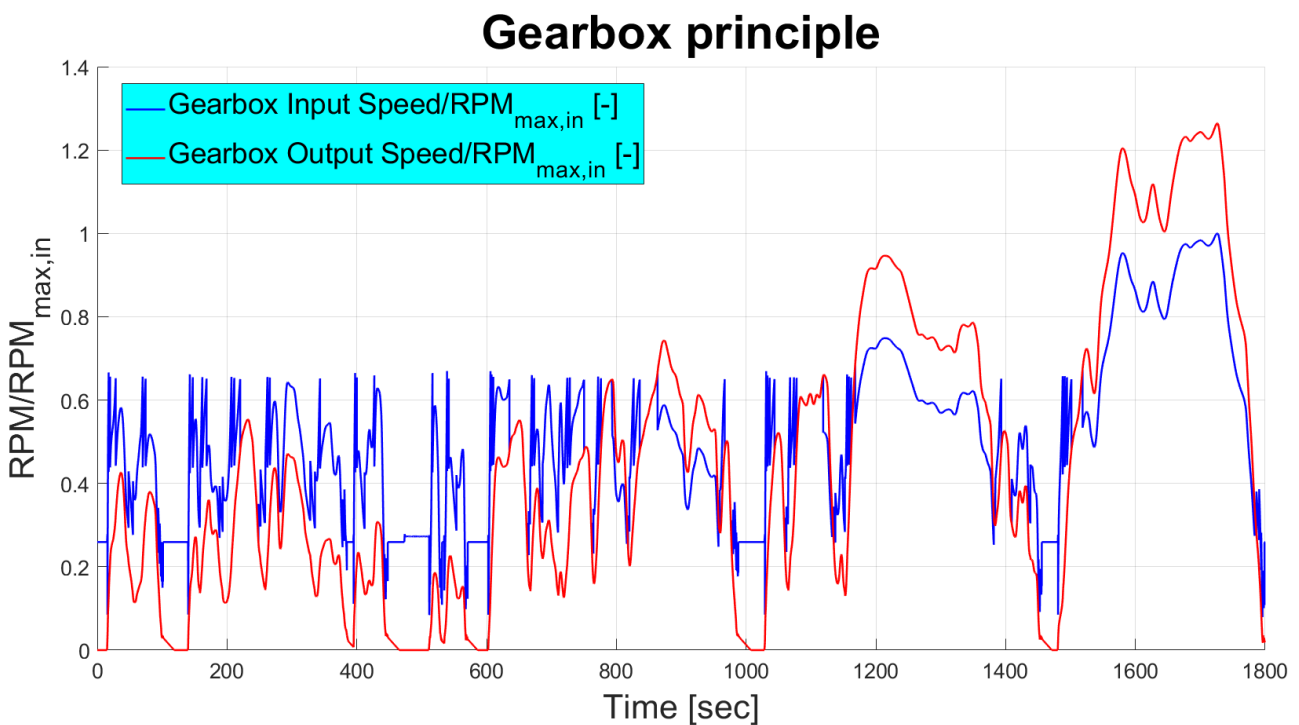


Figure 32. Gearbox principle – Speed conversion

The two speeds, normalised by the maximum value of the input one, are simply correlated by the transmission ratio realised thanks to the teeth coupling. In the Low speed phases, the selected gears are typically low and thus characterized by a reduction ratio (transmission ratio lower than 1), causing a normalized output shaft revolution speed lower than the input. By converse, the last gears are characterized by a transmission ratio higher than 1, as it is possible to notice in the Extra-High Speed section: here, the Gearbox Output Shaft is faster than the Input by more than 20% when the last gear is engaged, as the gearbox is acting as speed multiplier.

Consequently, the Speeds are always linked by the gear ratios. An exception is represented by the few cases in which the normalized Gearbox Output Speed is approaching a still condition. This can be better analysed in a more concentrated view, for example in the first 200 seconds:

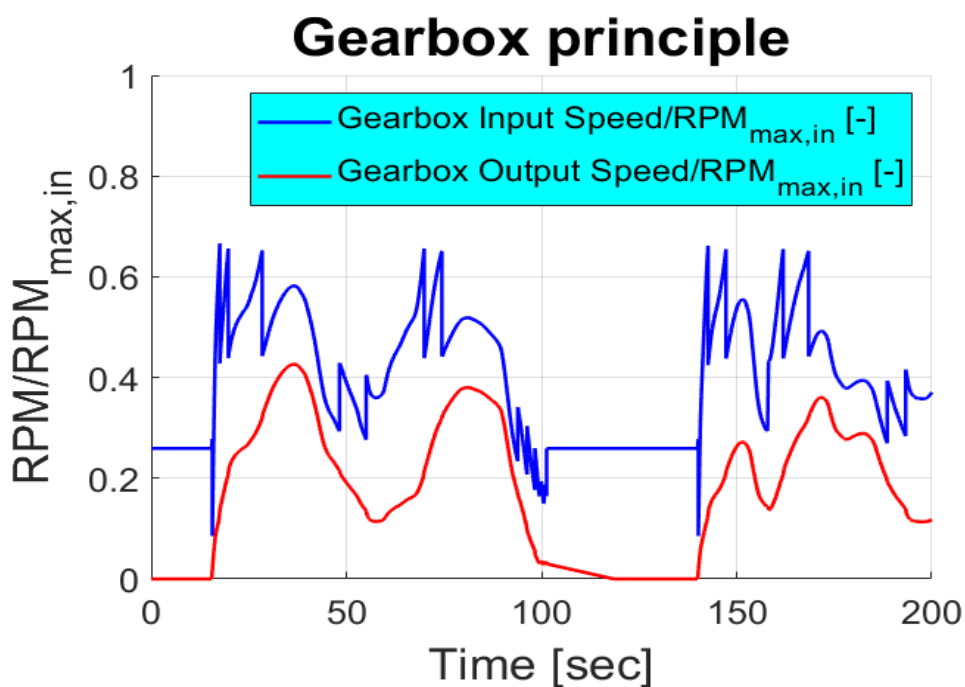
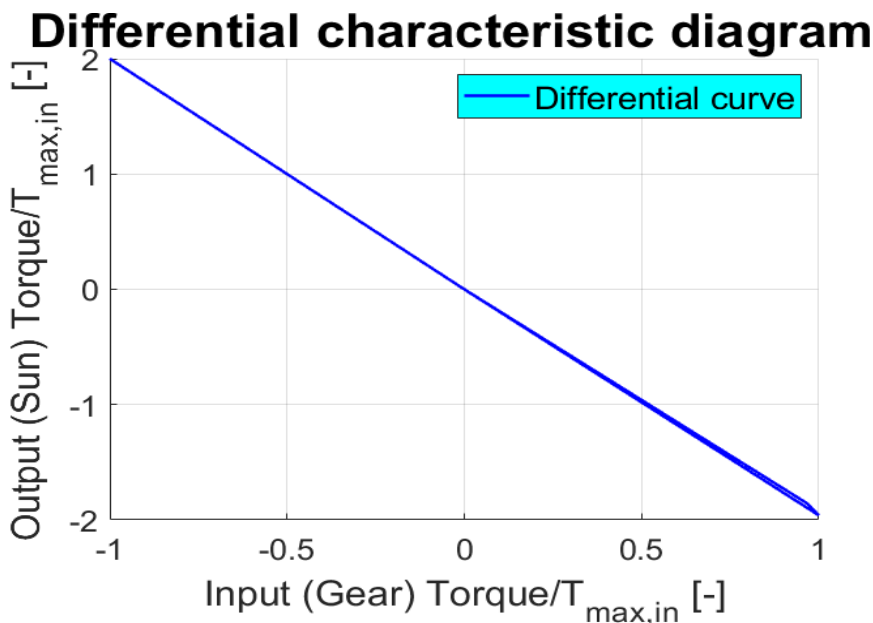


Figure 33. Gearbox principle – Detailed view of first 200 seconds

Reminding the engine functioning, when the neutral mode is on, the minimum regime is ongoing while the vehicle is still. For this reason, in this condition only, the input and output speed are not linked by a constant ratio. This is visible in the plot thanks to the horizontal blue lines, indicating a minimum rotation imposition to the engine. At the same time, the normalized Gearbox Output Speed is approaching the null value, since it is linked to the wheel rotation.

## 9.5 Final Drive

Concerning the differential, this is modelled as a real open differential, characterized by a mechanical efficiency very close to 1. Considering that the WLTC is conducted on the test bench, in straight wheels condition, the differential can be thought as an ideal differential, neglecting the quite insignificant Torque difference at its terminals. Thus, it is characterized by a Torque Bias Ratio (TBR) approximately equal to 1, meaning that the left sun gear and the right sun gear are constantly at the same torque, both in sign and magnitude, consequently transferring the same torque at the wheels. For this reason, the differential analysis can be reduced to base gear and one of the sun mechanisms, for example the left sun gear:



The output versus input Torque trend is an almost perfect linear correlation for this differential, with the output Torque increasing faster of the provided Torque. The Torque achieved at the sun is approximately double than the one at the input gear indeed, for each value of Torque at the gear level. This is due to the carrier-to-driveshaft teeth ratio and to the real efficiency.

Figure 34. Differential characteristic diagram

The differential perfectness hypothesis cause an exact over imposition on the same curve, computed for the right sun gear, since the two sides are transferring the same Torque to the wheel axle.

This mechanical stage is characterized by the final drive, usually included in the differential case. Thus, a further reduction ratio of the speeds downstream and upstream of it can be analysed. The input is mechanically connected to the Gearbox output through a dedicated shaft, while the Differential output is constituted by the half shafts, that are the wheel axle itself. Therefore, the speed conversion is characterized by a constant ratio:

## Differential principle

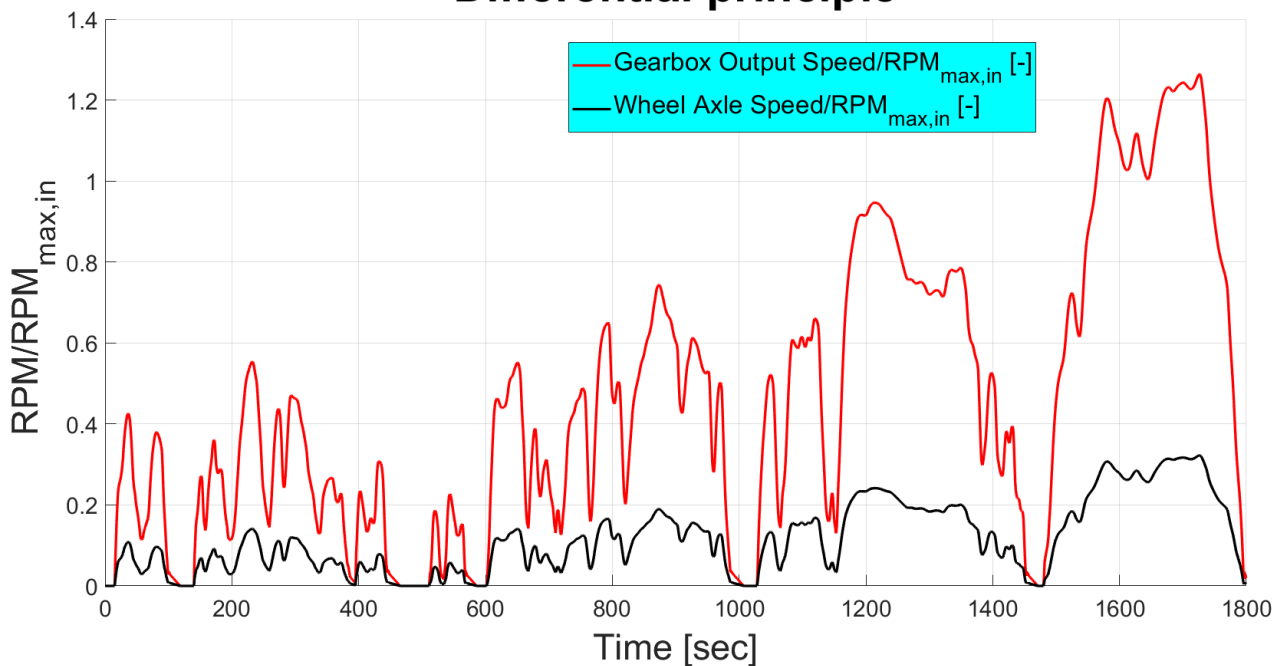


Figure 35. Differential principle – Speed conversion

To maintain the integrity of the results, the speeds are again normalized with respect to the maximum engine rotational speed.

Here, unlike the Gearbox, just one transmission ratio is applied throughout the entire cycle. Moreover, there is no possibility to disconnect it from the mechanical chain through a clutch.

As a consequence, the plot is displaying a constant relationship between the rotational speed curves at the inlet and outlet of the Differential mechanism.

## 9.6 Braking

The braking action is implemented in two passages. The first consists of converting the deceleration command (0/1) into a numerical value of Braking Torque. The latter is then passed to the Simscape circuit as physical signal to control effectively the Brake Torque Source as second step.

The first stage is merely mathematical, consisting of a simple conversion through a Gain element. The outcome is shown in the next chart:

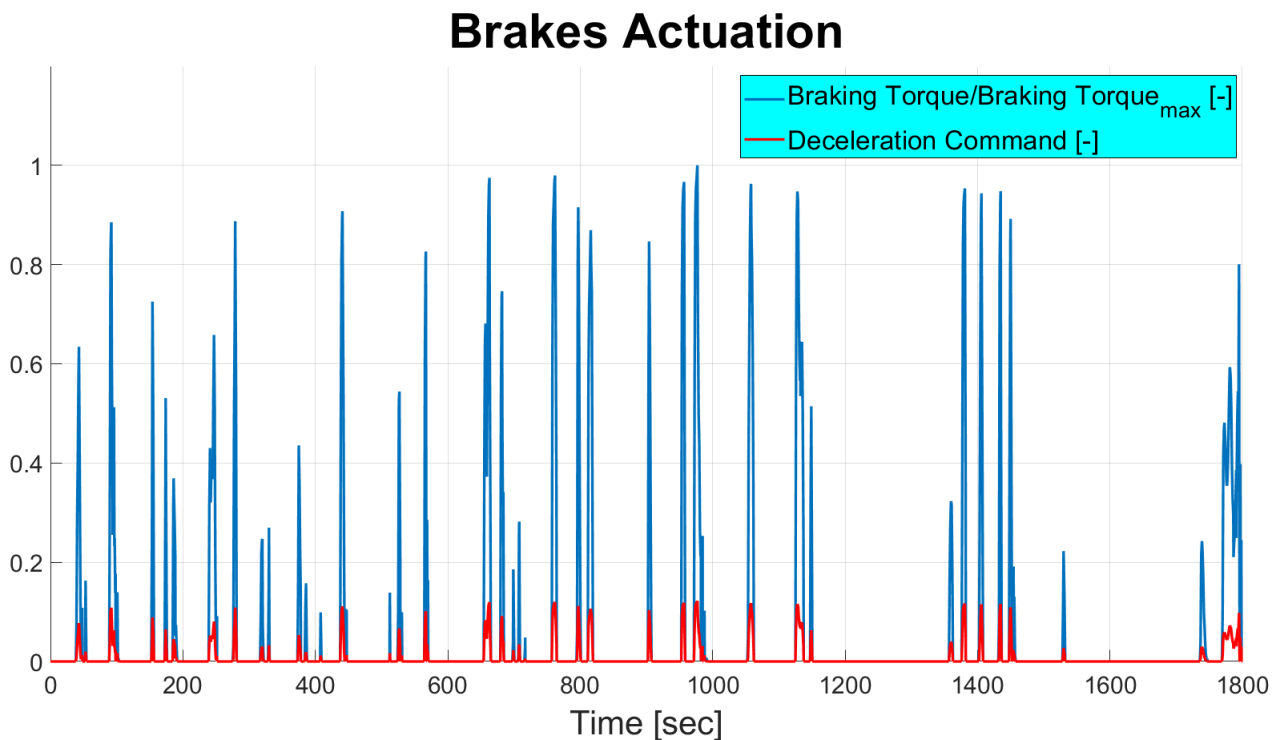


Figure 36. Brakes Actuation – From Deceleration Command to Braking Torque

Along the entire cycle, the braking command never exceeds the 20% of the maximum capability. This is due to the cycle construction itself, known for its soft accelerations and decelerations. In particular, the deceleration command is triggered few times and with a very similar extent. The maximum values achieved during each deceleration are quite similar indeed. This command is then converted into a Braking Torque, proportional to the deceleration command. Therefore, despite the spread of the velocities achieved during the test, the Braking Torques achieved during the brake actuations are very similar to each other.

To better verify the correct implementation in the physical circuit, it is good sense to consider the brakes actuation in combination with the Brake Torque effect on the Vehicle actual speed, compared to the WLTC speed profile. The situation on the entire cycle may be examined in the next diagram:

## Brakes Actuation

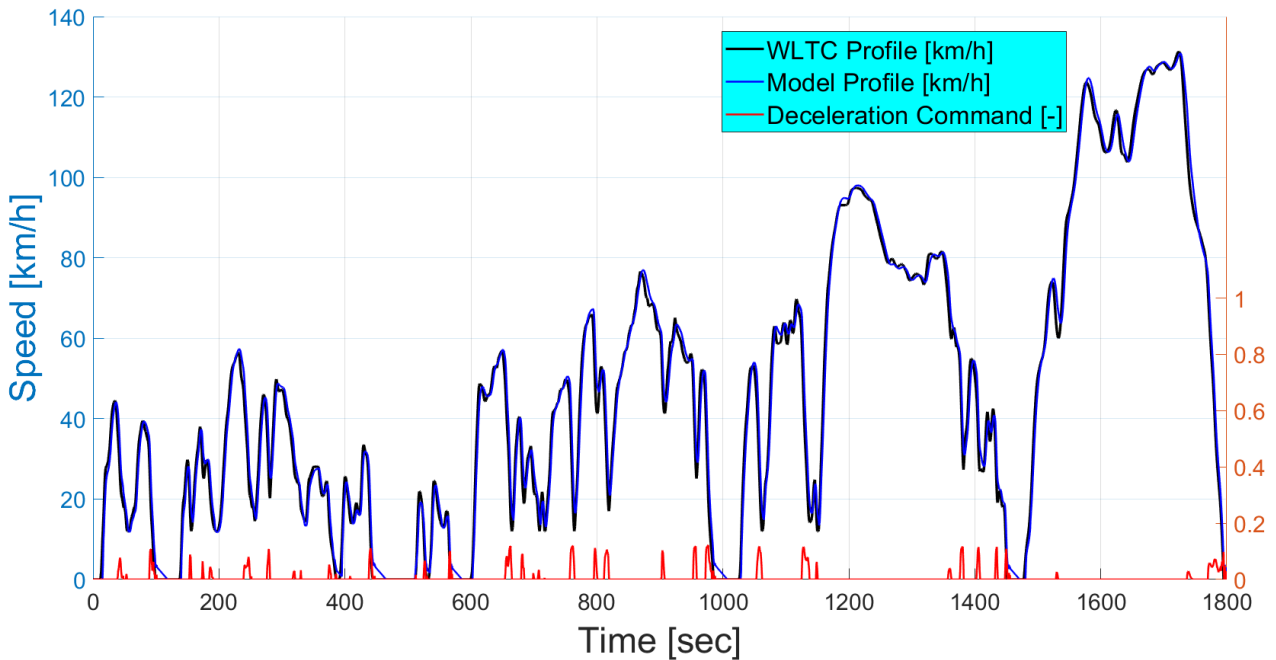


Figure 37. Brakes Actuation – Deceleration Command imposition on the Speed Profiles

It is already evident that the Brakes Actuation is always present in concomitance with the slowing down segments of the cycle, as expected. Nevertheless, not the entire deceleration phases are characterized by an imposed braking. The trend can be more thoroughly explored in the following zoom in of the chart:

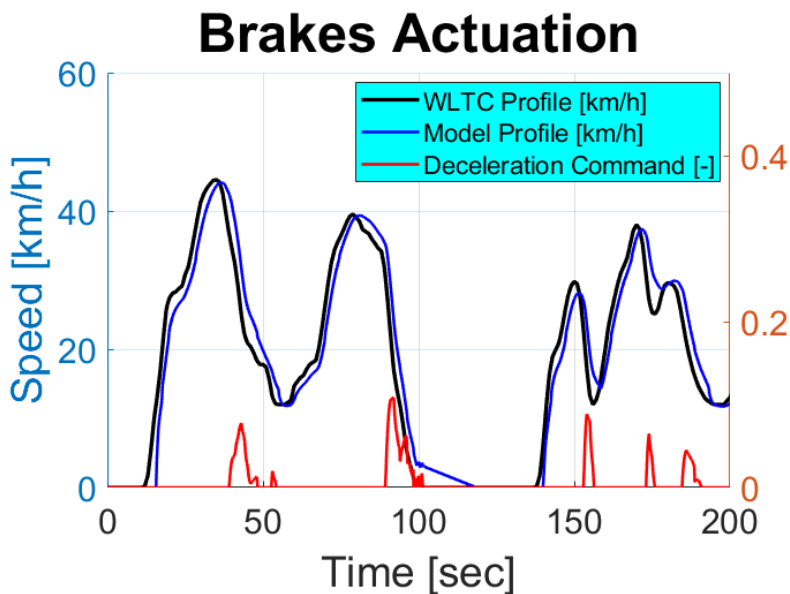


Figure 38. Brakes Actuation – First 200 seconds zoom in

Since the very first deceleration, when the computed vehicle velocity is above the WLTC reference profile, the Brakes Actuation is not immediately implemented. This is partially due to the Delay-State of the model, necessary for its resolution.

On the other hand, when the model senses that the vehicle speed should be decreased to follow the Reference speed, the delta is initially quite low. For this reason, the accelerator is progressively brought to zero at first, aiming at a self-deceleration of the vehicle itself, using the engine braking. When the delta is high enough to be impossible to recover it by using the engine action only, the Deceleration signal gets positive and it is sent to trigger the Brakes. This is confirmed by the next plot:

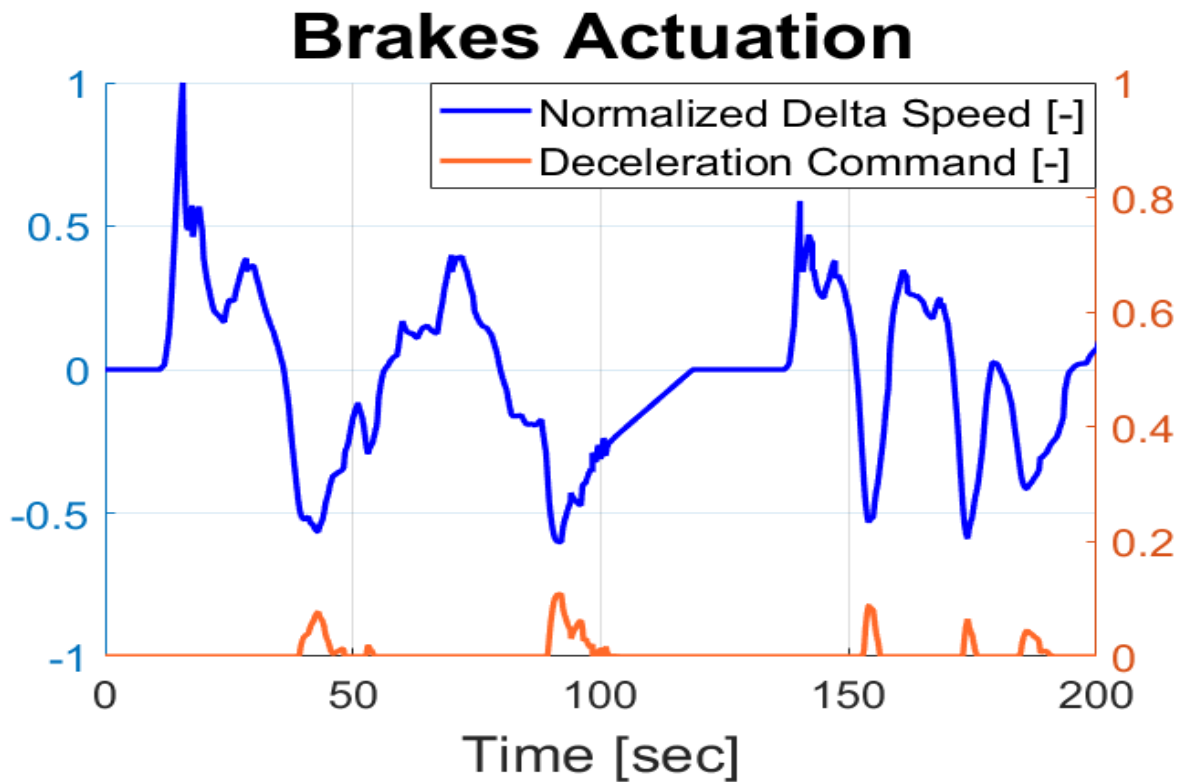


Figure 39. Brakes Actuation – Deceleration Command computation

By defining the Normalized Delta Speed as the difference between the WLTC Profile and Model Profile respectively, partitioned with respect to the max value, a positive value indicates a necessity of accelerating the vehicle and vice versa. Therefore, when the Delta Speed curve crosses the null threshold to approach the negative portion of the plot, a deceleration is required.

The delay in the Brakes actuation previously mentioned is here confirmed: every time, the deceleration command is rising only after a while that the delta becomes negative. Moreover, the full brakes triggering is achieved only when the difference of speeds gets maximum, in absolute value.

At this point, the vehicle speed is again aligning to the model speed and the brakes are progressively released, as the deceleration command is reducing. Even at the end of the deceleration phases, the engine braking is exploited as soon as the delta is low enough, releasing the brakes when the vehicle is still slightly faster than the WLTC reference. The whole is repeated during each slow down sector.

## 9.7 Wheels

Concerning the wheels duplication, a careful attention to the simultaneity of the motion must be paid. Since the test is ideally conducted on a test bench with straight wheels in identical conditions, the same rotational frequency must be observed at each time. This is displayed in the next plot:

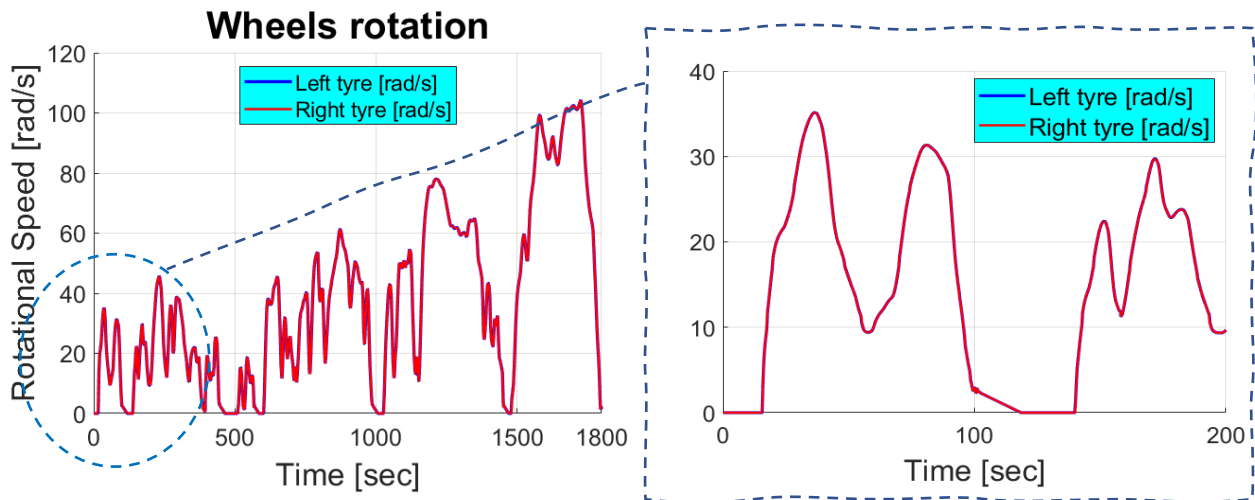


Figure 40. Left vs Right tyre rotational speed

The two rotational motions are perfectly over imposed, confirming the accurateness of the model.

Moreover, a constant coefficient rolling resistance model is implemented to simulate the tyre-to-ground interface. This model neglects the slight speed dependence of the tyre rolling resistance and applies a constant coefficient directly to the normal force computed at the wheel level by the vehicle body block.

Therefore, for the rolling resistance analysis it is essential to examine the wheel load distribution first. The study starts from the evaluation of the vertical or normal load applied at the wheels. Since the centre of gravity of the van is slightly off-centre, towards the front, in the no-loaded condition required by the test, the van is applying a lower weight on the rear axle and a little higher on the front. In the following, the load applied on a single wheel of the rear axle will be considered:

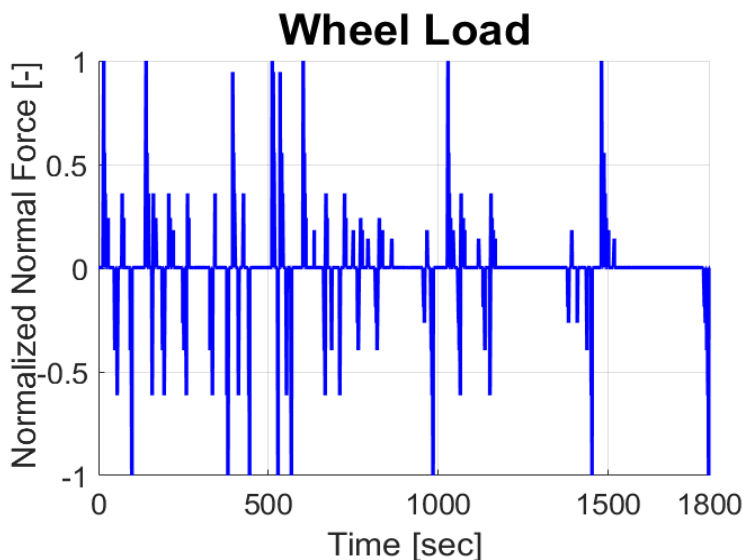


Figure 41. Wheel Normal Load trend

The plot in figure 41 shows a very strange trend, with the normal load peaking suddenly in specific instants only. Actually, the force is characterized by a baseline trend that is nearly imperceptible since it is almost 500x lower than the peaks limit. This trend is the actual wheel load distribution, whereas the enormous peaks are model-related and insignificant for the analysis. In fact, this peaks coincide exactly with the several change of gears, performed at extremely high clutch pressures to make the gearshift instantaneous by limiting the slipping phase of the clutch itself. As a consequence, an extremely high Torque is transferred immediately and for a fraction of time to the mechanical chain up to the tyres, excessively rising the wheel load. This is also confirmed by the sign of this peaks: positive during upshifts and negative otherwise.

For this reason, it is reasonable to neglect this clutch effect and obtain the “true” normal force distribution:

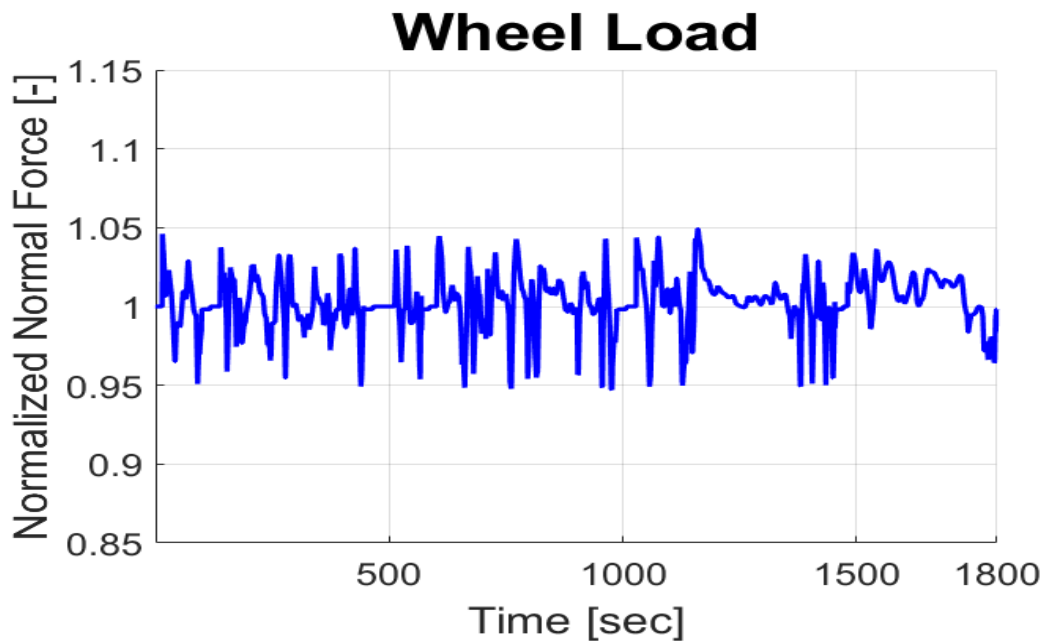
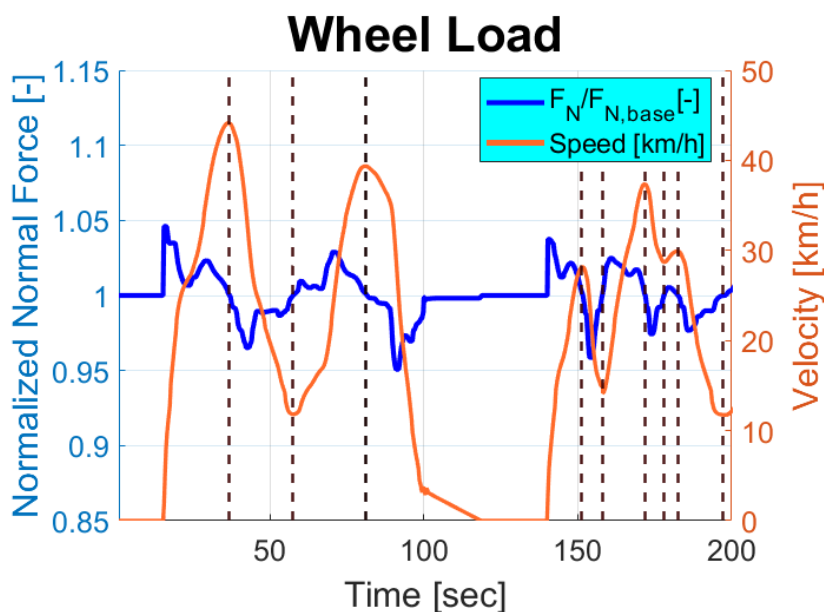


Figure 42. Wheel Normal Load trend – Filtered Signal

The normalization was performed with respect to the baseline value, obtained by the weight distribution in static condition.



Consequently, during the acceleration segments, the load transfer between the axles make the rear wheels Normal Force to grow, whereas the rear axle is discharged during the decelerating traits. The amount of the displacement from the unit value baseline is within the 5%, due to the low-level dynamicity of the cycle. The principle is proved in figure 43:

Figure 43. Wheel Normal Load trend vs Speed

Considering the Vehicle Speed Profile too, it is evident that the Normalized Normal Force trend is crossing the baseline condition exactly when the acceleration gets zero, that is in the minimum and maximum points of the Velocity curve. The behaviour is pointed out by the black vertical dotted lines.

At this point, it is immediate to understand the tendency of the Rolling Resistance, normalized again with respect to the vertical load in static conditions:

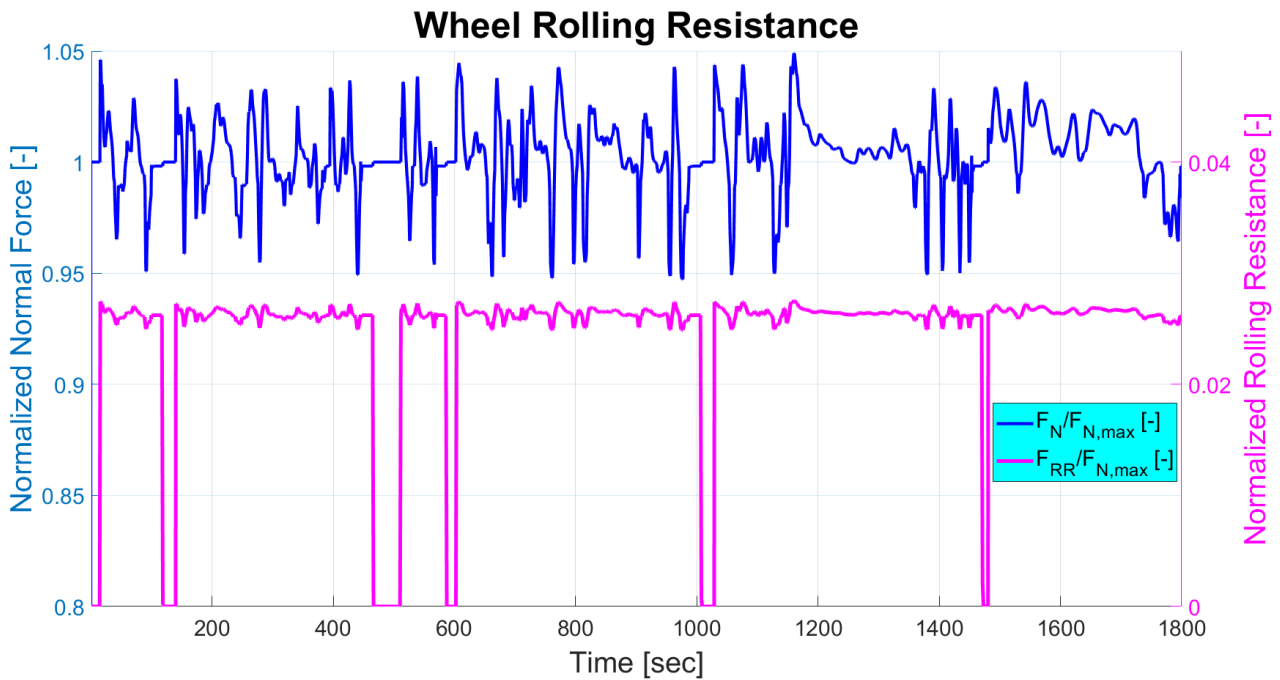


Figure 44. Wheel Rolling Resistance and Normal Load relationship

The Normalized Rolling Resistance (in magenta) is related to the Normalized Normal Force by a very small constant coefficient, as it is noticeable at a glance by looking at the chart, considering that the curves are obtained through a common normalizing factor. Nevertheless, initially and for other few times, the Rolling Resistance drops to zero. In these sections, the Reference Speed profile leads the vehicle to a standing still condition, where the rolling of the wheels is null and, as a consequence, the Rolling Resistance too.

Moreover, considering the Torque provided continuously by the engine, the total transmission ratio and the tyre rolling radius, the model is also able to compute the Force acting in longitudinal direction at the tyre-ground interface to let the vehicle move at the required speed. This Longitudinal tractive force is linked to the vertical load by the friction coefficient, provided that the adherence limit is not exceeded.

Thus, the overall loads distribution at the wheel level can be displayed, in both vertical and longitudinal direction:

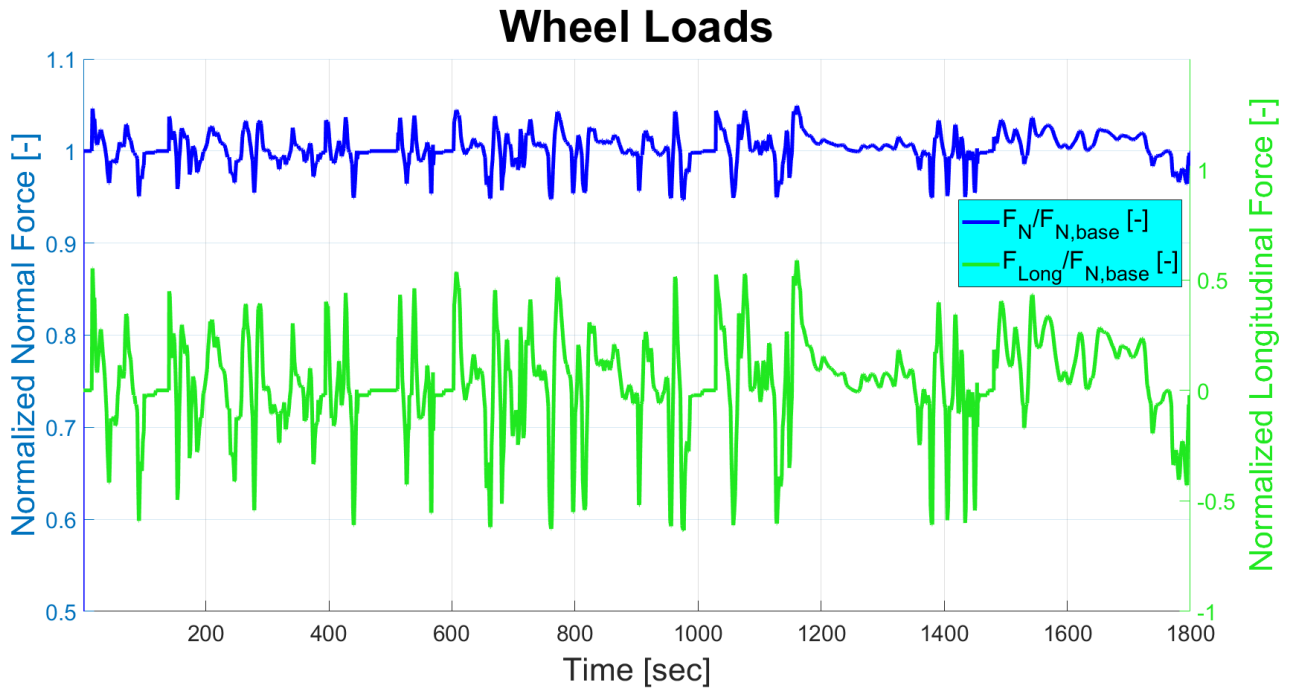


Figure 45. Wheel Normal Load vs Longitudinal Load trend

Comparing the Normal Force to the Longitudinal Force, both referred to the baseline value of the vertical load, it is evident that the latter is commonly more than halved, in absolute value, being linked to the friction coefficient. Moreover, it is characterized by a negative portion too, considering that this force is provided by the Engine Torque. Therefore, it is considered a tractive force, when the engine is accelerating the vehicle and thus the Torque is transferred from the engine to the wheels, or a braking force, in the opposite case.

## 9.8 Engine-out

Thanks to the GT-Power equivalent engine coupling, all the useful quantities at engine-out can be sensed on-the-fly. In particular, the most significant are the properties of the exhaust gas, such as its Temperature, the flow rate and NOx emission during the entire process.

The Temperature is the most important parameter, as the NOx and other emissions production is highly correlated to it. Moreover, it influences the gas stream density and consequently the flow rate. Also, the NOx treatment is affected by the Temperature of the exhaust flow indirectly, since the SCR wall Temperature is continuously varying due to the gas influence.

For these motivations, the thermal behaviour at the engine outlet is a pillar of next steps analysis and it must be carefully monitored. Therefore, the Temperature evaluation at the engine-out is the starting point of this examination. This can be appreciated in figure 46:

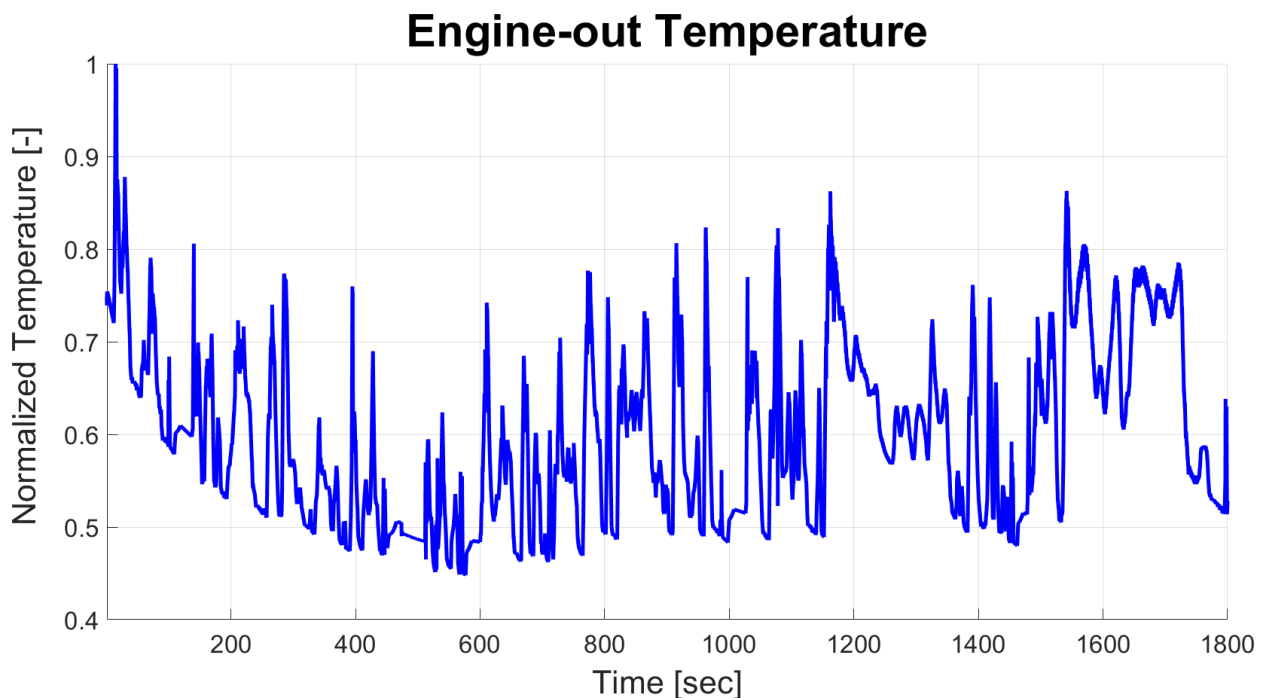


Figure 46. Engine-out Temperature

For confidentiality reasons, the original Temperature, expressed in Kelvin, is normalized with respect to the maximum value recorded during the cycle. In particular, this is achieved at the start of the vehicle run, around 15 seconds after the start of the collecting procedure since during this period of time the vehicle is still.

After that, the Temperature is oscillating approximately around 50 and 80 per cent of the highest value, according to the driving conditions, defined mainly by the amount of fuel burnt per each engine thermodynamic cycle, linked to the acceleration command consequently.

The association between acceleration command and exhaust gas Temperature can be verified in the following chart, considering the first 200 seconds for a better chart clean-up:

## Engine-out Temperature

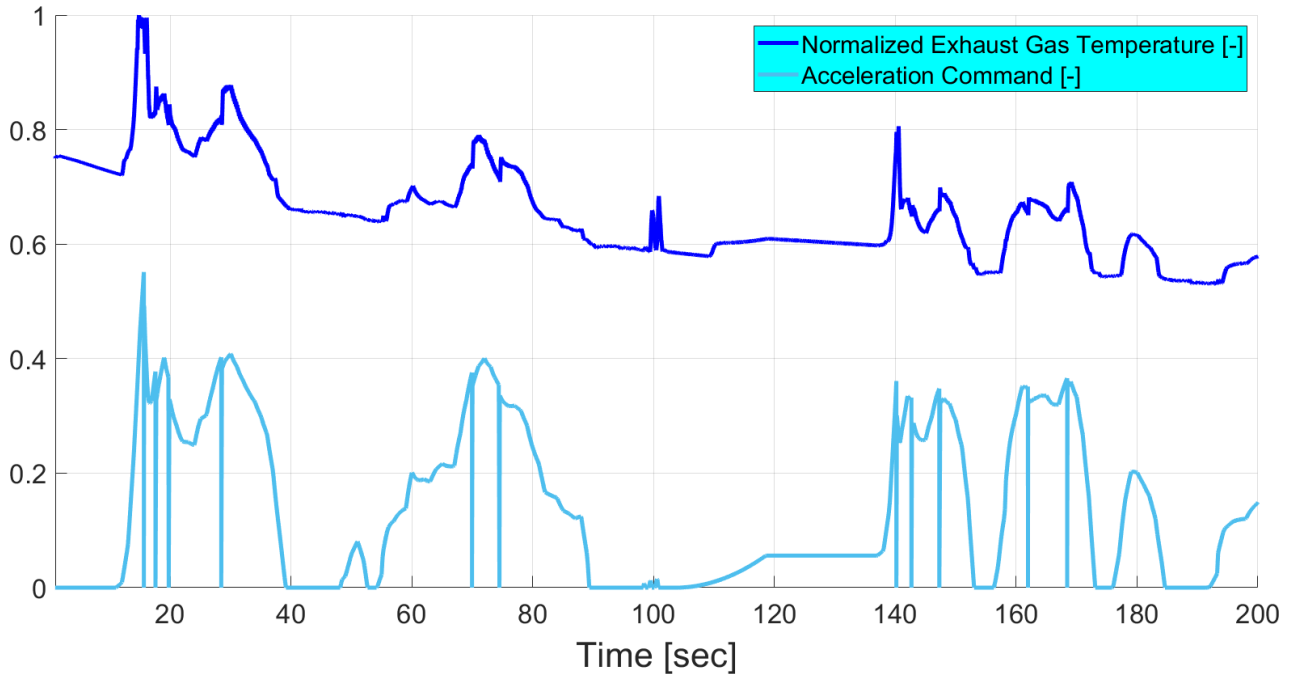


Figure 47. Engine-out Temperature vs Acceleration Command

The connection between the Acceleration action and the rise of the exhaust gas Temperature is evident, as the peaks in the normalized Temperature trend coincide with the sharper pressing of the accelerator pedal. Since the very first increase in speed, related to the greatest Accelerator Command value in the considered range of time, the Temperature of the burnt mixture is rising and it reaches here the maximum value indeed.

On the other hand, when the accelerator pedal is progressively released, the Temperature drops in a significant manner, even reaching a value lower than the Temperature prior to acceleration, when the deceleration lasts enough.

Instead, when the acceleration is null, or negative due to braking, the exhaust gases cool down slowly in an almost linear path. In this phase, the mass flow rate is minimized and the convective heat exchange with the hot exhaust pipes is amplified by the longest residence time.

The influence of the heat exchange residence time, and thus of the mass flow rate, is actually involved in all the Temperature transitions. Therefore, the next step is the evaluation of the exhaust gas mass flow rate along the WLTC. This quantity is originally expressed in [kg/s] and successively normalized with regard to the maximum sensed value.

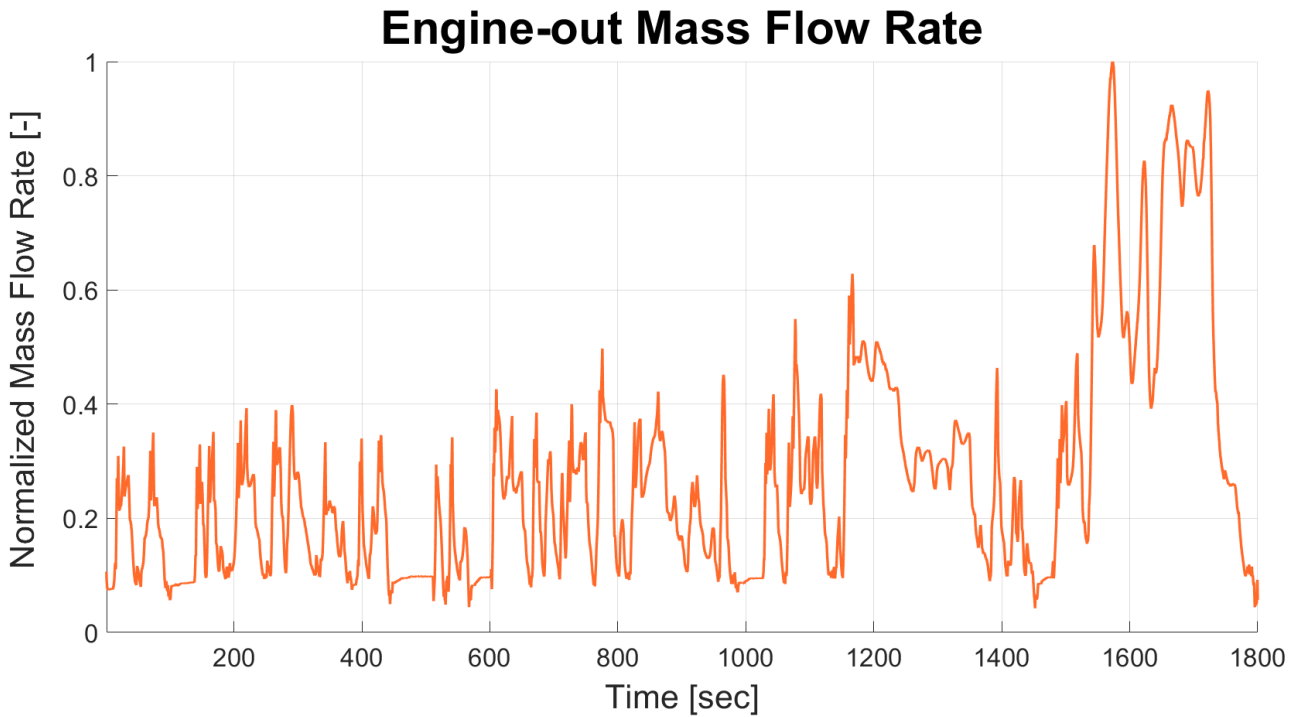


Figure 48. Engine-out Mass Flow Rate

As mentioned several times, the cycle starts in idling condition with the vehicle standing still. In this situation, the mass flow rate of the mixture coming out from the engine is approximately at 10% of the top amount achieved in the highest speed phase. After that, the mass flow rate boosts with the acceleration demands, whereas it drops when a deceleration is required, highlighting the oscillatory nature of the signal once again, according to the speed evolution.

This behaviour is explained by the continuity equation:  $\dot{m}_f = \rho \cdot A \cdot c$  (24)

Since the cross sectional area  $A$  is constant and the gas density variation can be neglected:  $\dot{m}_f \propto c$

This last statement is confirmed by the next plot, since the gas velocity is linked to the piston speed and to the engine speed in turn:

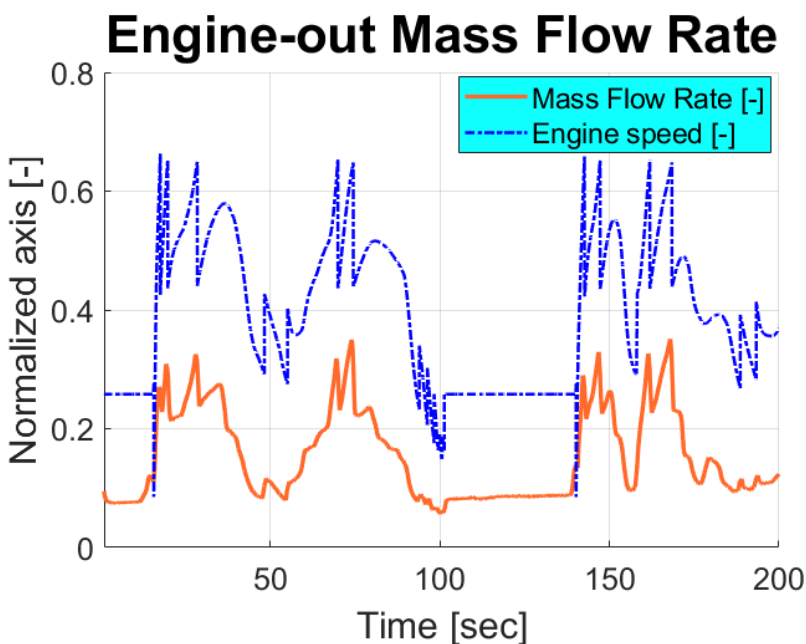


Figure 49. Engine-out Mass Flow Rate vs Engine Speed

The exhaust gas flow rate can be also expressed in volumetric terms, detecting the volumetric flow rate:

$$\dot{V}_f = \frac{\dot{m}_f}{\rho} \quad (25)$$

This parameter is computed by the GT-Power software at the engine outlet and originally specified in [L/s].

Another time, it is normalized considering the top value achieved for discretion motivations, obtaining the trend shown below:

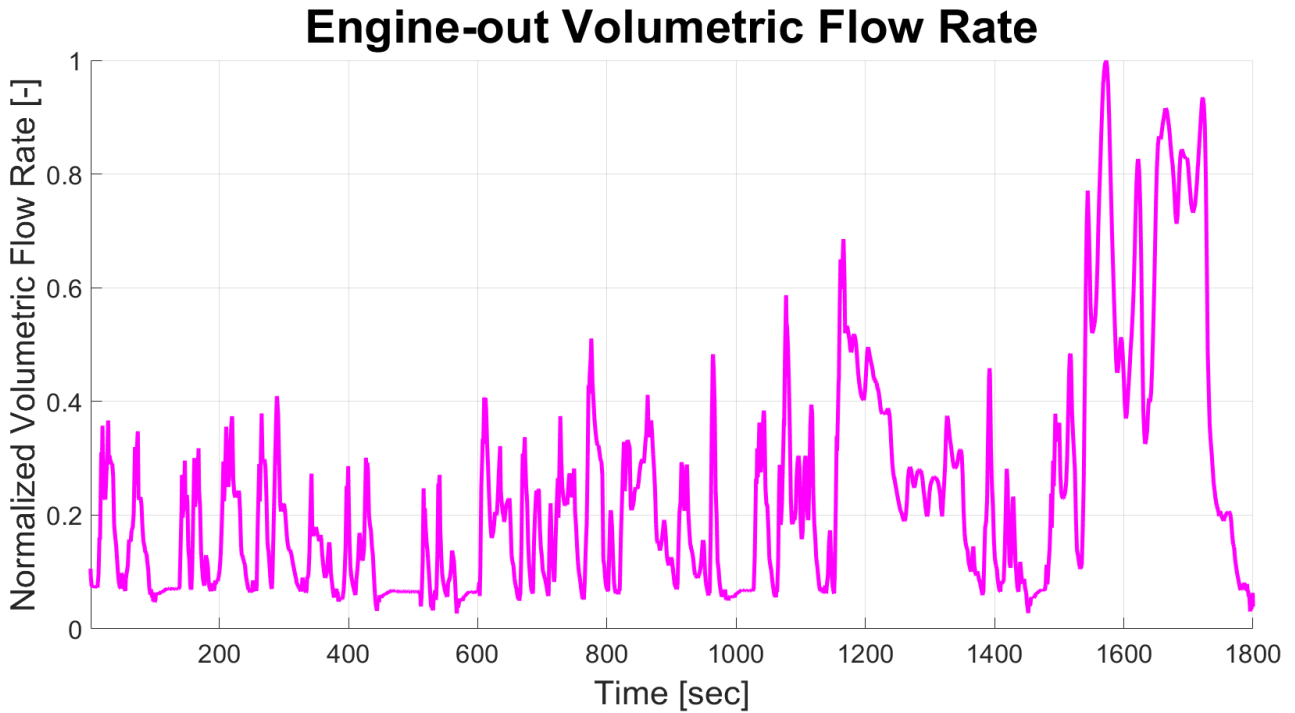


Figure 50. Engine-out Volumetric Flow Rate

At a glance, the trend could seem exactly identical to the mass flow rate chart and the general progression is pretty much the same indeed. Nevertheless, the variation of the engine-out gas density due to the Temperature and Pressure evolution at the exhaust level is affecting the tendencies, causing the achievement of slightly different normalized values for the same instant of time considered. This is confirmed comparing directly the two set of data:

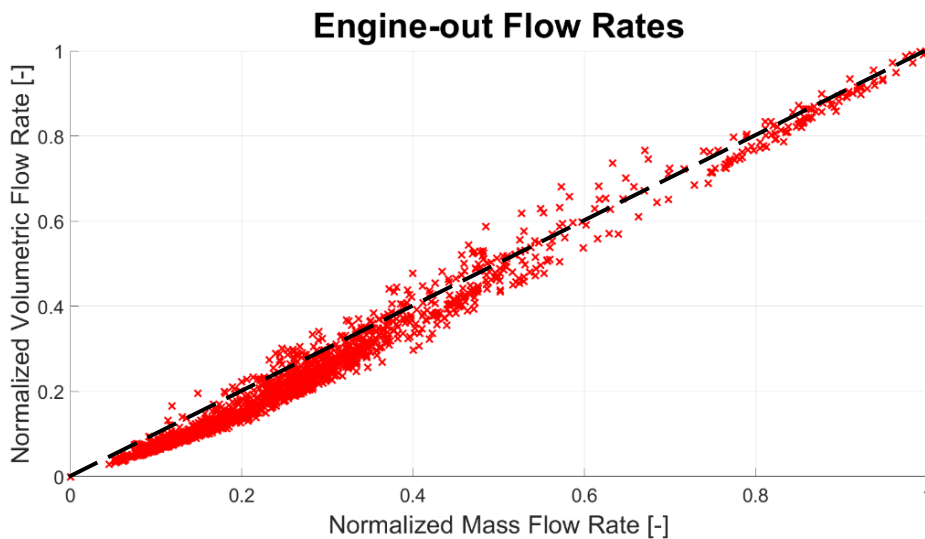


Figure 51. Engine-out Flows

The bisectrix, individuated by the black dashed line, is representing the constant density working points, since it constitutes the ratio of the normalized flow rates. As affirmed few sentences above, a variation of the gas density is present, according to the working conditions, in the neighbourhood of this line but the spread is typically contained. Therefore, the gas density difference along the cycle can be reasonably considered negligible for the next stages of the analysis.

Nowadays, a major topic of interest is the pollutants emissions, in particular for the Diesel Engines, such as the F1C. Especially, a huge concern is raising on the automotive field contribution to the global NOx release and on the feasible approaches to limit it. For this reason, the next phase is the evaluation of the Engine-out NOx emission, directly produced during the combustion in the dedicated chamber and up to the final part of the expansion stroke:

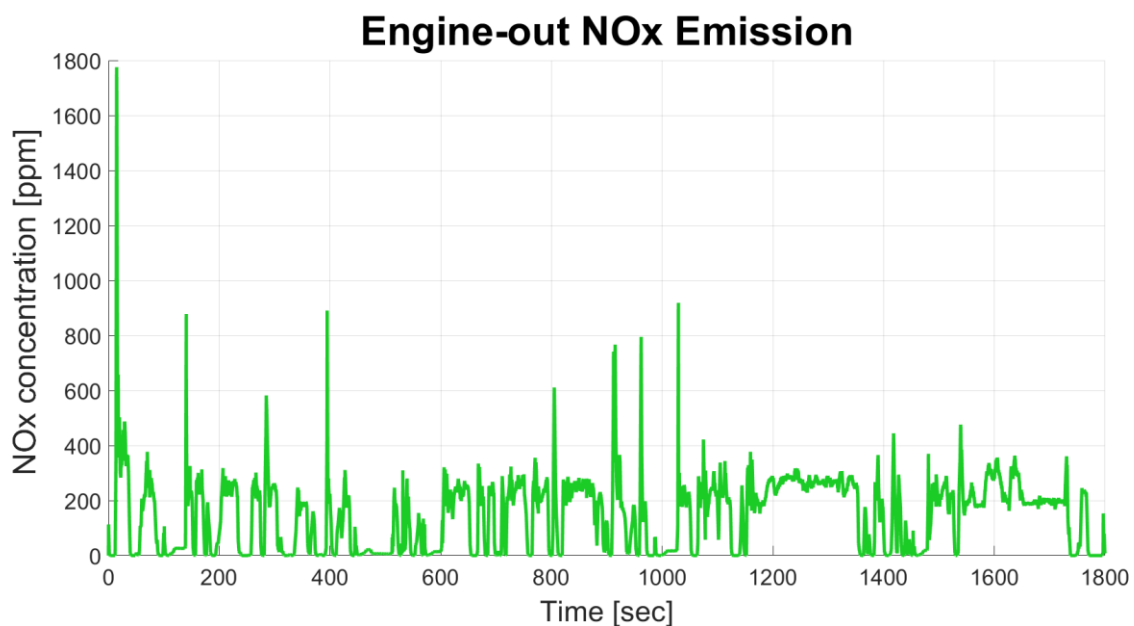


Figure 52. Engine-out NOx emission

In automotive Diesel engines, the standard NOx emission can overcome the  $10^3$  part per million [ppm], a sort of fraction in volume typically used for gaseous secretions. This suggests a good quality of the results shown in the last plot, displaying the NOx emission at the engine outlet, prior to their treatment in the dedicated device called SCR.

The trend in function of time is hardly predictable, as it is highly dynamic, according to the engine working conditions. In particular, it is well known that the NOx production is maximized in slightly lean mixture utilization, typical of Diesel applications and it is directly related to the Temperatures achieved during the combustion and expansion phase. The more elevated are the Temperatures, the more severe is the NOx formation. The Temperatures reached within the combustion chamber are not exactly equal to the exhaust gas Temperature at the engine-out due to the thermal exchange with the cylinder walls and pipes. Nevertheless, the Temperature of the gas exiting from the exhaust pipes can give a hint about the NOx amount emitted by the engine.

The relationship between NOx formation and Temperature is displayed in the subsequent diagram:

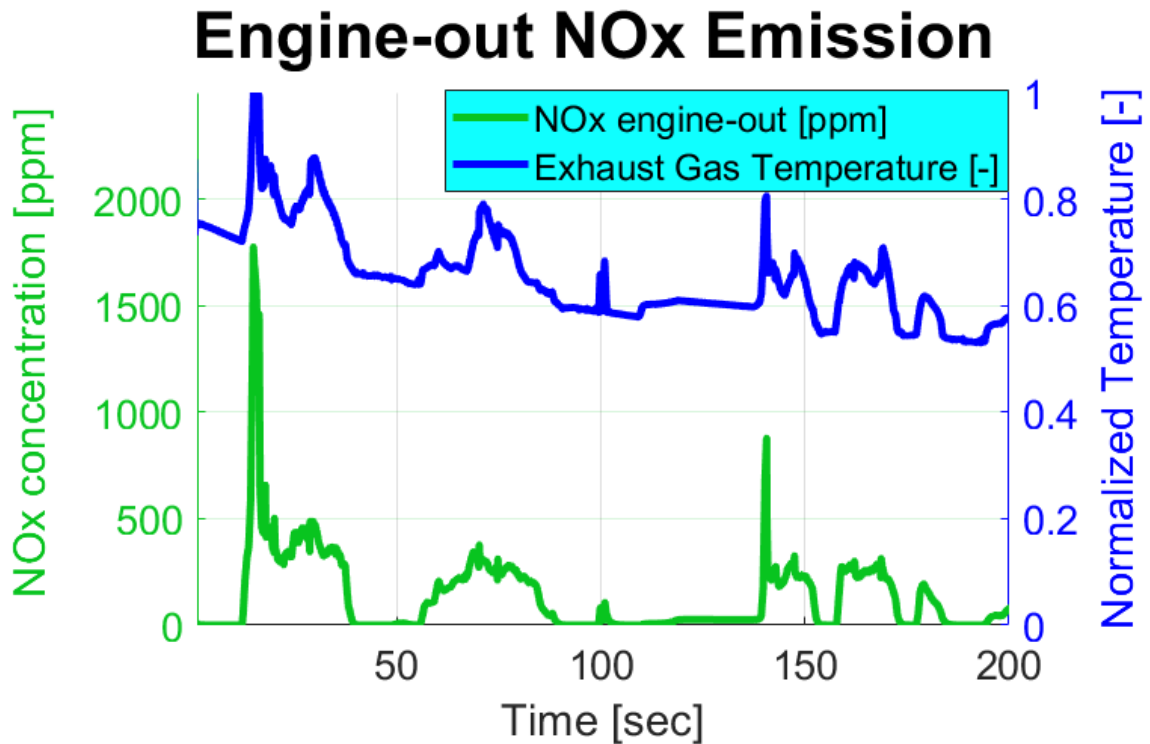


Figure 53. Engine-out NOx emission vs exhaust gas Temperature

The instantaneous NOx emission is represented by the green curve while the blue line is showing the normalized Temperature at the engine outlet, both considered for the usual initial phase. The accurate relationship between the two is evident, as they show similar trends.

When the vehicle starts its travel, the maximum NOx production rate is achieved, since this coincides with the maximum recorded Temperature, along the entire WLTC. By converse, a minimum threshold is reached during idling conditions. In general, a rise in Temperature involves a rise in NOx production and vice versa.

## 9.9 SCR

The last step is the treatment of the previously examined pollutants, in the so-called Selective Catalyst Reduction (SCR). This device dramatically abates the gaseous NO<sub>x</sub> emission prior to the release into the atmosphere, thanks to its several active sites disposed on to the wide surface available.

This process is governed by the Temperature of its walls and by the flow rate, linked to the residence time into the tool. The Volumetric Flow rate, which will be considered for this analysis, is directly obtained from the engine-out due to the mass conservation and it does not require further investigations. By converse, the Temperature of the catalyst walls is affected by the convectational heat exchanged with the fluid Temperature, crossing the catalyst itself. Therefore, the evaluation of a thermal model is essential in order to achieve the calculation of an accurate conversion efficiency.

### 9.9.1 Thermal Model

As already explained in chapter 6, the chosen thermal model is a 0D thermal model constituted by many blocks with no axial reference, meaning that all the variables involved in each block have to be intended as punctual measurements. Each block is characterized by a specific heat exchange area and mass, subdividing the original quantities of the entire SCR.

For the IVECO DAILY analysis, a 12 litres SCR was selected, with a total weight of 6.28 kg and 29.5 m<sup>2</sup> of area exploitable for the thermal exchange. The model discretization found the proper value in the 64 blocks subdivision, achieving the best compromise between results accuracy and computational power. The SCR is thought to be located directly after the engine, in order to neglect the influence of the environment on the exhaust pipes.

Starting from the first block, the fluid Temperature at the engine-out is imposed at its entrance.

At the beginning, the hot gases encounters the cold catalyst, characterized by a wall Temperature of 300K, approximately the Standard Ambient Temperature, since the WLTC provides for a cold starting condition of the vehicle. This has a mutual impact on the couple of Temperature trends, both the fluid and wall Temperatures, in figure 54.

Consequently, in the first static phase, the catalyst Temperature of the first block is approaching the fluid one, evaluated at the entrance of the SCR. The balance is not reached in these 15 seconds since the vehicle starts its motion at the end of this short timelapse, rising beyond the engine-out fluid Temperature and thus the fluid Temperature at the SCR inlet section.

Therefore, the walls of the catalyst gets hotter and hotter until a temporarily and unstable balance point with the fluid Temperature is reached during the second deceleration. At this point, the tendency is reversed as the fluid is now warmed by the SCR itself for a short transient.

At the following acceleration, the original condition is restored and the previously described principles apply cyclically along the entire testing procedure.

Every Temperature considered in the next steps is originally expressed in [K] and normalized according to the same maximum value, achieved by the fluid at the inlet of the SCR.

### SCR Thermal evolution - First Block

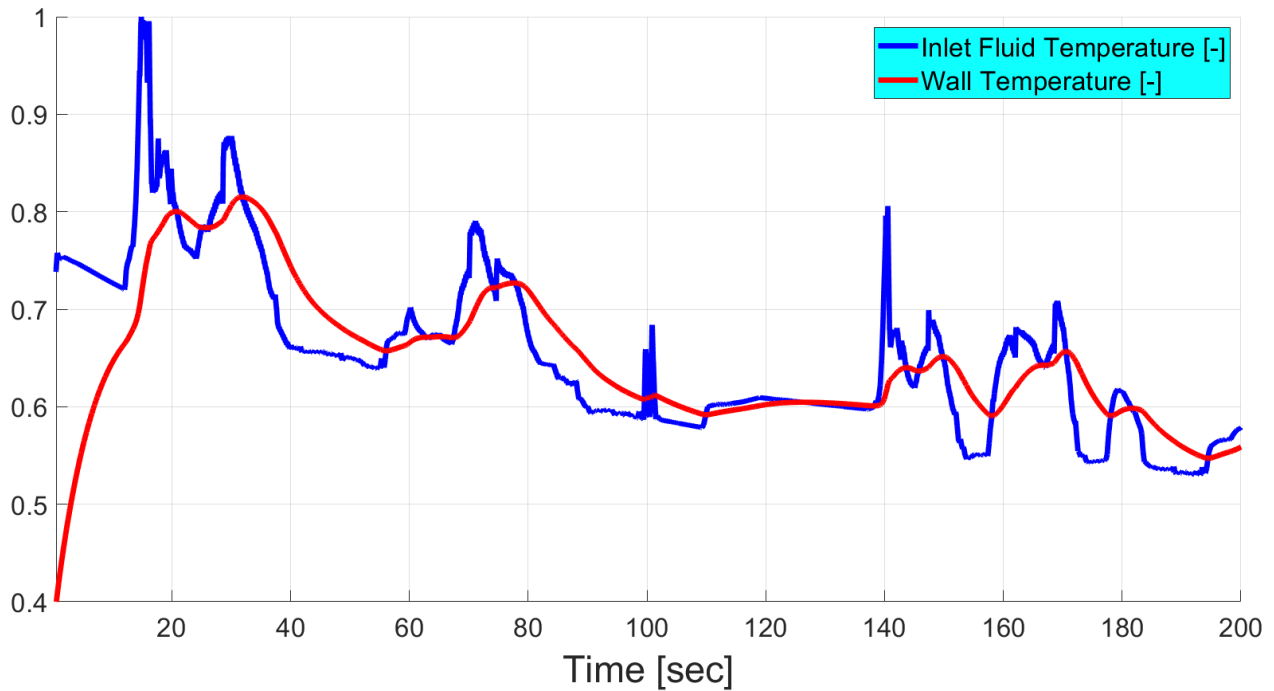


Figure 54. Inlet fluid Temperature vs Wall Temperature, first block – detailed

It is worth noticing that the wall Temperature evolution is much smoother and more progressive than the highly dynamic fluid characteristic but being still able to follow closely the trend. This ensures a fast warm-up of the catalyst at the start, for example, allowing a rapid achievement of the best conversion efficiency.

The overall trend recorded on the entire WLTC is reported below:

## SCR Thermal evolution - First Block

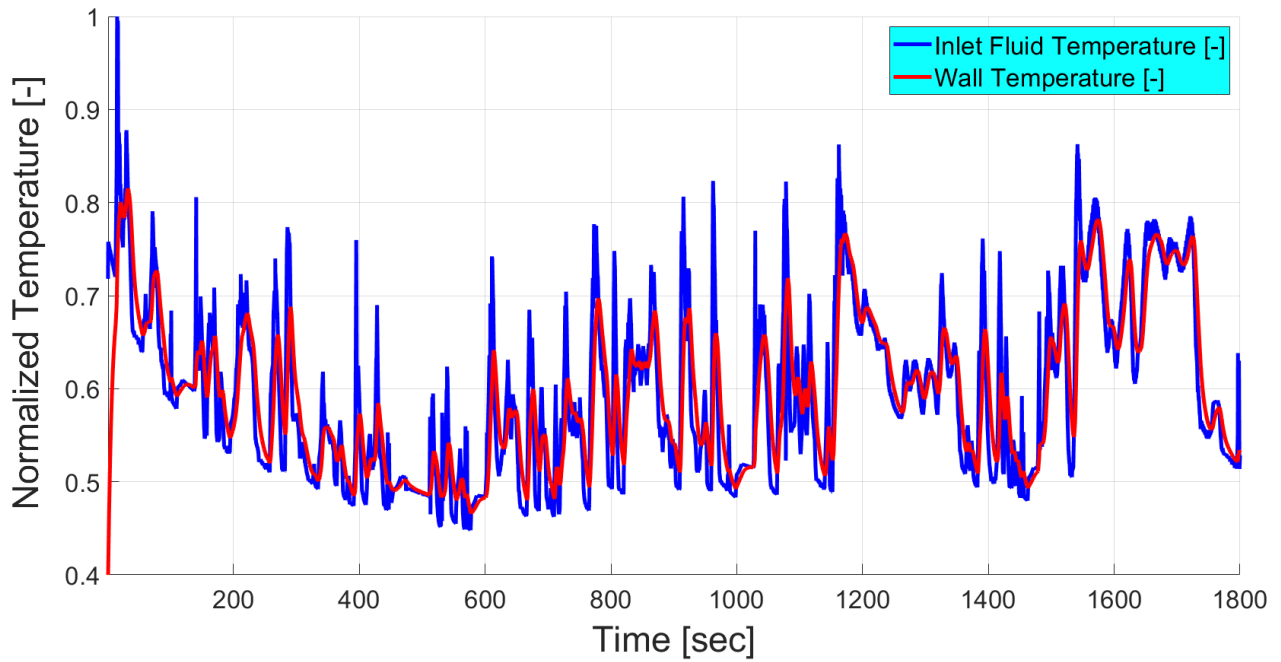


Figure 55. Inlet fluid Temperature vs Wall Temperature, first block

The SCR wall Temperature of the first block affects in turn the fluid Temperature itself, according to the formerly mentioned couple of thermal laws. Therefore, the fluid Temperature will be substantially modified at the outlet of the same block, in agreement with the thermal model implemented through the customized component source code.

The following charts testify this affiliation:

## SCR Thermal evolution - First Block

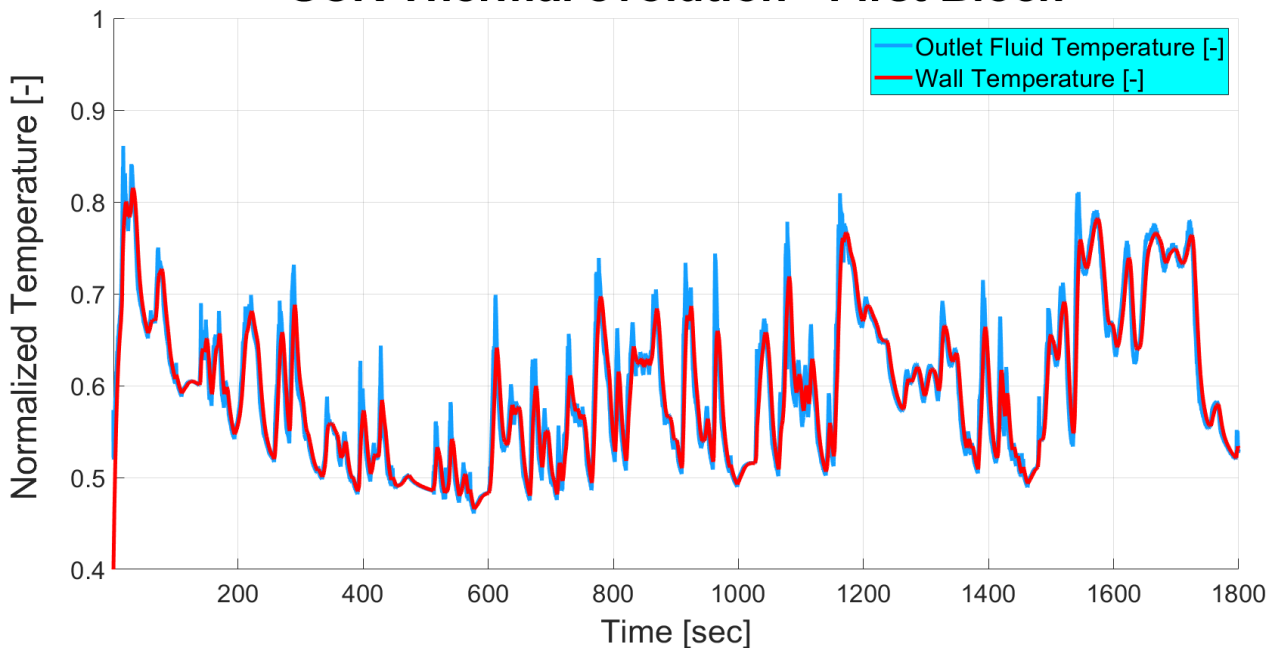


Figure 56. Outlet fluid Temperature vs Wall Temperature, first block

The end result is a fluid Temperature constantly close to the SCR Temperature, very near to the achievement of a continuous thermal balance condition between wall and fluid. This outcome is quite surprising considering that, at this stage, the analysis is dealing with the first block only, out of a total of 64.

Nevertheless, the single element area available for the thermal swap is already extended, being the total area almost 30 m<sup>2</sup>, more or less the equivalent of a squash court, condensed in a device shorter than a foot . Therefore, the thermal exchange is pretty intense in the first of the block set already.

Moreover, each block is characterized by its own wall Temperature, suggesting that the close-to-equilibrium condition must be achieved in every block with further interactions, exploiting all the available surface for the conversion.

The detailed situation is deepened in figure 57 and 58:

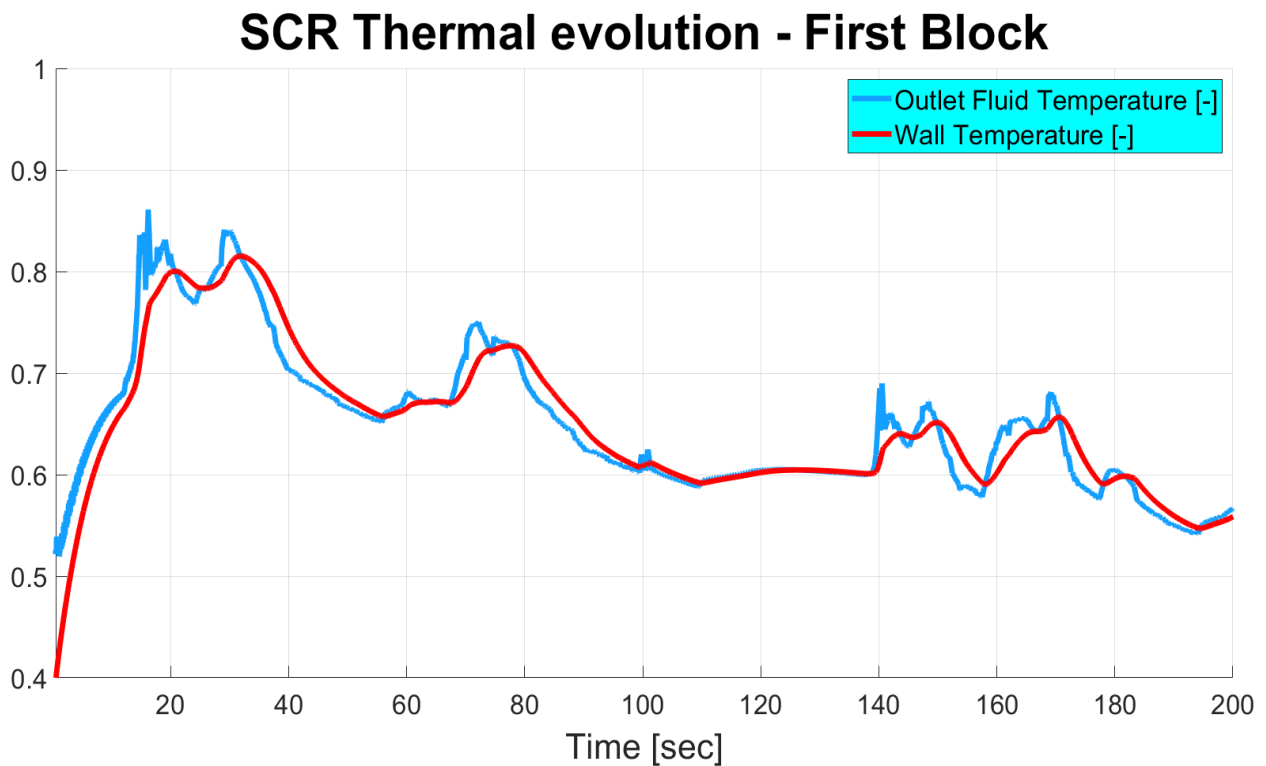


Figure 57. Outlet fluid Temperature vs Wall Temperature, first block - Detailed

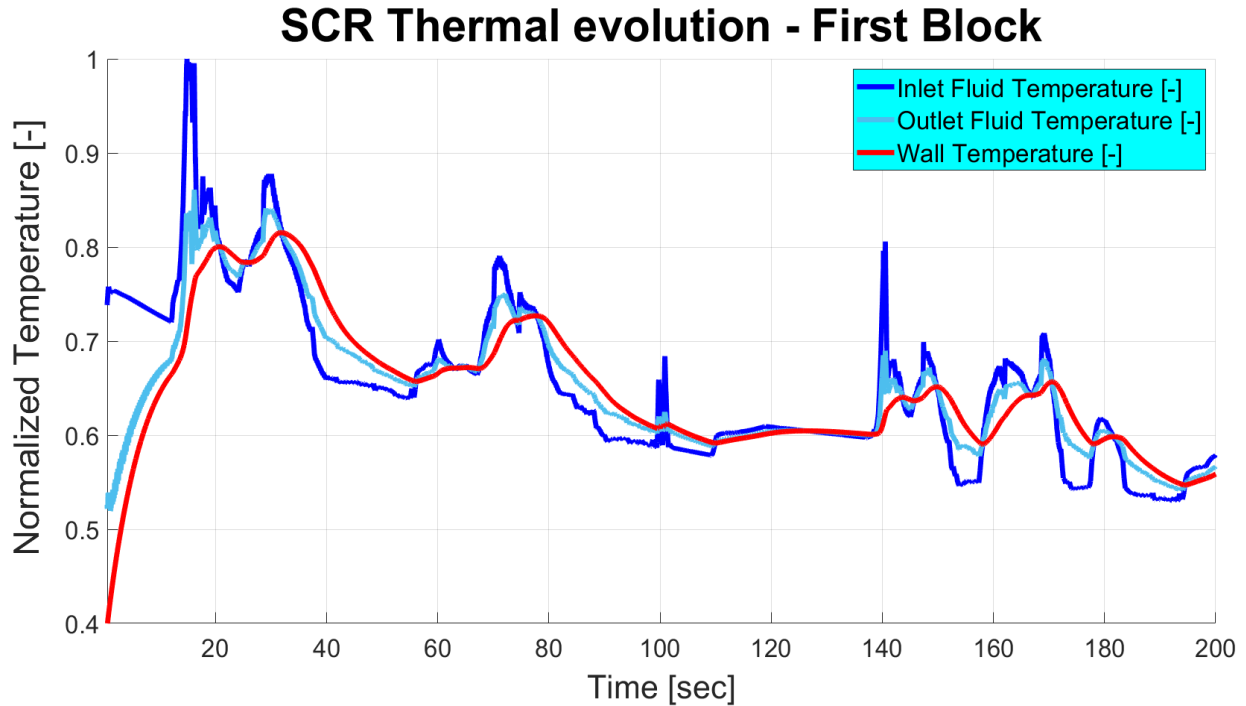


Figure 58. Complete thermal evolution, first block

The fluid is immediately cooled down by the cold SCR wall, responsible for reducing its Temperature of more than 25% at the very beginning. After that, the SCR is getting warmer too and this effect is progressively reduced, up to the start of the vehicle run. At this point, the rise of the fluid Temperature at the inlet is again mitigated by the colder SCR and the fluid reaches constantly an intermediate condition at the outlet. In fact, the Outlet Fluid Temperature is between the Inlet Fluid Temperature and the Wall Temperature curves for each instant of time studied. This holds even during the deceleration phases, when the fluid Temperature at the entrance of the device reduces enough to reverse the phenomena and the SCR warms up the fluid during the passage in the channels.

As expected, the fluid Temperature at the outlet is following a highly dynamic evolution, in agreement with the Inlet gas trend. Therefore, the SCR is capable of strongly affecting the magnitude of the fluid Temperature, from the block input to the outlet, but not its tendency.

The exchange phenomena between fluid and SCR is described by the heat flow rate law:

$$\dot{Q} = c_{p,f} \cdot \dot{m}_f \cdot (T_{f,out} - T_{f,in}) \quad (26)$$

Being  $c_{p,f}$ , the specific heat capacity of the fluid evaluated at constant pressure, assumed constant for the reasons discussed in the previous chapters, the heat flow rate is only depending by the delta of the fluid Temperature and by its mass flow rate. This statement can be verified by examining the Simscape empirical calculation in figure 59:

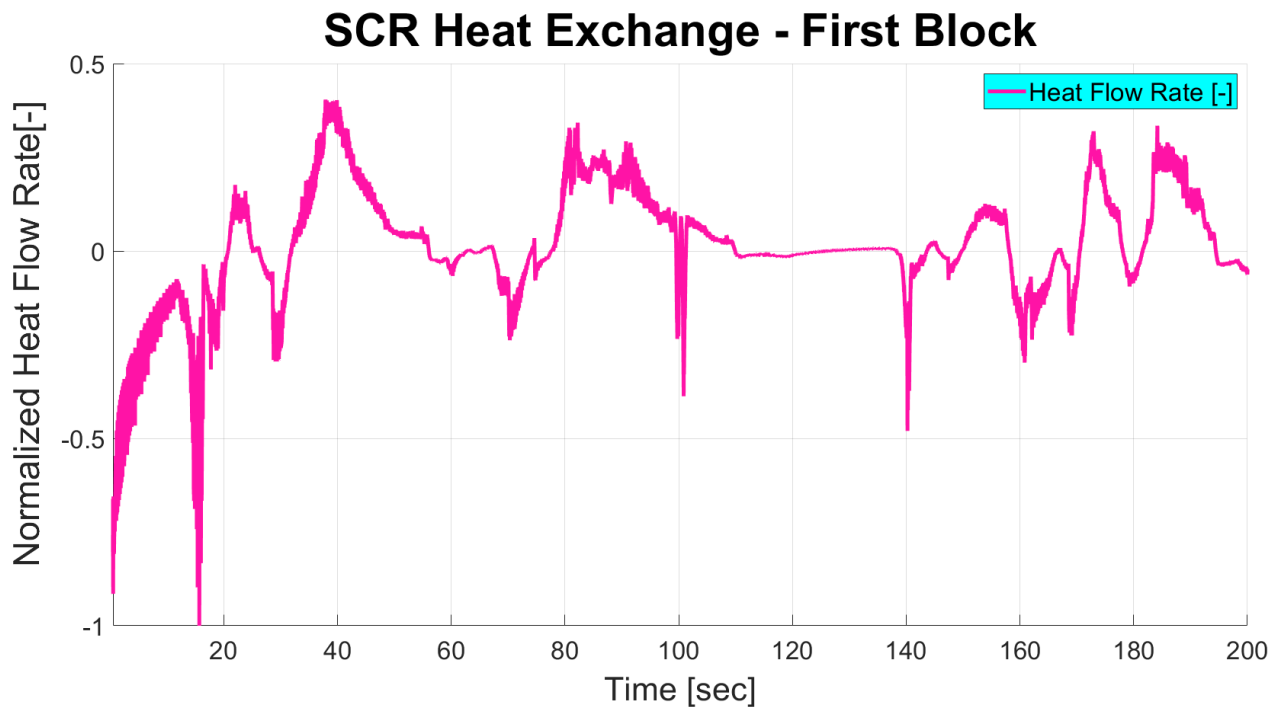


Figure 59. Heat Flow Rate, first block

Having in mind figure 58, when the fluid is getting colder due to the SCR action across the component, the heat is released by the gas and, by convection, a negative value is recorded (negative delta). By converse, the positive values are aligned with the fluid absorption of heat from the hotter walls (positive delta).

The strong variation of fluid Temperature at the beginning is compensated by the limited mass flow rate typical of the idling condition. Consequently, the heat flow rate at the opening of the test is not that extreme and the warm-up of the SCR is more critical than in an instantaneous start of driving.

Anyway, at the first acceleration the warm-up is not completed yet, resulting in a still huge delta of fluid Temperature across the sector, while the mass flow rate is already significant, determining the achievement of the maximum heat flow rate recorded, in absolute value.

Proceeding with the analysis, the successive action is the gas passage into the second block. Here, the fluid Temperature at the inlet coincides with the fluid Temperature at the outlet of the previous sector, the first block. This is necessary for the circuit continuity and the physical integrity of the variables involved.

Subsequently, the black curve represented in figure 60 can be added to the general picture of the first block. This line represents the fluid Temperature at the outlet terminal of the second element.

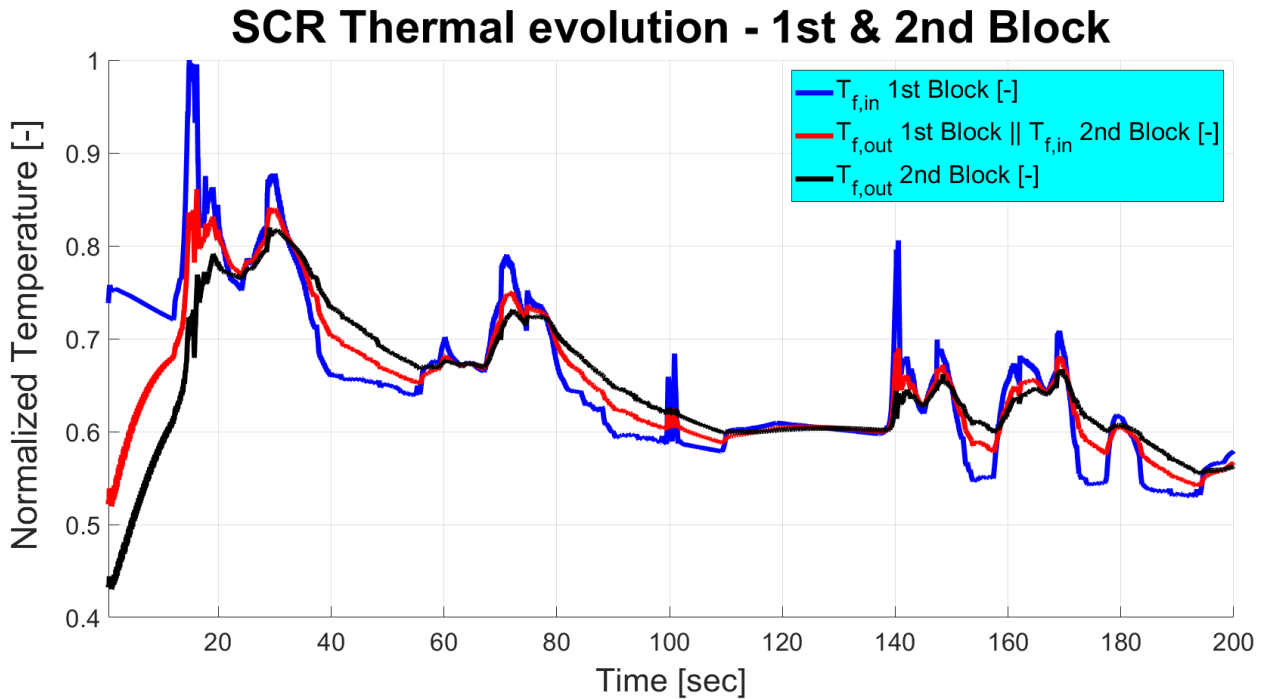


Figure 60. First block and Second block interaction

Obviously, the Temperature of the fluid at the outlet of the first block and the one at the inlet of the second block curves are identical, confirming the correct implementation of this concept in the model.

As one might expect, the second block and its walls, in particular, are mitigating the gas thermal condition once more (and vice versa). The most evident effect is displayed at the beginning of the cycle: in the second block, the gas is cooled down further, even below the wall Temperature of the first component. In a similar way, when the gas is getting hotter passing through the SCR, the fluid Temperature at the output port of the second element is rising even above the catalyst value in the first block.

This is due to the fact that the wall Temperature in the second block is characterized by its own evolution too, different from the first block feature and in some way delayed. The trend is clearer examined in the next plot, figure 61:

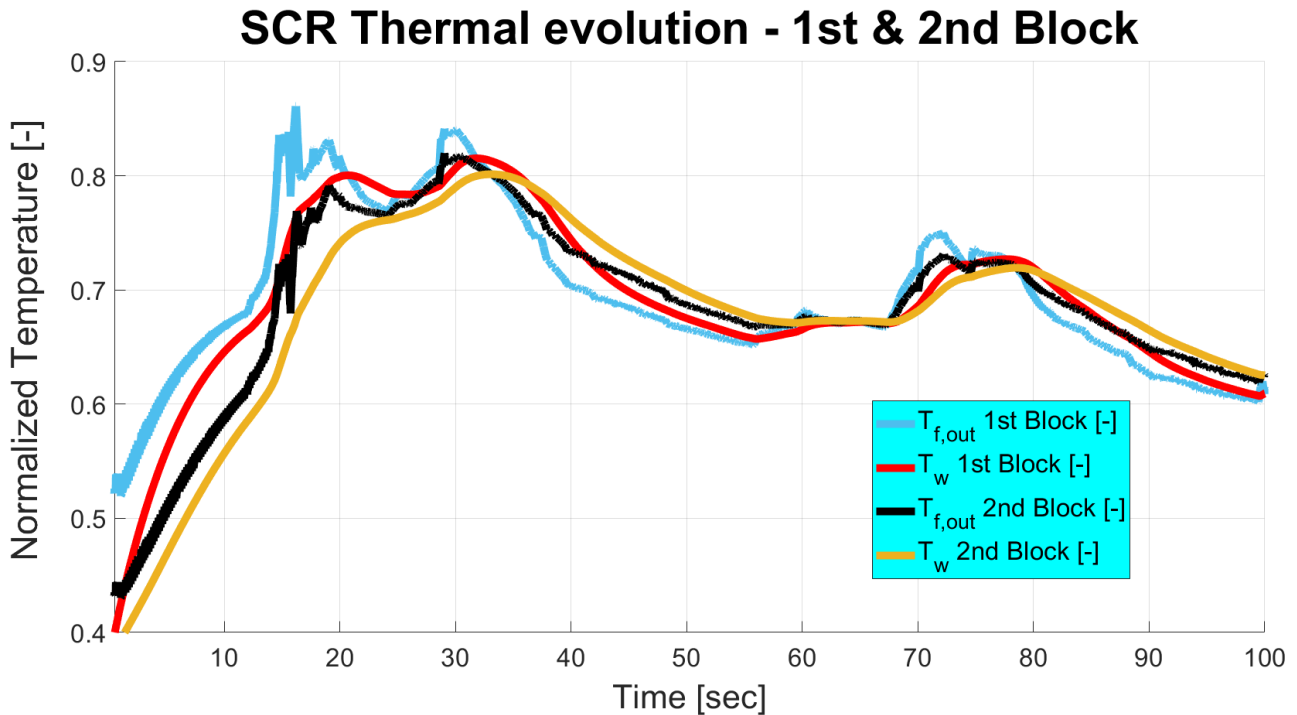


Figure 61. First block and Second block interaction with walls

In a very short period, the fluid Temperature at the second block outlet, whose trend is represented by the black curve, reaches values below the ones of the wall Temperature in the first sector ( $T_{w,1}$ ), in red colour. This is determined by the orange curve, symbolizing the wall catalyst Temperature in the successive element ( $T_{w,2}$ ). This curve is different from the wall catalyst condition in the previous sector, thanks to the discretization of the SCR. Therefore, the SCR Temperature is considered uniform in each element of the block set to satisfy the modelling assumptions but it varies from component to component, in order to better characterize the catalyst thermal evolution.

Considering this, it is now immediate to understand the trends in the second block. Here, the SCR walls are exchanging heat with the mixture, coming from the previous block, which is colder than the engine-out mixture in the first phase of the cycle, for example. For this reason, the SCR walls in the considered block, colder than the mixture, reach a condition ( $T_{w,2}$ ) even colder than the previous one ( $T_{w,1}$ ) in this timelapse.

As described for the first block, the fluid crossing the second element at the initial Temperature, indicated by the cyan curve, is in turn affected by the catalyst Temperature ( $T_{w,2}$ ), reaching a different condition at the outlet terminal, described by the black curve. Again, this curve is always an intermediate condition between the wall and inlet fluid Temperatures.

The same principles illustrated for the first block can be now applied to understand the behaviour of the second block as well as the behaviour of all the remaining ones.

Following the discretized model, the entire SCR thermal behaviour can be finally computed, in combination with the exhaust gas effect. Starting from the latter, the thermal evolution can be displayed at the extremities of the device and in the mid point, for example. This can be monitored in figure 62:

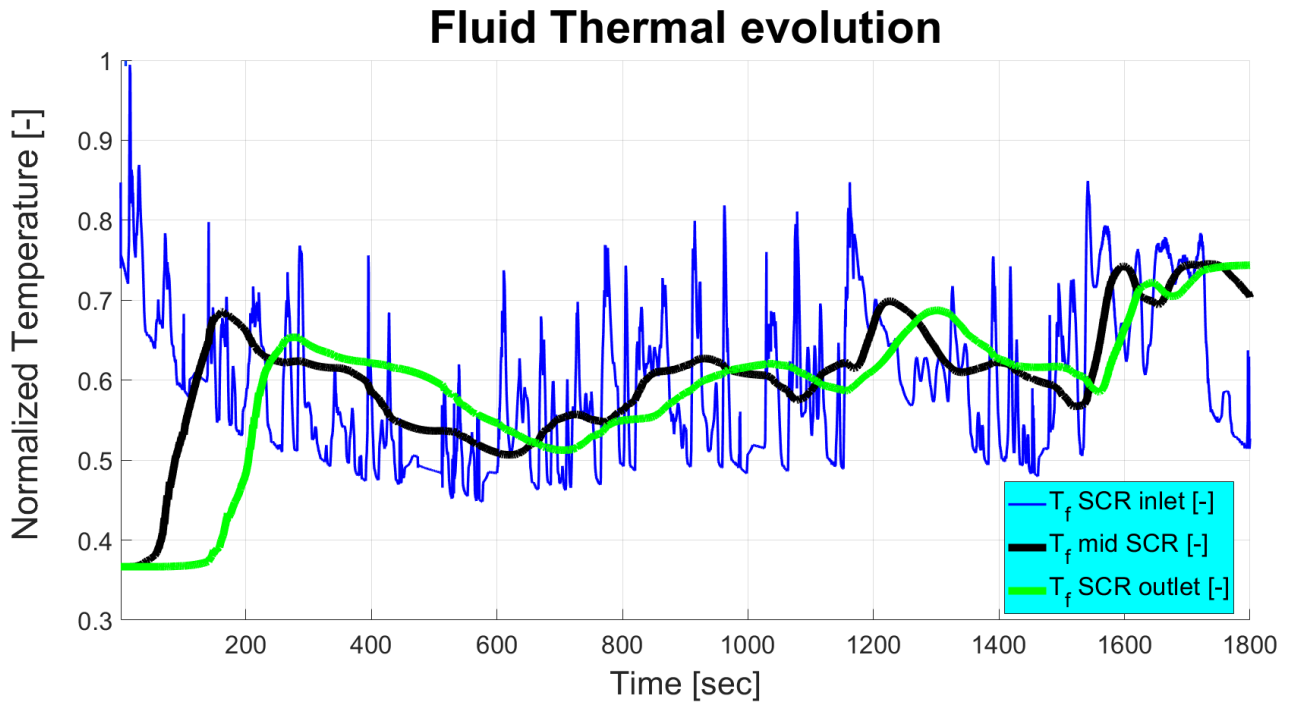


Figure 62. Fluid Thermal evolution across the catalyst

Due to the protracted thermal exchange during the gas passage into the channels, the fluid Temperature gets stabilized across the SCR. This is already evident in the mid SCR black curve, where the Temperature assumes a tendency similar to a filtering of the engine-out Temperature, or SCR inlet Temperature, highlighted in blue.

Going on along the aftertreatment system, the fluid is further affected by the walls, up to the achievement of the green curve, at the SCR outlet. This curve is showing a further cooling down at the beginning, due to the contact with the subsequent colder walls, and it is characterized by a similar but “delayed” trend with respect to the black curve, in general. Nevertheless, the maximum absolute values reached during each cooling/warming phase are not the same, as the green curve tends to reach a further regularized Temperature, due to the already clarified reasons.

For the sake of analysis completeness, the same chart can be plotted considering the catalyst walls Temperature (figure 63). The evaluation points are identical to the ones in the previous chart.

Being the effect between walls and fluid mutual, the walls Temperature trends are very similar to the fluid Temperatures at the outlet of the same evaluated blocks, especially going on along the SCR, when the fluid Temperature gets stabilized.

## SCR Thermal evolution

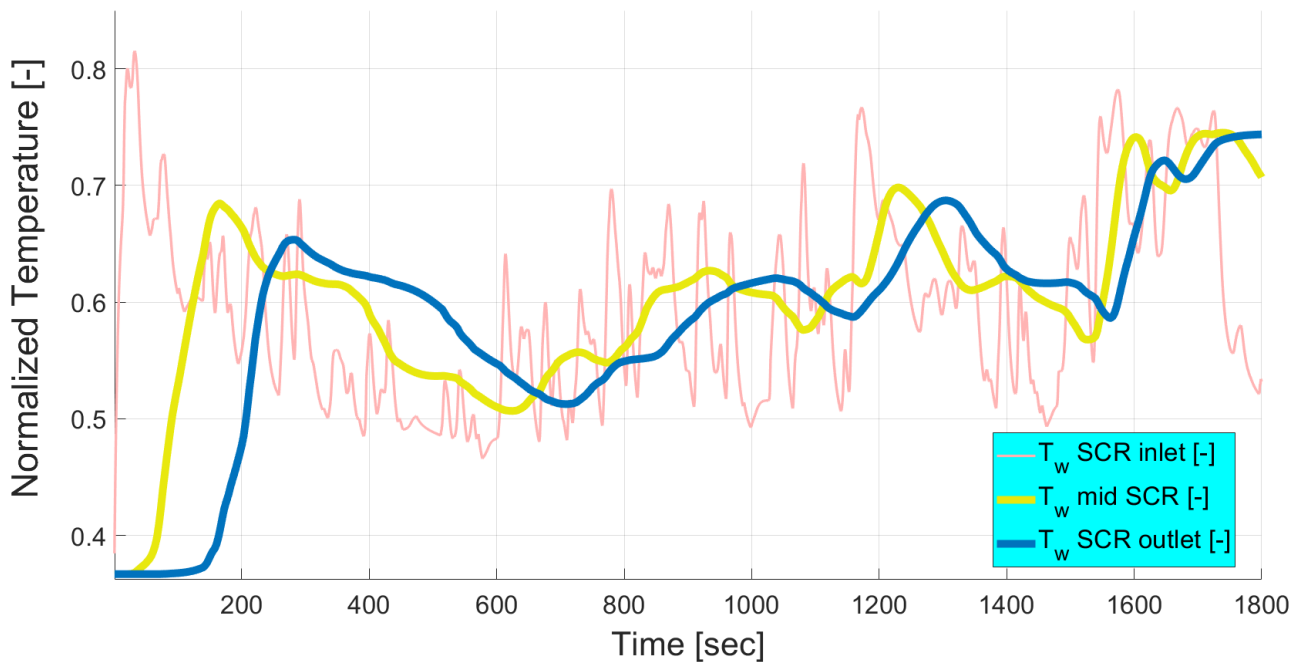


Figure 63. SCR Thermal evolution

Similar principles described for the fluid thermal evolution still hold for the catalyst thermal evolution. This is due to the missing description of the first blocks, in these plots, where the fluid Temperatures were still highly dynamic while the catalyst condition is more stable. Once this effect is damped down by the mutual interaction, the fluid and wall trends are very close to each other.

In conclusion, the catalyst thermal evolution is described by a huge variation of Temperature, proceeding in axial direction along its walls. Starting from a cold condition, the section immediately downstream of the engine is warming up very quickly, while the last portion takes more than 200 seconds to reach the proper level of Temperature, necessary for a significant abatement of the emissions.

This topic is linked to the fast achievement of the so-called light-off Temperature ( $T_{50}$ ), a conventional Temperature indicating the achievement of the 50% conversion efficiency, and it constitutes one of the biggest concern nowadays. The timelapse involved in the selected SCR model warm up is in line with the current aftertreatment systems (ATSS) State of Art, despite of the several simplifications implemented.

### 9.9.2 Chemical model

Combining the SCR mean Temperature, average value among the several walls Temperature trends just described, and the volumetric flow rate, showed in Figure and converted in [m<sup>3</sup>/h], the NO<sub>x</sub> conversion efficiency can be obtained by interpolating a dedicated look-up table. This step represents the chemical portion of the SCR model, according to which the NO<sub>x</sub> is converted exploiting the Ammonia and the abundance of Oxygen present in the mixture.

The NO<sub>x</sub> conversion efficiency trend can be plotted along the WLTC in figure 64:

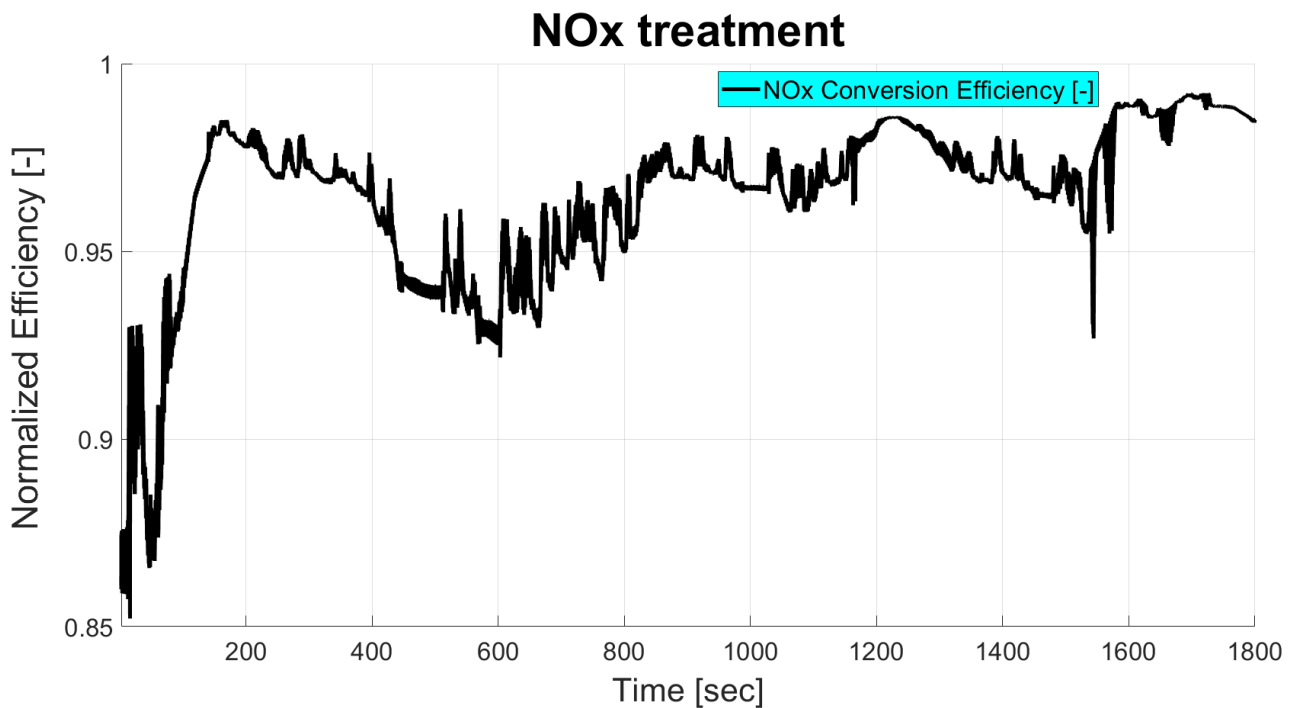


Figure 64. NO<sub>x</sub> conversion efficiency

The NO<sub>x</sub> conversion efficiency, related to the quality of the emission abatement across the SCR, starts at lower values due to the low Temperatures recorded during the first idling transient. Nevertheless, the mass flow rate too is low during this period, ensuring a longer residence time of the exhaust gases. Therefore, the drop in efficiency is not that remarkable as one might expect. After that, the flow rate and the SCR mean Temperature rise steeply and the NO<sub>x</sub> conversion efficiency largely overcomes the 90% threshold during the entire cycle, according to the driving conditions.

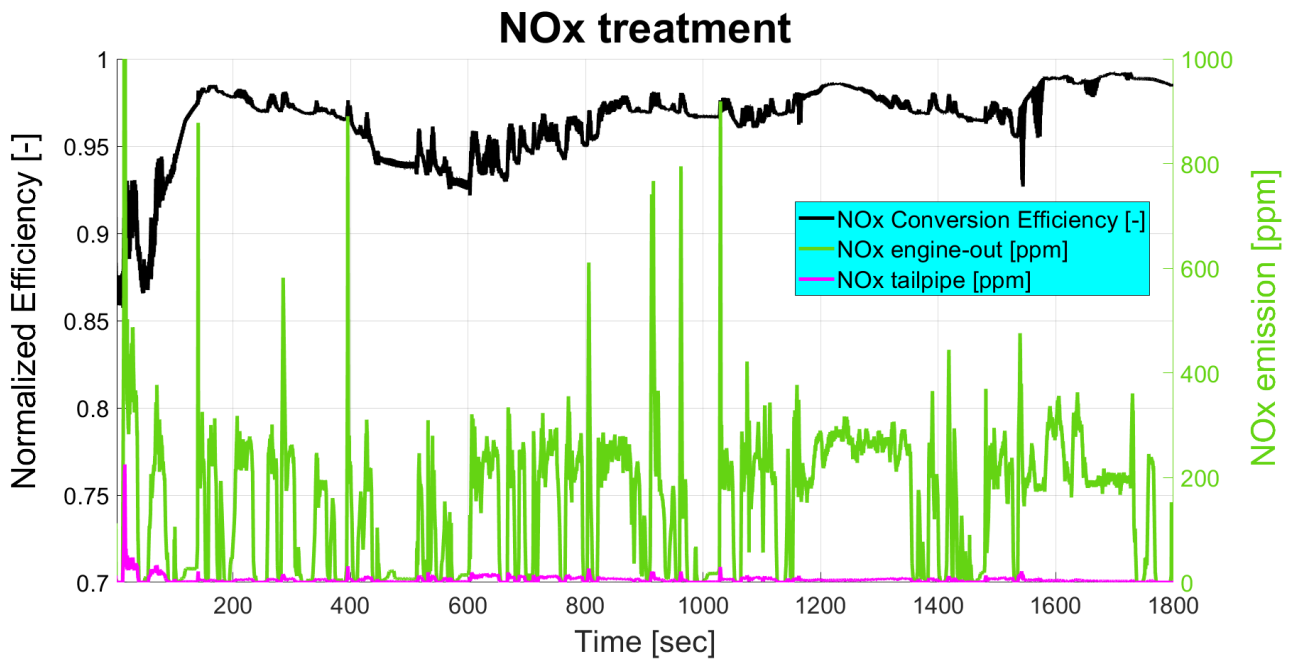


Figure 65. NOx conversion efficiency and emissions

Considering the engine-out NOx emission, through the knowledge of the NOx conversion efficiency the NOx at the outlet of the SCR can be extracted. This type of emission is also known as NOx emission at tailpipe level. Thanks to the incredibly high conversion efficiency, the tailpipe NOx emission is extremely limited during the vast majority of the time. In this sections, noticeable in figure 65, the SCR action is decreasing the emissions even by two order of magnitude, allowing the achievement of few part per million released.

On the other hand, in the most critical warm up phase the NOx discharge at the tailpipe is one order of magnitude higher than in the rest of the test, overcoming the 200 ppm. Here, despite of the huge emission, the SCR effect is already impressive, confirming the great reliability of the selected catalyst itself.

## 10. MODEL LIMITATIONS

The overall procedure has introduced several simplifications along the workflow. These are necessary to keep the required computational power and time under an acceptable level. Moreover, they avoid to overcomplicating the methodology during the first realization, before the achievement of concrete results. Nevertheless, these assumptions represent some limitations for the model accuracy and thus they must be inevitably recognized to master the full potentiality of the approach.

Following the energy path within the van, the starting point is the engine. This component is replicated simultaneously with the Simulink pace according to a working point computation principle, starting from the real characteristics of each component. Therefore, this approach is more common than the rougher map-based control because it offers a more complete characterization of every working point, at the expense of a longer simulation time. As a result, the engine modelling does not introduce loss of information, ensuring a high accurateness.

Going forward along the mechanical chain, the next element is the clutch. The latter is exemplified by a limited slip model, assisted by the exertion of an incredibly strong pressure on the friction-controlled disk and an immediate release afterwards. This is necessary to avoid a prolonged gear shifting that would increase the idling time of the model and consequently the relative speed error across the cycle. On the other hand, it causes a large drop in engine rotational speed during the subsequent clutch re-engagement. To solve this issue, a variable pressure model could be employed in the future, able to adjust the load applied according to the clutch stroke.

This would also solve the issue of the peaks of Torque transferred to the mechanical chain up to the wheels during the gears shifting. The peaks provided a distorted picture of the load involved in the process, affecting the design of the components involved. These include not only the wheels, deeply discussed in chapter 9.7, but also the gearbox, the differential,...

The next limiting element is the transmission logic. The StateFlow block implemented in this model governed the gear shifting according to constant speed thresholds. Moreover, a temporal reference was considered to avoid erroneous and continuous engagements and disengagements: the neutral gear is employed only when the engine rpm is below a minimum level for few seconds, a range of time long enough to avoid an automatic gear disengagement during normal driving at very low speeds. Even the other gears follow a similar approach.

This gearshift principle is known as *imposed engine speed strategy* and it is not so flexible as the WLTP prescribes. In fact, it determines a significant limitation on the stopping time, as verified in chapter 9.1.

On the contrary, the WLTP gearshift strategy is customised for the specific vehicle-engine coupling and follows the path of the real driving scenario. Therefore, a more thorough description of the transmission control, considering engine power and other factors too, would be beneficial to the model completeness.

Concerning the SCR analysis, the variables involved are infinite due to the complexity of the system and consequently several limiting aspects must be considered. The construction of the model itself requires some simplifying assumptions: uniform wall Temperature in each block and the heat transfer towards the environment is neglected, as well as the heat of the chemical reactions in the washcoat. These phenomena are strongly affecting the thermal evolution of the fluid-SCR interaction. To improve the accuracy of the thermal model, the number of blocks used to discretize the model must be raised up to a number ensuring the best trade-off between the computational power and the quality of the results. This approach was already passed through in this analysis and further actions would not bring other benefits. About the environment and chemical reactions heat transfers, these significantly influence the results and a dedicated model should be considered to improve the quality of the work.

With respect to a real SCR working principle, the urea oxidation at high Temperatures (beyond 500°C) is not included in this analysis. This causes a drop in the conversion efficiency since the urea is not fully involved in the active sites anymore. Therefore, the modelling of this process is of relevant interest and may represent a further improvement of the level of detail achievable by this methodology.

Moreover, to compare the tailpipe emissions with a real case, the entire After-Treatment System (ATS) line implementation is mandatory.

First of all, the SCR works in best efficiency conditions when the  $\text{NO}_2/\text{NO}_x$  ratio is approximately 50%. This condition is nearly achieved in extremely low load and low speed conditions only, at the engine-out. To easily reach this target, a Diesel Oxidation Catalyst (DOC) is interposed between the engine and the SCR and its implementation in the model should be included.

In addition, the Continuously Regenerating Trap (CRT) effect is not considered in this model. This process consists of the reaction of part of the  $\text{NO}_x$  emitted by the engine with the soot accumulated in the Diesel Particulate Filter (DPF), when the Temperatures upstream of the DPF itself are around 400°C. This determines an abatement of the  $\text{NO}_x$  level upstream of the SCR and thus the efficiency levels and the tailpipe  $\text{NO}_x$  emissions computed by the model are not comparable to the real case. The same is valid if the SCR is combined with the DPF in a single device named SCR on Filter (SCRoF).

## 11. CONCLUSIONS

The exploitation of the Simscape tool has granted the treatment of the several variables involved in the powertrain functioning as physical signals with units, recognized by the model and directly employed for the autonomous calculations. Moreover, the efforts in coupling the GT-Power engine mock-up to the Simulink/Simscape interface has led to a flawless engine replication, not even comparable to the Simscape dedicated engine block capabilities. This potential was not completely expressed in this examination since few features were required for the Simscape model definition but hundreds of characteristics could still be used in further studies (from the mixture composition up to the EGR valve position).

In this study, the focus was set on the Selective Catalyst Reduction characterization, thanks to the possibility offered by Simscape to customize the components. This allowed the computation of the thermal evolution in each point, despite of the complexity of the principles governing the heat exchange and of the catalyst intricated structure. The discretization approach was fundamental for this purpose and necessary due to the uniform wall Temperature assumption. Once the thermal behaviour is known, the chemical action of the SCR may be defined and the tailpipe NO<sub>x</sub> emission along the entire cycle is extracted.

Among the several benefits brought by this methodology, one of the most significant is the possibility to estimate the NO<sub>x</sub> amount immediately after the beginning of the test, whereas the sensor-based experimental data recording takes up to 800 seconds to achieve the proper conditions for the correct functioning. In this period, a plateau value is supposed or, as an alternative, an estimation model is employed. Moreover, this methodology does not require the availability of the physical components; once the target characteristics are designed, the high accuracy performances can be computed. Therefore, the application of this model-based approach has allowed to overcome these issues, leading to significant results in a flexible and immediate way.

Future works can be focused on the realization of a complete ATS model in order to compare its results with the real vehicle performances. Currently, this is not possible due to the missing DOC and DPF that determines significantly different conditions, compared to the real functioning. This would include the CRT effect and the achievement of the 50% NO<sub>2</sub>/NO<sub>x</sub> target, fundamental requirements for the reasons already explained in chapter 10. Moreover, the insertion of the urea oxidation activity would further refine the accurateness of the approach, especially at high Temperatures. In addition, the procedure is perfectible by relaxing the environmental and chemical reactions heat transfer assumptions, constructing proper models to embrace them.

Once all these limits are fixed, the final methodology would be able to correctly predict the experimental data coming from the tailpipe of a real vehicle, tested on a homologation cycle such as the WLTP, as done in this analysis. Here, this approach was employed for the emissions control but it may be extended to every car aspect, clearing the way to infinite possibilities in the future vehicle modelling.

## REFERENCES

- [1] Eriksson & Nielsen, 2014, *Modeling and Control of Engines and Drivelines*, John Wiley & Sons Ltd., Chichester (UK)
- [2] Gundlapally, Papadimitriou, Wahiduzzaman & Gu, 2016, *Development of ECU Capable Grey-Box Models from Detailed Models—Application to a SCR Reactor*, Springer, USA
- [3] Schär, Onder & Geering, 2006, *Control of an SCR Catalytic Converter System for a Mobile Heavy-Duty Application*, IEEE Transactions on Control Systems Technology, Vol.14, N°4
- [4] The Engineering Toolbox, 2009, <[https://www.engineeringtoolbox.com/air-properties-viscosity-conductivity-heat-capacity-d\\_1509.html?vA=300&degree=C&pressure=1bar#](https://www.engineeringtoolbox.com/air-properties-viscosity-conductivity-heat-capacity-d_1509.html?vA=300&degree=C&pressure=1bar#)>
- [5] M.W.Chase, 1998, *NIST-JANAF Thermochemical Tables, Fourth Edition*, Journal of Physics and Chemical Reference Data, Monograph 9
- [6] IVECO Press Room, 2014, <<https://www.iveco.com/en-us/press-room/release/Pages/new-daily-van-of-the-year-2015.aspx>>
- [7] IVECO, 2015, <[https://issuu.com/iveco1975/docs/iveco\\_cat-daily-ame-eng\\_lowres](https://issuu.com/iveco1975/docs/iveco_cat-daily-ame-eng_lowres)>
- [8] YouTube, 2017, <<https://www.youtube.com/watch?v=a5SuW6wO5mQ>>
- [9] Gamma Technologies, 2019, <<https://www.gtisoft.com/gt-suite-applications/propulsion-systems/gt-power-engine-simulation-software/>>
- [10] Mathworks Simscape, 2020, <<https://it.mathworks.com/products/simscape.html>>
- [11] IVECO, 2015, <[https://www.iveco.com/saudi-arabia-ar/collections/technical\\_sheets/Documents/Daily%20MY%202014/Daily%20MY%202014%20Cab/MCA\\_50C15\\_E3\\_UK\\_1%20.pdf](https://www.iveco.com/saudi-arabia-ar/collections/technical_sheets/Documents/Daily%20MY%202014/Daily%20MY%202014%20Cab/MCA_50C15_E3_UK_1%20.pdf)>
- [12] Wang, 2020, <<https://www.frontiersin.org/articles/10.3389/fenrg.2020.00067/full>>
- [13] IVECO, 2015, <[https://www.iveco.com/finland/Documents/Configurator/Brochure/Dailyvan\\_FI.pdf](https://www.iveco.com/finland/Documents/Configurator/Brochure/Dailyvan_FI.pdf)>
- [14] IVECO, 2015, <[https://www.iveco.com/SouthAfrica/collections/technical\\_sheets/Documents/DailyVanSpecificationSheet.pdf](https://www.iveco.com/SouthAfrica/collections/technical_sheets/Documents/DailyVanSpecificationSheet.pdf)>

